Microalgal photobioreactors:
Scale-up and optimisation

Promotor

Prof. Dr. Ir. J. Tramper

Hoogleraar in de Bioprocestechnologie, Wageningen Universiteit

Co-promotor

Dr. Ir. R. H. Wijffels

Universitair hoofddocent sectie Proceskunde, Wageningen Universiteit

Samenstelling promotiecommissie

Prof. Dr. A. Richmond *(Ben-Gurion University of the Negev, Israel)*

Prof. Dr. M. Tredici *(Università degli Studi di Firenze, Italia)*

Prof. Dr. Ir. W. H. Rulkens *(Wageningen Universiteit, Nederland)*

Prof. Dr. L. R. Mur *(Universiteit van Amsterdam, Nederland)*

Maria João Gante de Vasconcelos Barbosa

Microalgal photobioreactors: Scale-up and optimisation

Proefschrift

ter verkrijging van de graad van doctor
op gezag van de Rector Magnificus
van Wageningen Universiteit,
Prof. Dr. Ir. L. Speelman
in het openbaar te verdedigen
op vrijdag 12 september 2003
des namiddags te half twee in de aula.

Barbosa, M.J.G.V. 2003. Microalgal photobioreactors: Scale-up and optimisation.

Ph.D. Thesis, Wageningen University, Wageningen, The Netherlands – With summary in Dutch

Keywords: microalgae, cultivation, light regime, hydrodynamic stress, optimisation, productivity, photobioreactors, A-stat., scale-up.

ISBN: 90-5808-898-7

Aos meus pais

À minha avó Regina

Contents

Chapter 1	Introduction and thesis outline	9
Chapter 2	Microalgae cultivation in air-lift reactors: modeling biomass yield and growth rate as a function of mixing frequency	17
Chapter 3	Hydrodynamic stress and lethal events in sparged microalgae cultures	37
Chapter 4	Overcoming shear stress of microalgae cultures in sparged photobioreactors	57
Chapter 5	Optimisation of cultivation parameters in photobioreactors for microalgae cultivation using the A-stat technique	73
Chapter 6	Optimisation of biomass, vitamins and carotenoid yield on light energy in a flat panel reactor using the A-stat technique	91
Chapter 7	High-cell density cultures: design and operational characteristics of photobioreactors	115
References		137
Summary		149
Samenvatting		153
Acknowledgements		159
Curriculum Vitae		163

1 Introduction and thesis outline

Products from microalgae and cyanobacteria

For millennia, aquatic environments have been a source of food, minerals and natural products. Concomitant to the increase in Human population and its needs, there is an urge for the discovery and sustainable development of new resources. In the sea, very different and extreme environments can be found, hosting unusual biochemical processes of importance to industry, nutrition, medicine, research and the environment. Marine organisms represent therefore a vast resource with potential benefits in many different areas (Table 1.1).

Table 1.1. Products from microalgae

	Product	**Applications**
Biomass	Biomass	Health food Functional food Feed additive Aquaculture Soil conditioner
Coloring substances & Antioxidants	Xantophylls (astaxanthin and canthaxanthin) Lutein β-carotene Vitamins C and E	Food and feed additives Cosmetics
Fatty acids-FA	Arachidonic acid-AA Eicosapentaenoic acid-EPA Docosahexaenoic acid-DHA γ-linolenic acid–GCA Linoleic acid-LA	Food additive
Enzymes	Superoxide dismutase-SOD Phosphoglycerate kinase-PGK Luciferase and Luciferin Restriction enzymes	Health food Research Medicine
Polymers	Polysaccharides Starch Poly-β-hydroxybutyric acid-PHB	Food additive Cosmetics Medicine
Special products	Peptides Toxins Isotopes Aminoacids (proline, arginine, aspartic acid) Sterols	Research Medicine

Among aquatic microorganisms microalgae and cyanobacteria are a very interesting source of a wide range of compounds (Table 1.1) (Benemann et al., 1987; Cohen, 1999; Skulberg, 2000; Pulz et al., 2001). They do not only have the capacity to produce high-value compounds, but also the ability to do it using only sunlight, carbon dioxide and seawater. For this reason microalgae and cyanobacteria are called photoautotrophic microorganisms, i.e. they need light as their main energy source (phototrophic) and they can grow on a very simple culture medium (autotrophic). This is possible due to the only biological process of importance that can harvest energy from the sun – photosynthesis.

Photobioreactors

After identification of a strain and product of interest, the step to follow is the development of bioprocesses to establish the link between discovery and commercialisation. Reactor design and optimisation is an essential step to bring the new product to the 'store shelf'.

The cultivation system can vary depending on the product and strain. Open systems can be used for very fast growing strains or for strains that grow at extreme conditions, such as high pH or high salinities. However, for the majority of the strains and products with applications in the pharmaceutical industry, monoalgal or even axenic cultures are required. In order to meet these standards and aiming at attaining a cost-effective process, several closed systems have been developed in the last years (Pulz and Scheibenbogen, 1998; Tredici, 1999). As in conventional heterotrophic cultivations, also in microalgal biotechnology high volumetric productivities are required to reduce the size of cultivation systems and consequently reduce production and downstream processing costs. This entails a high efficiency of light utilization besides high biomass concentrations because light energy is the growth limiting substrate. The basic idea of using sunlight to produce high-value compounds brings along several limitations, which are related to the light regime inside the cultivation system and have to be considered in the design and scale-up of photobioreactors.

High-cell density cultures can be achieved in microalgae biotechnology with a proper reactor design and process optimisation (Richmond, 2000). For this reason it is important to build up general knowledge in this field, with emphasis on the most critical scale-up and operational parameters: light and mass transfer, shear and mixing rates. These parameters are closely interrelated and they determine the productivity and efficiency of the system (Figure 1.1).

Moreover, maximisation of productivity also implies the optimisation of cultivation parameters and knowledge on growth and production kinetics (Figure 1.1).

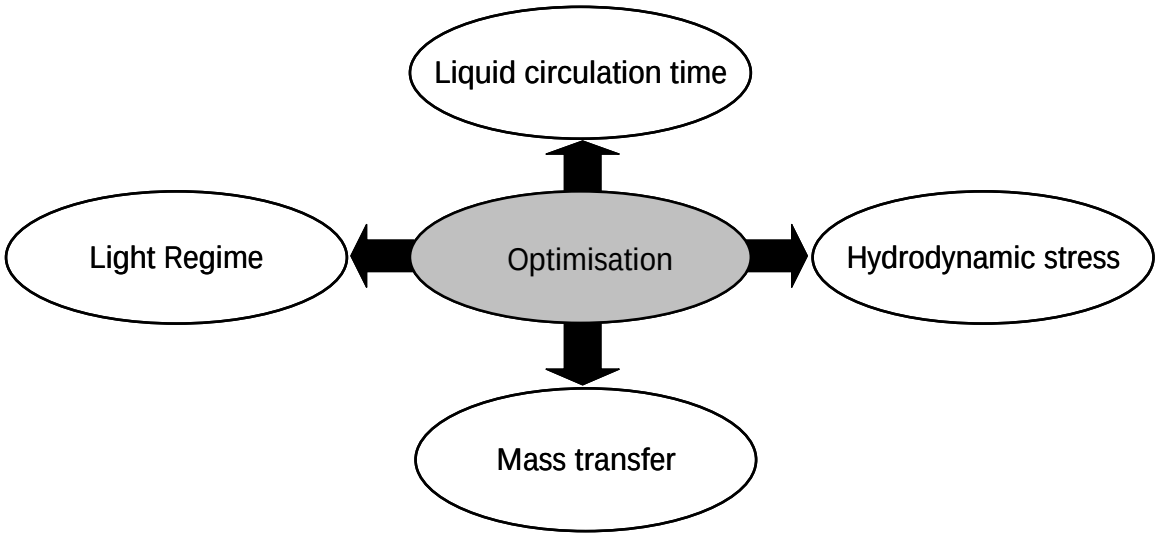

Figure 1.1. Scale-up parameters of photobioreactors.

In this thesis we have only considered vertical gas-sparged photobioreactors such as air-lift reactors, bubble columns and flat panels, due to its simple construction and operation. Moreover, these configurations show clear advantages for microalgae biotechnology: (1) the mass transfer is high in these systems and (2) short liquid circulation times can be obtained.

The aims of the present thesis are:

- Characterize the most critical scale-up aspects of gas-sparged photobioreactors, with emphasis on light regime and hydrodynamic stress.
- Develop optimisation tools for photobioreactors

Light regime, productivity and light efficiency

In a high cell-density culture, a light gradient inside the photobioreactor will always occur due to light absorption and mutual shading by the cells. Depending on the mixing characteristics of the system, the cells will circulate between light and dark zones of the reactor. The main limiting factor for the development of microalgal biotechnology is that light energy cannot be stored and homogenized inside the reactor.

In photobioreactors, the light regime is determined by the light gradient and the liquid circulation time. Strong light can be efficiently used by working at the optimal cell density in combination with a proper liquid circulation time (Richmond, 2000).

Light/dark cycles have been proven to determine the light efficiency and productivity of photobioreactors. Very fast alternations between high light intensities and darkness (from less

than 40 μs to 1 s) can greatly enhance the photosynthetic efficiency (Kok, 1953; Phillips and Myers, 1954; Terry, 1986; Matthijs et al., 1996; Nedbal et al., 1996), more pronounced for the shorter cycles in this range. The short cycle-time flashing light effect is thought to result from the fast reduction of the electron acceptors, associated with the photosystem II (PSII), followed by their oxidation in the dark period (Matthijs et al., 1996). This results in a maximum 'photo-accepting capacity' of PSII during light flashes.

This range of liquid circulation times is however not found in the most common and studied photobioreactors such as air-lifts and bubble columns. These reactors have liquid circulation times in the order of 10-100 s and 1-4 s, respectively. It was thought that medium duration light/dark cycles, of several seconds to tens of seconds, which are much easier to apply on photobioreactors, could also maintain maximal growth rate (Lee and Pirt, 1981; Merchuck et al., 1998). This was supported by the believe that energy-rich compounds were stored during the light period to be utilized during the dark period (Lee and Pirt, 1981) It was even suggested that photoinhibitory damage was less pronounced under these light/dark cycles (Merchuck et al., 1998). However Janssen et al. (2000a; 2000b; 2001) has shown that medium-duration light/dark cycles lead to a decrease in the yield of biomass on light energy in optically thin cultures.

Moreover Janssen et al. (2000a) showed that the light gradient during the light period strongly influences the biomass yield on light energy. As a consequence the light/dark cycle data obtained in the past, which were obtained with optically thin cultures, could not be used to estimate the performance of photobioreactors. For this reason, In Chapter 2 the effect of medium duration light/dark cycles of 10 to 100 s on the growth rate and biomass yield on light energy of the microalgae *Dunaliella tertiolecta* is studied. A statistical model and a corresponding experimental design are used to quantify this relation. In these experiments the light period is characterized by a light gradient and therefore the model developed could be used to simulate the implications of theses cycles on the design and operation of air-lift reactors. It is shown that air-lifts seem to be inefficient for microalgae cultivation due to the presence of these light/dark cycles which lead to low productivities and low yields on light energy, even at high gas inputs. These findings reinforce the need for shorter cycles that can be obtained in bubble columns and flat panels at high gas inputs.

Hydrodynamic stress

A high degree of turbulence is desirable in microalgae cultivations in order to promote a fast circulation of the cells from the dark to the light zone of the reactor. Its importance increases with scale-up.

According to Gudin and Chaumont (1991), the key problem of microalgae cultivation in photobioreactors is cell damage due to shear stress. However, few quantitative studies have been done regarding hydrodynamic stress in microalgae cultures cultivated in gas-sparged photobioreactors (Suzuki et al., 1995; Camacho et al., 2001). The growth rates of some microalgae have been reported to increase initially with increasing turbulence, probably due to the improved supply of light or CO_2. But upon an optimum level of turbulence, the growth decreases sharply with further increase of the superficial-gas velocity (Silva et al., 1987; Suzuki et al., 1995; Merchuk et al., 2000) and this is believed to be due to cell damage. It is therefore important to understand why and how cells are damaged in sparged photobioreactors in order to be able to avoid the decline in productivity associated to it.

Cell damage can take place during bubble formation, bubble rising or bubble break-up. It has been suggested that the main cause for cell damage was the bubble bursting at the liquid surface (Suzuki et al., 1995, Camacho et al. 2001). However very few quantitative data have been given and other possible causes for cell death have been overlooked. In this thesis, Chapter 3 and 4, the clarification and quantification of cell death rates in gas-sparged photobioreactors was done. In Chapter 3, the sensitivity of different microalgae strains, with and without a cell wall (*Dunaliella tertiolecta*, *Chlamydomonas reinhardtii* wild type and cell wall lacking mutant), to high superficial gas velocities is investigated. The cell wall is confirmed to provide protection against hydrodynamic shear and indications that cell damage occurred at the sparger site are shown. These indications are supported by a critical analysis of literature. In order to confirm this finding and to further investigate other possible causes for cell damage, the effect of gas entrance velocity, liquid height and nozzle diameter on the cell death constant is studied in Chapter 4 for the microalgae *Dunaliella tertiolecta* and *Dunaliella salina*. Bubble bursting and bubble rising are proven not to contribute to cell death. Cell damage is strain dependent and each strain has a critical gas-entrance velocity above which cell death occurs. Small nozzles, which produce small bubbles, are found to be more detrimental to cells than bigger nozzles. These findings show the importance of a proper sparger design to avoid cell death and the decline in productivity associated to it.

Optimisation

The maximization of productivity and light efficiency implies the optimisation of cultivation parameters. The knowledge on the response of microorganisms to changes in the physical environment is an essential step to obtain a cost-effective process. Steady-state culture characteristics are generally used to study growth and production kinetics as well as physiological characteristics of microorganisms. Usually these characteristics are determined in chemostat cultivations, which are very time-consuming especially when a large number of steady-state points are necessary. In contrast, acceleration–stat (A-stat) cultivations in which a cultivation parameter is continuously changed with a controlled and constant acceleration rate are not so time consuming and a wider range of steady states can be studied (Paalme et al., 1995) (Figure 1.2).

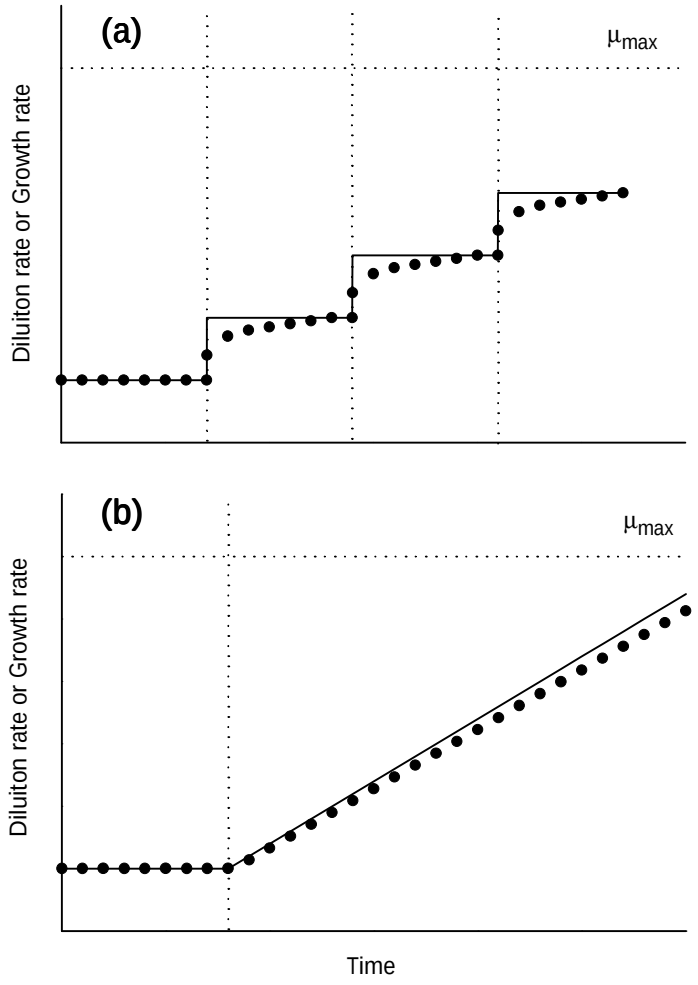

Figure 1.2. Schematic figures of: (a) several chemostats and (b) one A-stat. Solid line represents dilution rate and circles represent the specific growth rate.

The acceleration rate is the key parameter of the A-stat because it determines if the cultivation is kept in pseudo steady state. It should be a compromise between a fast and an accurate process, where the microorganism has time to adapt to the continuous change in the physical environment (Sluis et al., 2001). The A-stat has been previously used in heterotrophic microorganisms such as yeasts and bacteria, where the substrate is evenly diluted inside the reactor. However, given that in microalgae cultures the only energy source is the light falling on the reactor surface, the system changes dramatically and the applicability of the A-stat to photoautotrophic microorganisms on different cultivation systems needs to be proven and compared to the conventional chemostat cultivations. Optimisation of biomass yield on light energy of *Dunaliella tertiolecta* cultivated in a pilot-plant bubble-column is done in Chapter 5. The results show that the A-stat is a fast and accurate tool to determine kinetic parameters in continuous cultivations. Moreover it can be used as a tool to optimise cultivation parameters in a specific photobioreactor. Its applicability to another photobioreactor (flat panel), to other light regimes and to optimise the production of compounds of interest (vit C, vit E, lutein and β-carotene) is proven in Chapter 6. As described in this chapter, the acceleration rate is very important as it determines whether the system will be in steady state during the A-stat. With the proper acceleration rate, the results obtained with the A-stat are similar to the ones obtained with chemostat cultivations.

Finally, in Chapter 7 the possibility to attain high-dell density cultures in flat panels with a small optical path, in which short liquid circulation times can be induced, is discussed. An overview of the important operational and design parameters to be considered for an optimal process is given as well as new aspects and challenges that will be decisive for the success of high-cell density cultivations in photobioreactors.

2 Microalgae cultivation in air-lift reactors: modeling biomass yield and growth rate as a function of mixing frequency

Abstract

The slow development of microalgal biotechnology stems from the failure in the design of large-scale photobioreactors where light energy is efficiently utilised. Due to the light gradient inside the reactor and depending on the mixing properties, algae are subjected to certain light/dark cycles where the light period is characterised by a light gradient. These light/dark cycles will determine productivity and biomass yield on light energy.

Air-lift reactors can be used for microalgae cultivation and medium frequency light/dark cycles will be found in these systems. Light/dark cycles are associated with two basic parameters: first, the light fraction, i.e. the ratio between the light period and the cycle time and second, the frequency of the light/dark cycle. In the present work, light/dark cycles found in air-lift reactors were simulated taking into account the light gradient during the light period. The effect of medium frequency cycle time (10 - 100 s) and light fraction (0.1-1) on growth rate and biomass yield on light energy of the microalgae *Dunaliella tertiolecta* was studied. The biomass yield and growth rates were mainly affected by the light fraction, whereas cycle time had little influence. Response surface methodology was used and a statistical model describing the effect of light fraction and cycle time on growth rate and biomass yield on light energy was developed. The use of the model as a reactor design criterion is discussed.

This chapter has been published as: Maria J. Barbosa, Marcel Janssen, Nienke Ham, Johannes Tramper and René H. Wijffels. 2003. Microalgae cultivation in air-lift reactors: modeling biomass yield and growth rate as a function of mixing frequency. Biotechnol Bioeng 82:170-179.

Introduction

Algal biotechnology has progressed relatively slowly in spite of its recognised utility as a potential source of high-value compounds for the pharmaceutical and food industry (Apt and Behrens, 1999). A constraining factor is the lack of efficient large-scale cultivation techniques. Several of the microalgae applications demand the use of monocultures and controlled cultivation systems. This requirement has led to increased emphasis on the development of closed photobioreactors. Many engineering problems still need to be worked out in order to develop cost-effective production systems. For this reason it is important to build up general knowledge in this field, with emphasis on the most critical scaling up parameters.

One of the major subjects on which efforts in microalgal biotechnology should be focused is the efficient utilization of high light intensities, with the aim of increasing the biomass yield on light energy. In dense microalgal cultures light intensity decreases with distance from the irradiated surface due to self-shading and light absorption. As a result of this light gradient across the reactor, depending on the mixing frequency, algae are exposed to certain light/dark cycles where the light period is characterised by a gradient. For this reason, such cycles, which are commonly found in photobioreactors, will be referred to as light gradient/dark cycles (Figure 2.1).

Cells of mass cultures therefore receive light intermittently, which is the most practical mode to dilute strong light and could result in an effective use of light by the culture (Richmond, 2000). Light intermittence is associated with two basic parameters: first, the light fraction, i.e. the ratio between the light period and the cycle time (ε) and second, the length of the light/dark cycle (t_c).

In photobioreactors, the reactor design, length of the light path, cell concentration, extent of culture turbulence and light intensity, will determine the frequency and light fraction of the cycles. The degree of mixing is known to significantly affect the reactor productivity and the yield of biomass on light energy due to the resultant light/dark cycles (Hu and Richmond, 1996; Hu et al., 1996). High frequency fluctuating light ($t_c \leq 100$) has been reported to lead to higher growth rates and higher photosynthesis rates than with continuous light (Kok, 1953; Matthijs et al., 1996; Nedbal et al., 1996). In some of these experiments the light intensity during the light period was chosen equal to the intensity of the continuous light. In other experiments the time-averaged intensity was equal under intermittent and continuous light. However, these short cycles are not found in photobioreactors, where medium frequency fluctuations prevail. The behaviour seems to be different for medium frequency fluctuations. Light/dark cycles in the range 6 to 87 s leads to similar or lower growth rates and biomass yields on light energy in comparison to the ones obtained under continuous light of the same light intensity as during the light period of the light/dark cycles (Janssen et al., 1999; 2000a; 2000b). No influence of light/dark cycles in the

range 1-263 s was found on the volumetric productivity, specific oxygen production or carbon dioxide fixation (Grobbelaar, 1989; 1991).

In contradiction to the above findings, Lee and Pirt (1981) and Merchuck et al. (1998) observed maximal growth rates under light/dark cycles with a dark period of 9 and 6 s, respectively. Bosca et al. (1991) reported a higher carbon dioxide fixation under 4 s light/dark fluctuations in comparison to continuous light. The effect of medium frequency light/dark cycles is thus to be clarified. Moreover most of the earlier studies mentioned above have the drawback of being done with diluted cultures in order to avoid a light gradient. As a result (high) light periods were followed by periods of total darkness. However, the reality in photobioreactors with dense cultures is different. The cells move randomly with the flow from photic to light-limited zones. The light intensity never cycles sharply from total darkness to homogeneous light; instead, there is a continuous change in the light intensity from the photic to the light-limited levels (Figure 2.1).

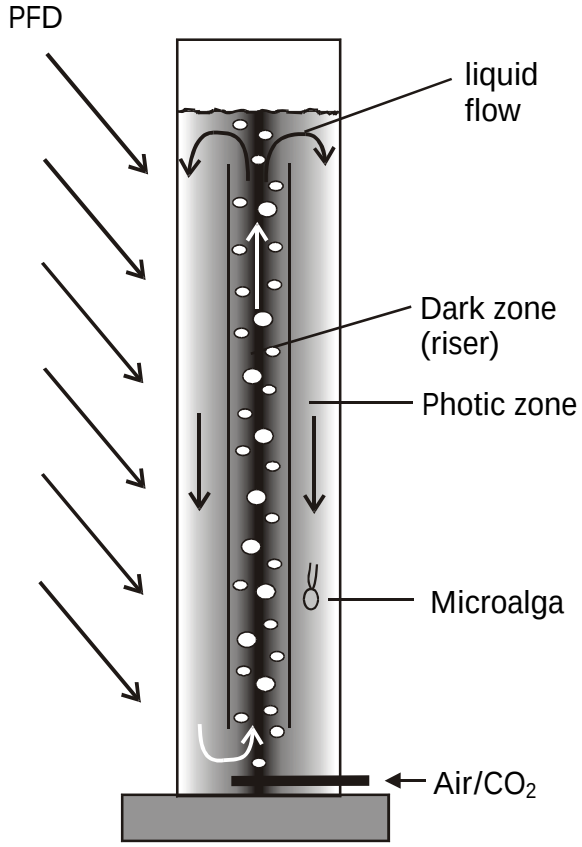

Figure 2.1. Air-lift loop reactor: liquid flow, light regime and resulting light gradient/dark cycles. PFD is the photon flux density.

Janssen et al. (2000a) showed that the light gradient during the light period strongly influences the biomass yield on light energy. As a consequence the light/dark cycle data obtained in the past can not be used to estimate the performance of photobioreactors. Clarifying and modeling the

effect of medium-duration light gradient/dark cycles on microalgal productivity still needs to be done as it is an important design tool for photobioreactors.

Air-lift reactors can be used for microalgae cultivation. A concentric draught-tube internal loop air-lift reactor could be designed in such a way that the riser comprises the dark zone and the downcomer the photic zone (Figure 2.1). Consequently the time algae spend in the dark and photic zone is determined by liquid circulation time (10-100 s), which depends on the superficial gas velocity and reactor design (Chisti, 1989).

In the present work the effect of cycle time (10 - 100 s) and light fraction (0.1-1) on biomass yield on light energy and on the specific growth rate was studied. The biomass yield and growth rates were mainly affected by the light fraction. Cycle time had a small influence on the yield and growth. A statistical model describing the effect of light fraction and cycle time is proposed. An empirical model was preferred to a theoretical model because it allows the study of a wide range of mixing frequencies (and thus light gradient/ dark cycles) and it is an established method to study main effects and two-factor interactions with relatively few experimental trials (Hwang and Hansen, 1997; El Helow et al., 2000). The development of a theoretical model would require extensive knowledge on the metabolism response to different light gradient/dark cycles, which is not available yet.

The use of the developed statistical model as a reactor design criterion is discussed.

Materials and Methods

Experimental design

The 11 different runs (Table I) were done according to an experimental design (central composite design (Haaland, 1989). The observations obtained in the experiments were fitted to the following model:

$$Y = b_0 + b_1 \cdot X_1 + b_2 \cdot X_2 + b_{11} \cdot X_1^2 + b_{22} \cdot X_2^2 + b_{12} \cdot X_1 \cdot X_2 \qquad \text{Eq 2.1}$$

Where Y is the dependent variable (growth rate or biomass yield on light energy); X_1 and X_2 are the independent variables (cycle time and light fraction, respectively); b_o is the regression coefficient at center point; b_1 and b_2 are linear coefficients; b_{11} and b_{22} are quadratic coefficients; b_{12} is a second-order interaction coefficient.

Strain and culture medium

Dunaliella tertiolecta CCAP 19/6B was obtained from the Culture Collection of Algae and Protozoa (Oban, UK). *D. tertiolecta* was cultivated in artificial seawater medium (ASW) composed of

(quantities in g L^{-1}): NaCl, 24.5; $MgCl_2 \cdot 6H_2O$, 9.8; $CaCl_2 \cdot 2H_2O$, 0.53; Na_2SO_4, 3.2; K_2SO_4, 0.85. The following nutrients were added (quantities in mmol L^{-1}): KNO_3, 16.0; $NaH_2PO_4 \cdot 2H_2O$, 1.0; $NaHCO_3$, 5.0. Also the following trace elements were added (quantities in µmol L^{-1}): $Na_2EDTA \cdot 2H_2O$, 61.6; $FeCl_3 \cdot 6H_2O$, 23.3; $CuSO_4 \cdot 7H_2O$, 0.210; $ZnSO_4 \cdot 7H_2O$, 0.303; $CoCl_2 \cdot 6H_2O$, 0.085; $MnCl_2 \cdot 4H_2O$, 1.83; Na_2MoO_4, 0.052.

D. tertiolecta was maintained as pure suspended culture in 250 mL-Erlenmeyer flasks containing 50 mL of medium. The cultures were kept at 20ºC, under a light intensity of 50-70 µmol m^{-2} s^{-1} and a 16/8 h day/night cycle. Every three weeks 0.5 mL of a culture was transferred to a new flask containing fresh medium. The reactor was inoculated directly with the 3 weeks old culture of one flask.

Cultivation system

A turbidostat-type reactor was used for cultivation of *D. tertiolecta* for 2 weeks under each light regime. The reactor is shown in Figure 2.2, the suspension volume was about 100 mL and the light path was 3 cm. The turbidostat was equipped with a water jacket connected to a temperature-controlled water bath at 30ºC. The pH was maintained between 7.70–7.85 by adding pulses of carbon dioxide to the air or nitrogen flow.

The culture was bubbled with nitrogen during the 16-h day period and air during the 8 h night period at a flow rate of 2.3 L h^{-1}.

Light was provided by a slide projector equipped with a halogen lamp (150 W) and connected to a timer to apply a 16/8 h day/night cycle. A shutter placed between the reactor and the light simulated the light/dark cycles by cutting off the projector light beam. The biomass concentration in the turbidostat was maintained constant by continuously measuring the out-going photon flux density (PFD_{out}) with a 2π PAR sensor (IMAG-DLO, The Netherlands) (Figure 2.2). A CR 10 datalogger (Campbell Scientific, UK) was programmed to control the shutters (VSR25, Uniblitz, NY, USA) and to measure and register PFD_{out} and dilute the reactors whenever PFD_{out} was below the set point (PFD_{set}). The continuous dilution in the turbidostat was stopped during the 8 h night period.

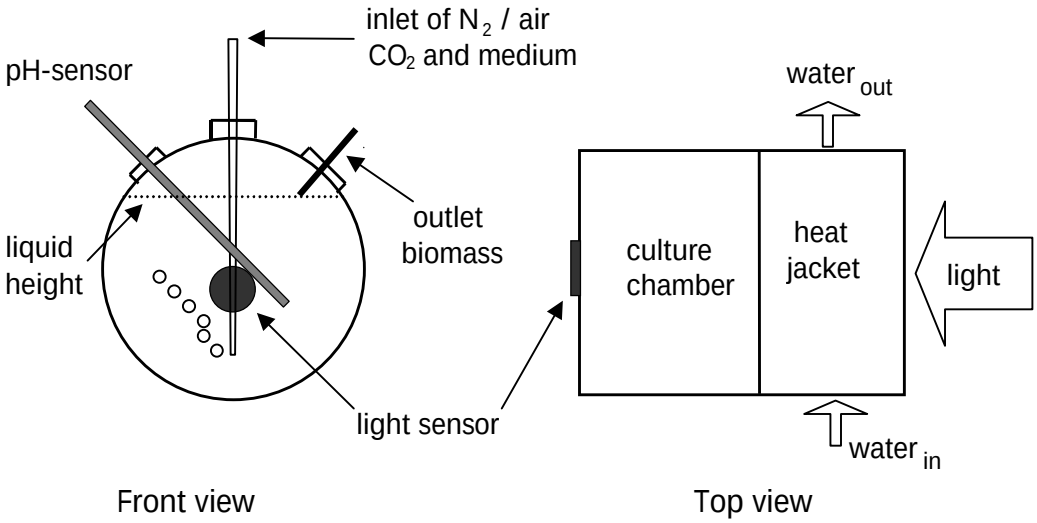

Figure 2.2. Reactor set-up: front and top view.

Photon flux density (PFD)

The photon flux density was always measured as PAR (Photosynthetic Active Radiation 400-700 nm).

PFD_{in}

The in-going PFD was measured with a LI-190SA 2π PAR-sensor, (LI-COR, Lincoln, NE, USA) at seven different spots of the illuminated area of a dummy reactor full with water, which simulated the heat jacket of the reactor. The average PFD will be referred as PFD_{in}.

PFD_0

Before inoculation, the outgoing PFD (with only medium in the reactor) was continuously measured for 2 hours with a 2π PAR sensor (IMAG-DLO, The Netherlands). The average PFD during this time will be referred to as PFD_0.

PFD_{out}

The outgoing PFD (with algae biomass in the reactor) was continuously measured during experiments with a 2π PAR sensor (IMAG-DLO, The Netherlands) as shown in Figure 2.2. This PFD_{out} was set in order to keep the transmittance constant for all the experiments. The transmittance (T) was kept at 4.2%.

The set points (PFD_{set}) for each experiment were calculated according to Eq 2.2.

$$PFD_{set} = \frac{T}{100} \cdot PFD_0 \qquad \text{Eq 2.2}$$

Photoacclimation

In order to avoid photoinhibition and to assure the same initial culture conditions for all the experiments the cultures were initially grown under the same conditions before imposing the experimental light/dark cycles. During this period (one week) the light intensity was gradually increased as follows:

1- Low light intensity (PFD_{in} = 200-400 µmol m^{-2} s^{-1}) and continuous light

2- High light intensity (PFD_{in} = 900-1200 µmol m^{-2} s^{-1}) and continuous light

3- High light Intensity (PFD_{in} = 900-1200 µmol m^{-2} s^{-1}) and experimental light/dark cycles

The average ± 95% confidence interval of the growth rates at the beginning of each experiment (phase 2) was 0.056 ± 0.004 h^{-1} which shows that experiments were started with the same initial conditions, i.e. 'physiological state' of the algae. All measurements were done for 4 consecutive days after the acclimation week.

Suspension collection

The suspension collected from the reactor was centrifuged at 5000 *g*, 4ºC, for 5 min. The supernatant was centrifuged again. Both pellets were resuspended in ASW to a final OD_{680} of 1.4. This concentrated suspension was used for the determination of protein.

Protein determination

The concentrated suspension (5.5 mL) was centrifuged at 5000 *g*, 4ºC for 5 min. The supernatant was centrifuged again. Both pellets were resuspended in sodium-phosphate buffer (10 mL) containing 1% w/v sodium dodecyl sulphate (SDS) and sonicated on ice water (Meijer and Wijffels, 1998). The suspensions were centrifuged and samples from each supernatant were stored at –80ºC until analysis. Protein was quantified with bicinchoninic acid (BCA) (Smith et al., 1985) using a commercially available kit (Pierce BCA protein assay kit, Rockford, Illinois, USA).

Growth rate (µ)

As the reactor was run as a turbidostat the specific growth rate corresponds to the dilution rate, which was followed by daily measurement of the diluted volume. The dilution rate was calculated by dividing the daily collected volume with the reactor liquid volume and with 16 hours, which corresponds to the day period. A small difference between protein concentration inside the reactor and in the suspension collected was found. This discrepancy might be caused by the fact that the samples taken in the reactor reflect only one moment of the 24 h day/night cycle while the other suspension was collected over the full 24 h day/night period. Nevertheless, this difference was assumed to be constant in all experiments so that if the absolute growth rate is not precise, the comparison between experiments is still possible.

Light absorption

The light absorbed (E_{abs}) by the culture was calculated according to Eq 2.3:

$$E_{abs} = PFD_{in} \cdot (1 - \frac{T}{100}) \cdot (\varepsilon \cdot 16 \cdot 3.6 \cdot A) \qquad \text{Eq 2.3}$$

where E_{abs} is the light absorbed by the culture (mmol d^{-1}), T is transmittance (-) which was set at 4.2 %, A is the illuminated area (m^2). The factors 3.6 and 16 are needed to convert µmol s^{-1} into mmol d^{-1} including the 16/8 h day/night cycle.

Biomass yield on light energy ($Y_{X,E}$)

The biomass yield on light energy ($Y_{X,E}$) was calculated as gram protein produced per mol photons absorbed according to Eq 2.4.

$$Y_{X,E} = \frac{P_X}{E_{abs}} \qquad \text{Eq 2.4}$$

where P_X is the productivity, i.e. the amount of protein produced per day (mg d^{-1}). The daily productivity (P_X) was calculated multiplying the volume of culture suspension diluted during one day with the protein concentration of that suspension.

Results and Discussion

Light fraction and cycle time

The efficiency of light utilisation by the microalgae *Dunaliella tertiolecta* under medium – duration light gradient/dark cycles in comparison to continuous light was investigated. During all experiments a light gradient was maintained in the light period, from 1066 to 1331 µmol m^{-2} s^{-1} (PFD_{in}, Table 2.1) to 4.2% of this range (45 - 56 µmol m^{-2} s^{-1}).

In Table 2.1 the turbidostat productivity (P_X) and the light absorption (E_{abs}) during all the experimental runs are presented. As was expected a correlation was found between P_X and E_{abs}; P_X is high when E_{abs} is high and vice-versa. The exact ration between P_X and E_{abs} gives the biomass yield on light energy ($Y_{X,E}$) in (m)gram protein per (m)mol photons (Eq 2.4). For all 11 experiments of the design, the biomass yield and growth rate are presented in Figure 2.3 as a function of the light fraction, ε, and cycle time, t_c.

Table 2.1. Productivity (P_x, mg protein d^{-1}) and light absorption (E_{abs}, mmol photons d^{-1}) inside the turbidostat as a function of light fraction (ε) and cycle time (t_c) of light-gradient/dark cycles. Also PFD_{in} is presented; the transmittance of the culture was maintained at 4.2%. P_X and E_{abs} are averages of four independent determinations on consecutive days.

t_c (s)	ε (-)	PFD_{in} (μmol m^{-2} s^{-1})	E_{abs} (mmol d^{-1})	P_X (mg d^{-1})
23.1	0.231	1168	44	3.8 (1)
23.1	0.869	1331	202	47.1
86.9	0.231	1091	---	0.0 (2)
86.9	0.869	1066	174	47.1
10.0	0.550	1154	111	24.3
100.0	0.550	1248	117	17.5
55.0	0.100	1103	---	0.0 (2)
55.0	1.000	1247	237	64.7
55.0	0.550	1219	123	19.8
55.0	0.550	1237	129	19.5
55.0	0.550	1172	123	17.6

t_c – cycle time

ε **-** light fraction: time that cells are exposed to light divided by the total cycle time

(1) - value based on first two days after acclimation, P_x dropped and on day 3 production was too low to be measured

(2) - algae did not grow under these cycles

The effect of the two main parameters associated to light/dark cycles, i.e. light fraction (ε) and cycle time (t_c), on biomass yield on light energy ($Y_{X,E}$) and specific growth rate (μ) can be deduced from Figure 2.3. The increase in light fraction led to a significant increase in both yield and growth rate (Figure 2.3 a, b) as previously reported (Janssen et al., 1999; 2000a; 2000b). Biomass production was found not to be possible at ε smaller than 0.231 but under a light fraction of 0.869, $Y_{X,E}$ was almost as high as under continuous illumination. Furthermore, it can be observed in Figure 2.3 that under light fractions smaller than or equal to 0.55, short cycle times resulted in higher growth rates and biomass yields than longer cycles at the same light fraction (growth rate and biomass yield increased 55% and 52%, respectively, when cycle time decreased from 55 to 10 s and the light fraction was 0.55). On the other hand, at ε equal to 0.869, longer cycle times seemed to be more beneficial with respect to the biomass yield (Figure 2.3). This was not expected and will be discussed later. These results show the importance of well defining each parameter (cycle time and light fraction) to study the effect of medium-duration light gradient/dark cycles in microalgae cultivation.

The biomass yield on light energy under continuous illumination agrees with previous work where a yield of 0.261 g mol^{-1} was found in a 15 s light gradient/dark cycle with ε equal to 0.67 and the same light gradient in the light period (Janssen et al., 2000a). That value is close to the maximal yield of 0.272 g mol^{-1} found under continuous illumination in this study (Figure 2.3).

Light/dark cycles will result in a lower average PFD, which can induce photoacclimation. In *D. tertiolecta* acclimation to lower PFDs occurs by an increasing number of photosystems (Falkowski and Owens, 1980; Falkowski et al., 1981) with a consequent increase of the specific light absorbing surface. Two situations can be foreseen; (1) more light can be fixed at the reactor surface where the PFD is high, resulting in a more efficient use of light energy; (2) the thermal dissipation of the light energy absorbed increases due to the fact that concomitantly the specific light absorption increases and the absolute irradiance in the light period is high, resulting in a less efficient use of light energy.

In the present study light gradient/dark cycles of medium frequency (10-100 s) lead to a similar or lower photosynthetic efficiency in comparison to continuous light (Figure 2.3) which supports the hypothesis on the increase in thermal dissipation.

The biomass yield on light energy obtained under continuous illumination agrees with previous work done in a 1-L turbidostat with a light path of 3 cm (Janssen et al., 2000a). In that study a yield of 0.261 g mol^{-1} was found in a 15 s light gradient/dark cycle with ε equal to 0.67 and the same light gradient in the light period. That value is close to the maximal yield of 0.272 g mol^{-1} found under continuous illumination in this study (Figure 2.3). But, it must be noted that a yield of 0.272 g mol^{-1} is still significantly lower than the yield of 1.20 g mol^{-1} determined under a PFD of only 58 μmol m^{-2} s^{-1} (Janssen et al., 2000a). The yield under low photon flux densities is a good measure for the maximal efficiency of light utilisation.

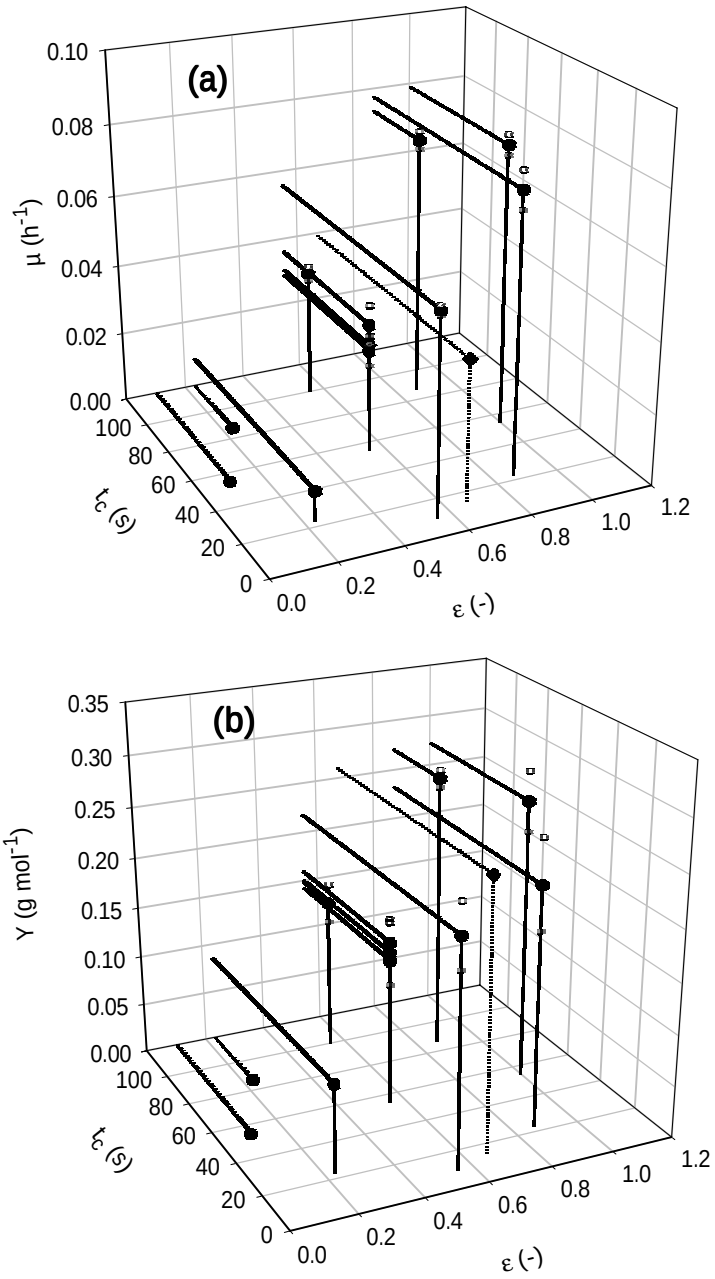

Figure 2.3. Effect of light fraction (ε) and cycle time (t_c) on: (a) specific growth rate (μ) and on (b) biomass yield on light energy ($Y_{X,E}$) of *Dunaliella tertiolecta*. Non-filled circles represent 95% confidence intervals. One data point (◆, with dashed drop lines) is from a previous work (Janssen et al., 2000a)

High PFDs can lead to photoinhibition, which is characterised by a decrease in the photosynthetic capacity (Melis, 1999). It is thought that the introduction of a dark zone could reduce photoinhibition by avoiding long exposure to high PFDs and providing dark time for reparation of the photo-induced damage (Grima et al., 1996, Merchuck et al., 1998). Our results show that under medium-duration light gradient/dark cycles at photon flux densities lower than 1200

μmol m^{-2} s^{-1} the presence of a dark zone did not lead to an improvement in the efficiency of light utilisation. At higher photon flux densities (> 1200 μmol m^{-2} s^{-1}) photoinhibition took place and it was clearly more pronounced for longer cycles.

It was already mentioned that it was not expected that the biomass yield would be higher at longer cycle times. But this was observed at the light fraction of 0.869 (Figure 2.4). At t_c equal to 86.9 s the yield was higher than at 23.1 s. Moreover, $Y_{x,E}$ under the 86.9 s cycle was almost equal to the yield determined under continuous light, 0.271 g mol^{-1} as opposed to 0.272 g mol^{-1}. This result is possibly related to the fact that PFD_{in} was higher under the 23.1 s cycle in comparison to the 86.9 s cycle, 1331 as opposed to 1066 μmol m^{-2} s^{-1} (Table 2.1). The 'additional' PFD of 275 μmol m^{-2} s^{-1} under the 23.1 s cycle possibly cannot be utilized as efficiently as the 'original' PFD_{in} of 1066 μmol m^{-2} s^{-1} applied under the 86.9 s cycle.

Two experiments out of the 11-experiment design were also done at a PFD_{in} of approximately 1600 μmol m^{-2} s^{-1}. Comparing these extra experiments with the corresponding experiments from the experimental design, carried out under PFD_{in} of 1240 μmol m^{-2} s^{-1}, shows that the biomass yield drops considerably under higher PFD_{in} (Figure 2.4). Once more it appears that 'additional' PFD added to PFD_{in} cannot be utilized as efficiently as the original photon flux supplied to the microalgae. Moreover, it seems that photoinhibition occurs under 1600 μmol m^{-2} s^{-1}. In Figure 2.4 can be seen that an increase in the in going light intensity from 1240 to 1600 μmol m^{-2} s^{-1} lead to a decrease in growth rate, more pronounced for longer cycles at a constant light fraction. This finding shows that the optimal light/dark cycle strongly depends on the light intensity in the photic period and that photoinhibition could not be prevented by the presence of a dark period.

Although photoinhibition was demonstrated this does not mean that light/dark cycling might be better than continuous light as was suggested by Merchuk et al. (1998). It can be safely concluded that, up to in-coming photon flux densities of at least 1200 μmol m^{-2} s^{-1}, the suggested reparation of photo-induced damage during the dark period did not lead to more efficient light utilization under medium-duration light-gradient/dark cycles in comparison to continuous light. On the contrary, it seems more likely that introduction of significant dark zones will lead to a higher vulnerability to light-induced damage. Due to the process of photoacclimation (Janssen et al., 2000a), the specific light absorbing surface of the microalgae increases under light gradient/dark cycles. As a result, the algae will intercept even more light in the high light zone possibly leading to more photodamage and energy dissipation. This is in agreement with Melis et al. (1999) who proved the possibility of maximizing solar use efficiencies and photosynthetic productivity by minimizing the number of the light-harvesting antenna pigments of the photosystems.

At photon flux densities higher than 1200 μmol m^{-2} s^{-1} the role of photoinhibition becomes more pronounced as can be seen in Figure 2.4. In this situation light-gradient/dark cycling might be more attractive with respect to the efficiency of light utilization than a continuous light-gradient. However, the negative effect of photoinhibition on the biomass yield on light energy can be reduced with an increased rate of cycling between light and dark zones in a photobioreactor. This was demonstrated by others (Vonshak, et al., 1994; Torzillo, et al., 1996; Grima, et al., 1996) and this effect can also be seen in Figure 2.4 comparing the 55 s and 100 s cycles.

Shorter light/dark cycles can attenuate or even prevent photoinhibition due to the smaller length of the light period, which would be advantageous in outdoor cultivation of microalgae where an over-saturating PFD will exist in the photic zone.

The effect of medium-duration light/dark cycles on microalgal productivity has been shown to have a strong influence on biomass yield and growth rate. Modeling it would thus be a very important design tool for photobioreactors.

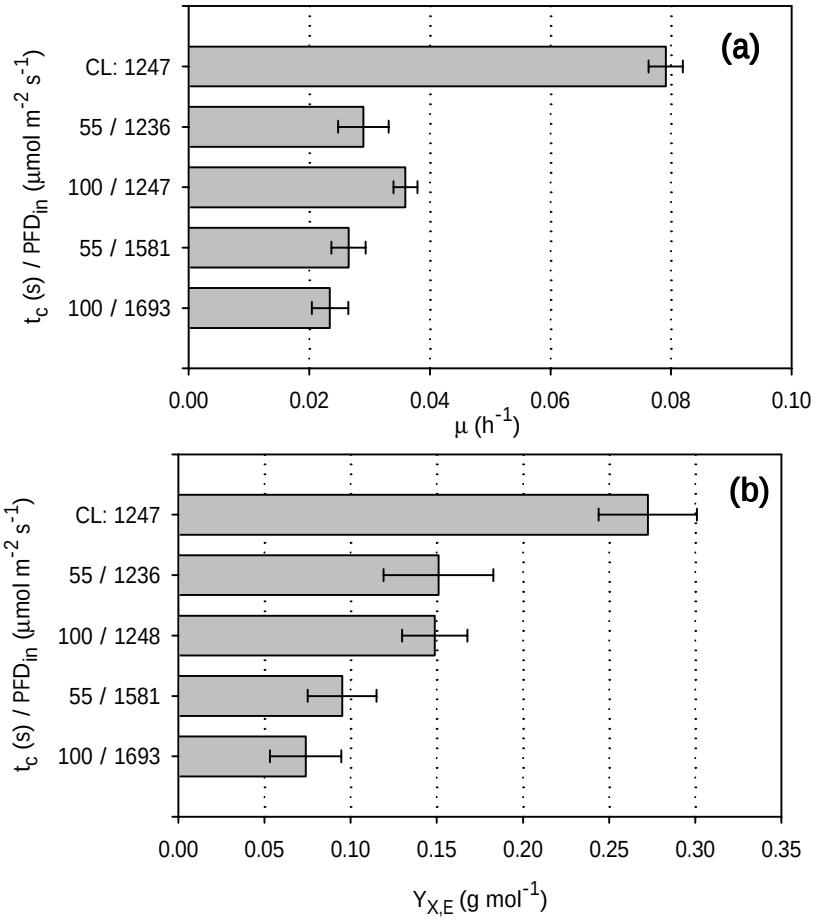

Figure 2.4. Cultivation of *Dunaliella tertiolecta* under light-gradient/dark cycles, effect of PFD_{in} on: (a) specific growth rate (μ); (b) biomass yield on light energy ($Y_{X,E}$) in gram protein per mol photons. All 4 light/dark cycle experiments were done at ε equal to 0.55; CL is continuous light (ε = 1). Error bars represent 95% confidence intervals.

Statistical model

Response surface methodology is an empirical modeling technique devoted to the evaluation of the relationship of a set of controlled experimental factors and observed results (Annadurai, 2000). An empirical model was preferred here to a theoretical model because the first one is an established method to study main effects and two factor interactions with relatively few experimental trials (Hwang and Hansen, 1997; El Helow et al., 2000). The development of a theoretical model would require extensive knowledge on the metabolism response to different light gradient/dark cycles, which would severely limit the range and number of combinations of the two variables. A statistical model overcomes this limitation.

This is the first study on the demonstration of the response surface method to optimise biomass yield on light energy as a function of light dark cycles in microalgae cultivation.

Eleven runs were done according to a central composite design (Haaland, 1989). A second-order polynomial function was fitted to the experimental results of biomass yield on light energy ($Y_{X,E}$) and growth rate (μ):

$$Y_{X,E} = 0.1084 - 0.0037 \cdot t_c + 0.2650 \cdot \varepsilon + 1.28 \cdot 10^{-5} \cdot t_c^2 - 0.1063 \cdot \varepsilon^2 + 0.0030 \cdot \varepsilon \cdot t_c \quad \text{Eq 2.5}$$

$$\mu = 0.0170 - 0.0009 \cdot t_c + 0.0602 \cdot \varepsilon + 6.22 \cdot 10^{-6} \cdot t_c^2 - 0.0307 \cdot \varepsilon^2 + 0.0001 \cdot \varepsilon \cdot t_c \quad \text{Eq 2.6}$$

The fit of the model is expressed by the coefficient of determination, r^2, which was calculated to be 0.990 and 0.978 for the biomass yield and growth rate, respectively. The closer the r^2 value to 1.00, the stronger the model is and the better it predicts responses (El Helow et al., 2000). Accordingly, our calculated r^2 value indicates that the model could explain 99.0 and 97.8% of the variability in the response. The contour plots for the biomass yield and growth rate adjusted to the model are shown in Figure 2.5.

According to the results obtained from the model, an increase of light fraction, for a constant cycle time, always leads to an increase of biomass yield and growth rate**.** The rate of increase slows down significantly at higher ε (Figure 2.5). The effect of cycle time on biomass yield is less pronounced and depends on the light fraction. In general it can be said that shorter cycle duration leads to higher efficiencies. Only at high light fraction ($\varepsilon \geq 0.8$) the efficiency is highest at short but also at long cycle times, which is very questionable (Figure 2.5). However, as discussed, this effect may be due to experimental variability of which the variation in PFD_{in} is probably the most important. Another explanation could also be the fact that the area correspondent to the outer limits of the variables ($\varepsilon = 1$, $\varepsilon = 0.1$, $t_c = 100$ and $t_c = 10$) are not very precise. Moreover, for continuous light ($\varepsilon = 1$) the cycle time is irrelevant, which is not taken into account in the present model. These limitations of the model should be considered as well as the main advantage of the

model here presented which is the wide range of light gradient/dark cycle times that could be studied and the information obtained from it.

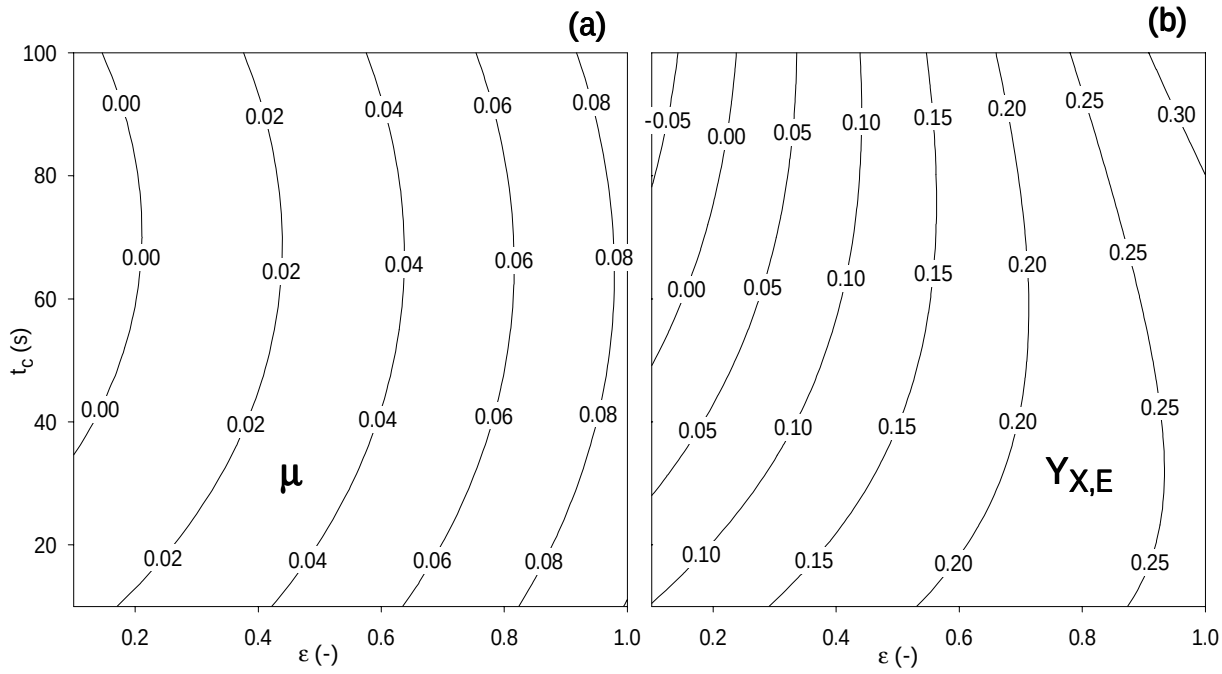

Figure 2.5. Contour plot of light fraction (ε) and cycle time (t_c) on: (a) specific growth rate (μ) and on (b) biomass yield on light energy ($Y_{X,E}$) of *Dunaliella tertiolecta*.

Reactor design

Air-lift reactors can be used for microalgae cultivation. A concentric draught-tube internal loop air-lift reactor could be designed in such a way that the riser comprises the dark zone (PFD ≤ 50 μmol m^{-2} s^{-1}) and the downcomer equals the photic zone. Consequently the time algae spend in the dark and photic zone is determined by liquid circulation velocity, which on its turn, depends on the superficial gas velocity and reactor design.

The superficial liquid velocity in the riser (U_{lr}), cycle time (t_c) and therefore the light fraction (ε) can be calculated for each specific reactor design using relations as described by (Chisti, 1989). By knowing these two parameters (t_c and ε), the biomass yield on light energy and growth rate can be estimated by using the developed statistical model (Eqs 2.5 and 2.6). This can be done only under the assumption that PFD_{in} is approximately equal to 1200 μmol m^{-2} s^{-1}, the light gradient is kept constant (1200 to 50 μmol m^{-2} s^{-1}), $10 < t_c < 100$ and $0.1 < \varepsilon < 1$. The effect of reactor height, superficial gas velocity in the riser and the downcomer to riser cross-sectional area (A_d/A_r) on cycle time, light fraction and consequently on biomass yield on light energy were simulated and are depicted in Figure 2.6 a, b and c, respectively. Some examples of possible combinations between air-lift dimensions, operation conditions and the respective estimated biomass yield will

now be given. It can be seen in Figure 2.6 that only A_d/A_r influences light fraction and it should be higher than 1.041 (dark volume = 43% of the total reactor volume) to keep the light fraction above 0.55. Downcomer to riser cross-sectional areas of 3 (Merchuk et al., 1998) and in the range 0.8 - 1.1 have been previously used for microalgae cultures (Camacho et al. 1999; Merchuck et al., 2000; Miron et al., 2000). By using the developed model the biomass yield on light energy can be estimated. Assuming $\varepsilon = 0.55$ and $t_c = 25.0$ s the biomass yield on light energy would be 0.18 ± 0.03, which corresponds to 66% of the yield estimated for continuous light ($\varepsilon = 1$). An increase in light fraction can lead to a significant improvement of the biomass yield on light energy. With light fractions closer to 1, such as with $\varepsilon = 0.79$ and $t_c = 27.6$ s the yield estimated would be 82.0% of the one estimated for continuous light ($\varepsilon = 1$). This light gradient/dark cycle could be obtained in the same reactor and operation conditions as used for the simulation depicted in Figure 2.6c, by setting the A_d/A_r on 3.43 (dark volume = 20.2% of the total volume).

Figure 2.6 clearly shows that the light fraction is the main variable affecting biomass yield on light energy as both trends are similar. In an air lift photobioreactor the light fraction can be increased by increasing the downcomer to riser cross-sectional area (A_d/A_r) which will lead to an increase of the biomass yield on light energy. However, optimising light efficiency has a drawback in volumetric productivity. A_d/A_r is inversely proportional to biomass concentration i.e., if the cross sectional area of the downcomer is increased in order to reach higher yields on light energy (Figure 2.6c) the biomass concentration should decrease in order to keep the same light gradient (from 1200 to 50 µmol m^{-2} s^{-1}) (Figure 2.6) which would lead to lower volumetric productivities.

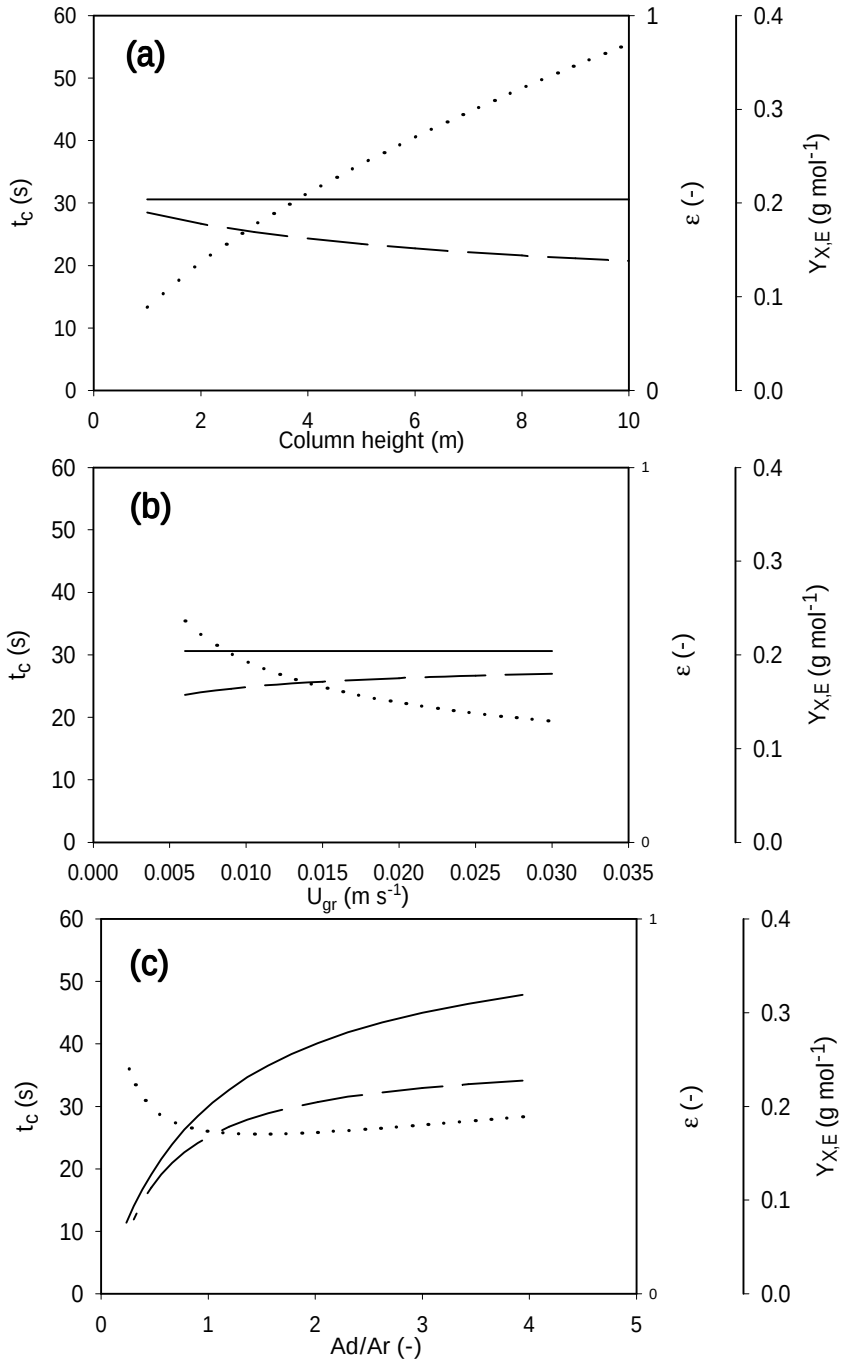

Figure 2.6. Simulations of the effect of (a) reactor height, (b) superficial gas velocity in the riser (U_{gr}) and (c) downcomer to riser cross-sectional area (A_d/A_r) on the circulation time (t_c), light fraction (ε) and biomass yield on light energy ($Y_{X,E}$). Dotted line refers to t_c, solid line to ε and the long dashed line to $Y_{X,E}$.

(a): T_v = 0.2 m; A_r = 0.015 m^2; U_{gr} = 0.025 m s^{-1}; (A_d/A_r) = 1.041; C_b = 0.10 m

(b): H = 2 m; T_v = 0.2 m; A_r = 0.015 m^2; (A_d/A_r) = 1.041; C_b = 0.10 m

(c): H = 2 m; T_v = 0.4 m; U_{gr} = 0.025 m s^{-1}; C_b = 0.10 m

Air-lift reactors seem to be inefficient for microalgae cultivation due to the presence of medium duration light/dark cycles (10 – 100 s) that are associated with these reactors. Only at high light

fractions ($\varepsilon > 0.67$) biomass yield will be comparable to the yield obtained under a continuous light gradient (from 1200 to 50 µmol m^{-2} s^{-1}) without a dark period ($\varepsilon = 1$). This yield, on its turn, is much lower than the yield obtained at low PFDs: 0.27 (Figure 2.4) as opposed to 1.2 g mol^{-1} determined under a constant PFD of only 58 µmol m^{-2} s^{-1} (Janssen et al., 2000a). The yield under low photon flux densities is a good measure for the maximal efficiency of light utilisation, which should be the target for photobioreactor design. Photoinhibition took place under over-saturating PFDs (> 1200 µmol m^{-2} s^{-1}), which led to low biomass yields on light energy and low growth rates. These results stand for the need of using systems where short light/dark cycles can be attained, such as bubble columns and flat panels.

Conclusions

In the present work a model describing the effect of medium duration light/dark cycles (10 – 100 s) on the growth rate and biomass yield on light energy was proposed. For the first time the light gradient during the light period was considered. The implications on reactor design were simulated and air-lift reactors seem to be inefficient for microalgae cultivation due to the presence of these light/dark cycles which lead to low yields on light energy. The validation of the model in an airlift should be done in the future. Shorter light/dark cycles that can be found in reactors such as bubble columns and flat panels should be further considered.

Appendix I: Light /dark frequency in air-loop reactors

The liquid circulation velocity in air-lift loop reactors was calculated according to the procedure of Chisti (1989). The superficial liquid velocity in the riser was calculated with Eq 2.7.

$$U_{lr} = \left[\frac{2 * g * h_d * (\varepsilon_{gr} - \varepsilon_{gd})}{K_B * \left(\frac{A_r}{A_d}\right)^2 * \frac{1}{(1-\varepsilon_{gd})^2}} \right]^{0.5} \qquad [m\ s^{-1}] \qquad \text{Eq 2.7}$$

The hold-up in the riser and downcomer was estimated with the following Eqs (Eq 2.8 and Eq 2.9):

$$\varepsilon_{gr} = \frac{U_{gr}}{0.24 + 1.35 \cdot (U_{gr} + U_{lr})^{0.93}} \qquad [-] \qquad \text{Eq 2.8}$$

$$\varepsilon_{gd} = 0.89 \cdot \varepsilon_{gr} \quad [-] \quad \text{Eq 2.9}$$

The parameters h_d, the height of liquid dispersion, and K_B, the friction loss coefficient for the bottom zone, could be calculated using reactor dimensions (Chisti, 1989) and the hold-up. Since U_{lr} appears also in Eq 2.7 an initial estimation has to be made followed by an iteration procedure. Liquid circulation time finally is calculated with Eq 2.10.

$$t_c = \frac{V_l}{v_{lsr} \cdot A_r \cdot (1 - \varepsilon_{gr})} \quad [s] \quad \text{Eq 2.10}$$

Nomenclature

A	illuminated area	[m^2]
A_d	cross sectional area downcomer	[m^2]
A_r	cross sectional area riser	[m^2]
C_b	bottom clearance air-lift reactor	[m]
E_{abs}	light absorbed by the culture	[mmol d^{-1}]
g	gravitational acceleration	[ms^{-2}]
H	height of the column	[m]
h_d	liquid dispersion height	[m]
K_B	friction loss coefficient bottom zone air-lift reactor	[-]
P_X	productivity, on protein basis	[mg d^{-1}]
PAR	photosynthetic active radiation, 400-700 nm	
PFD	photon flux density in PAR range	[µmol photons m^{-2} s^{-1}]
PFD_{in}	in-going PFD	[µmol photons m^{-2} s^{-1}]
PFD_0	outgoing PFD (with medium in the reactor)	[µmol photons m^{-2} s^{-1}]
PFD_{out}	outgoing PFD (with algae biomass in the reactor)	[µmol photons m^{-2} s^{-1}]
PFD_{set}	set point of PFD_{out}	[µmol photons m^{-2} s^{-1}]
T	transmittance	[%]
T_v	vessel diameter	[m]
t_c	circulation time = duration L/D cycle	[s]
U_{gr}	superficial gas velocity in the riser	[m s^{-1}]
U_{lr}	superficial liquid velocity in the riser	[m s^{-1}]
$Y_{X,E}$	biomass yield on light energy, protein per photons	[g mol^{-1}]
ε	light fraction within light/ dark cycles	[-]

μ	specific growth rate	[h^{-1}]
ε_{gd}	fractional gas hold-up downcomer	[-]
ε_{gr}	fractional gas hold-up riser	[-]

3 Hydrodynamic stress and lethal events in sparged microalgae cultures

Abstract

The effect of high superficial gas velocities in continuous and batch culture of the strains *Dunaliella tertiolecta*, *Chlamydomonas reinhardtii* wild type and cell wall lacking mutant was studied in bubble columns. No cell damage was found for *D. tertiolecta* and *C. reinhardtii* (wild type) up to superficial gas velocities of 0.076 and 0.085 m s^{-1}, respectively suggesting that high superficial gas velocities alone can not be responsible for cell death and consequently the bursting of the bubble can not be the sole cause for cell injury. A death rate of 0.46 ± 0.08 h^{-1} was found for *C reinhardtii* (cell wall lacking mutant) at a superficial gas velocity of 0.076 m $s^{-1}$and increased to 1.01 ± 0.29 h^{-1} with increasing superficial gas velocity to 0.085 m s^{-1}. Shear sensitivity is thus strain dependent and cell wall plays to some extent a role in the protection against hydrodynamic shear.

When studying the effect of bubble formation at the sparger in batch cultures of *D. tertiolecta* by varying the number of nozzles, a death rate of 0.047 ±0.016 h^{-1} was obtained at high gas entrance velocities.

D. tertiolecta was cultivated in a pilot plant reactor under different superficial gas velocities up to 0.026 m s^{-1} and relatively low gas entrance velocities and no cell damage was observed. There is indication that the main parameter causing cell death and damage is the gas entrance velocity at the sparger.

This chapter has been published as: Maria J. Barbosa, Marco Albrecht and René H. Wijffels. 2003. Hydrodynamic stress and lethal events in sparged microalgae cultures. Biotechnol Bioeng 83:112-120.

Introduction

Microalgae are a natural source of high-value compounds for the pharmaceutical and food industry, such as bioactive compounds, vitamins, pigments, fatty acids. Production of these compounds requires the development of large-scale photobioreactors.

Shearing action in sparged photobioreactors such as bubble columns and flat panels is necessary for mixing, heat elimination and mass and light transfer; its importance increases with scale-up. However, excessive shear can lead to impaired cell growth, cell damage and eventually cell death.

Cell damage due to shear stress has been referred to as the key problem of culture of microalgae in photobioreactors (Gudin and Chaumont, 1991). However, few quantitative studies have been done to characterise algal cells with respect to their shear sensitivity and within these few works, very different types of equipment, methodology and reactor configurations have been used. Hardly any data on cell death rates have been reported and it is extremely difficult to draw conclusions about the actual stress levels to which cells are exposed and their response to it by comparing results obtained for example in free jets or stirred-tank reactors with turbine impellers agitated at different speeds (Bronnemeier and Markl, 1982) or when sparging gas into the culture vessel (Silva et al., 1987; Suzuki et al., 1995).

In some papers the negative effects of hydrodynamic stress on cell growth and productivity have been reported (Gudin and Chaumont, 1991; Merchuck et al., 2000), which has led to a common opinion among researchers in this field that microalgae are intrinsically shear-sensitive. Presently shear sensitivity is an easy way out to explain low productivities and growth rates in microalgae culture systems.

The growth rates of some microalgae have been reported to increase initially with increasing turbulence, probably due to the improved supply of CO_2 or light, but upon an optimum level, the growth decreases sharply with further increase of the superficial gas velocity. Silva et al. (1987) reported this behaviour for *Dunaliella* cells (strain was not specified) as well as Merchuk et al. (2000) for *Phorphyridium sp*. ($0.00054 < U_g < 0.0082$ m s^{-1}). Suzuki et al. (1995) reported that for increasing values of superficial gas velocities (U_g) above 0.017 m s^{-1} and a decreasing number of nozzles (from 3 to 1) i.e. an increase in the gas entrance velocity, an increase in death rate of *Dunaliella tertiolecta* was observed, more pronounced for the increase in superficial gas velocity. These results show that algae death was mainly due to the bursting of the bubbles at the surface and it might have occurred to some extent at the sparger site. The same authors found a linear correlation between the specific death rate and the inverse of culture height but no explanation was given. However, these experiments were performed in the dark making it impossible to discriminate between growth limiting and damaging conditions. Camacho et al. (2000) reported

the inverse behaviour: an increase in culture height resulted in an increase in death rate. The authors related the effect of fluid height to cell attachment to bubbles: a greater height of rise means that more cells can be captured by the rising bubbles and carried to the surface where cells die as the bubbles rupture. Camacho et al. (2001) reported that the microalgae *Phaeodactylum tricornutum* is sensitive to hydrodynamic stress in bubble columns and that the break-up of small bubbles on the liquid surface seems to be the cause of cell damage ($0.01 < U_g < 0.05$ m s^{-1}). The same authors found that hydrodynamic conditions, which do not promote cell damage in the laboratory-scale, could not be extrapolated to pilot-scale, while using similar spargers and superficial gas velocities. These results show that there is still a lack of knowledge on how to minimise cell damage when scaling up.

The effect of hydrodynamic forces generated by air bubbles on animal cells in suspension has been extensively studied (Tramper and Vlak, 1988; Chalmers, 1996). Tramper et. al. (1986) distinguished 3 regions in a bubble column where cell death might occur: (1) at the sparger where the bubbles are formed, (2) in the region where the bubbles rise, and (3) at the surface where bubble disengagement occurs.
There is convincing evidence that cell death mainly occurs at bubble rupture (Jobses et al., 1991), although the sparger region is not excluded as a possible place for cell death. (Murhammer and Goochee, 1990).

Cell death rate can be described by first order kinetics as described by Eq 3.1, provided that the cell growth rate is zero or negligible compared to the cell death rate.

$$\ln\left(\frac{C_{Xv}(t)}{C_{Xv}(0)}\right) = -k_d \cdot t \qquad \text{Eq 3.1}$$

where $C_{xv}(t)$ and $C_{xv}(0)$ are the viable-cell concentration (cell m^{-3}) at time t = t and t = 0 (h) respectively, k_d is the first-order death-rate constant (h^{-1}) and t is the time (h).
Tramper et al. (1988) proposed a model for cell damage caused by sparging, in which a hypothetical killing volume, is associated with each air bubble during its live time. This model has been validated for insect cells and hybridomas in lab scale bubble columns (Tramper et al., 1988; Jobses et al., 1991). Jobses et al. (1991) further elaborated the model by specifying it for each event (bubble formation, bubble rising and bubble break-up) to yield verifiable correlations between the cell death rate and particular culture parameters. It was found that if bubble rising is the cause of cell death, the specific death-rate constant will be independent of culture height (at a constant reactor cross sectional and a constant bubble size). If the bubble formation at the sparger is the cause, the specific death rate will increase with decreasing number of nozzles, i.e.

with increasing gas-entrances velocities (provided that the total gas flow rate, bubble size, orifice diameters and culture volumes are constant). The latest, if bubble break up at the liquid surface is the cause the death rate will be proportional to the gas flow rate per unit volume (as long as fluid viscosity, surface tension and bubble size are constant).

In the present work the effect of superficial gas velocities and gas entrance velocities in continuous and batch cultures of the strains *Dunaliella tertiolecta*, *Chlamydomonas reinhardtii* wild type and cell wall lacking mutant was studied in lab scale and pilot plant bubble columns. *D. tertiolecta* and *C. reinhardtii* were selected because they are reported as being the most sensitive microalgae strains due to the lack of a rigid cell wall. *D. tertiolecta* only possesses a thin cytoplasmic membrane and *C. reinhardtii* has a relatively thin cell wall (Märkl et al., 1991). Both *C. reinhardtii* wild type and cell wall deficient mutant were chosen to verify the protective effect of the cell wall against hydrodynamic shear.
The gas velocities at the sparger were calculated, when possible also from literature, and results were compared. There is indication that the main parameter causing cell death is the gas entrance velocity at the sparger and that it could be used as a tool for reactor design.

Materials and Methods

Organism and culture medium

Chlamydomonas reinhardtii CC 1690 wild type 21 gr mt+ and *Chlamydomonas reinhardtii* CC1883 cell wall mutant 15 (nit+) mt- were kindly provided by Dr. Elizabeth Harris from the Chlamydomonas Genetics Center (Duke University, Durham, NC, USA). The organism was cultivated in a Sueoka high salts (HS) medium as described by Harris (1989), it is composed of (amounts in g L^{-1}): NH_4Cl, 0.5; $MgSO_4 \cdot 7H_2O$, 0.02; $CaCl_2 \cdot 2H_2O$, 0.01; K_2HPO_4, 1.44; KH_2PO_4, 0.72; $NaHCO_3$, 0.84 and 1 mL L^{-1} of Hütner's trace-elements solution (Harris, 1989).
Both *Chlamydomonas* strains were maintained as pure suspended culture in 250 mL-Erlenmeyer flasks containing 50 mL of medium. The cultures were kept at 20ºC, under a light intensity of 50-70 µmol m^{-2} s^{-1} and a 16/8 h light/dark cycle. Every three weeks 0.5 mL of a culture was transferred to a new flask containing fresh medium. The reactor was inoculated directly with the 3 weeks old culture of one flask.

Dunaliella tertiolecta CCAP 19/6B was obtained from the Culture Collection of Algae and Protozoa (Oban, UK). *D. tertiolecta* was cultivated in artificial seawater medium (ASW) composed of

(quantities in g L^{-1}): NaCl, 24.5; $MgCl_2 \cdot 6H_2O$, 9.8; $CaCl_2 \cdot 2H_2O$, 0.53: Na_2SO_4, 3.2; K_2SO_4, 0.85. The following nutrients were added (quantities in mmol L^{-1}): KNO_3, 16.0; $NaH_2PO_4 \cdot 2H_2O$, 1.0; $NaHCO_3$, 5.0. Also the following trace elements were added (quantities in µmol L^{-1}): $Na_2EDTA \cdot 2H_2O$, 61.6; $FeCl_3 \cdot 6H_2O$, 23.3; $CuSO_4 \cdot 7H_2O$, 0.210; $ZnSO_4 \cdot 7H_2O$, 0.303; $CoCl_2 \cdot 6H_2O$, 0.085; $MnCl_2 \cdot 4H_2O$, 1.83; Na_2MoO_4, 0.052. In the fed-batch cultivation the concentration of KNO_3 and $NaH_2PO_4 \cdot 2H_2O$ were increased to 32 and 2 mmol L^{-1}, respectively. In the batch cultivation 100 mM of buffer Tris was added to the medium.

D. tertiolecta was maintained as pure suspended culture in 250 mL-Erlenmeyer flasks containing 50 mL of medium. The cultures were kept at 20ºC, under a light intensity of 50-70 µmol m^{-2} s^{-1} and a 16/8 h light/dark cycle. Every three weeks 0.5 mL of a culture was transferred to a new flask containing fresh medium. The reactor was inoculated directly with the 3 weeks old culture of one flask.

Cultivation system

Turbidostat

D. tertiolecta, C. reinhardtii wild type and cell wall lacking mutant were cultivated in identical lab scale bubble columns with an inner diameter of 0.0354 m and a height of 0.4 m (top and bottom not included). The working volume was 0.30 L.

The bubble columns were equipped with a water jacket connected to a temperature-controlled water bath operated at 30ºC. pH was maintained between 7.70-7.85 by adding pulses of carbon dioxide to the air. The air flow rate was controlled with a mass flow controller (5850E, Brooks Instrument BV, The Netherlands).

Light was continuously provided by 10 fluorescent light tubes (LYNX LE, 55W, Sylvania, Germany) placed at one side of the reactor and a mirror placed at the opposite side. The ingoing photon flux density (PFD) was measured at 8 different spots inside the reactor with a LI-190SA 2π PAR-sensor, (LI-COR, Lincoln, NE, USA) and an average light intensity of 540 µmol m^{-2} s^{-1} was calculated from 8 different measurements along the column.

The biomass concentration in the turbidostat was maintained constant by continuously measuring the light transmitted by the culture. An external loop was built together with a device containing a light emitting diode (LED, L-53SRC-F, Kingbright) and a 2π PAR sensor (IMAG-DLO, The Netherlands). The culture circulated between the LED and the light sensor and the light transmitted by the culture was continuously measured.

A CR 10 datalogger (Campbell Scientific, UK) was programmed to measure and register the light transmitted by the culture and dilute the reactors whenever it was below the set point which corresponded to a biomass concentration of 0.5 g L^{-1}. This biomass concentration was arbitrarily

chosen and it is a compromise between a low level of mutual shading and sufficient biomass for analysis and accurate turbidostat control.

In order to assure the same initial culture conditions for all the experiments the cultures were initially grown under a low superficial gas velocity (0.005 m s^{-1} for 1 week) before imposing the experimental gas velocity.

As the reactor was operated as a turbidostat the specific growth rate (μ) corresponds to the dilution rate, which was followed by daily measurement of the diluted volume. The dilution rate was calculated by dividing the volume collected, with the reactor liquid volume, and with 24 h, which is the time of collection. All measurements were done for 4 consecutive days.

Repeated batch

Dunaliella tertiolecta was cultivated in a pilot plant bubble column with a height and diameter of respectively 2.5 and 0.21 m. The working volume was 69 L. The reactor was surrounded by 62 fluorescent tubes (Britegro 2023, Sylvania) with a correspondent light intensity of 400 μmol m^{-2} s^{-1} at the reactor wall, measured with a LI-190SA 2π PAR-sensor, (LI-COR, Lincoln, NE, USA).

A Bio controller (Applikon, The Netherlands) controlled the cultivation conditions (pH and temperature) and the software BioExpert (Applikon, The Netherlands) acquired the on-line data (temperature, pH, air and carbon dioxide flow rate). The reactor was equipped with a water jacket connected to a water bath, which allowed controlling the temperature at 30ºC. The pH was controlled at 7.8 by adding carbon dioxide to the air flow. The total gas flow rate was kept constant by automatic decrease of the gas flow rate when the CO_2 flow rate increased.

Batch cultures

D. tertiolecta was cultivated in lab scale bubble columns with an inner diameter of 0.0354 m and a height of 0.4 m (top and bottom not included). The working volume was kept at 0.30 L.

The bubble columns were equipped with a water jacket connected to a temperature-controlled water bath operated at 30ºC. pH was maintained between 7.70-7.85 by buffering the medium with 100 mmol Tris. The effect of Tris concentrations up to 100 mM were found not to affect the growth rate of *D. tertiolecta* (data not published). The air flow rate was controlled with a mass flow controller (5850E, Brooks Instrument B.V., The Netherlands)

Light was continuously provided by 10 fluorescent light tubes (LYNX LE, 55W, Sylvania, Germany) placed at one side of the reactor and a mirror placed at the opposite side. The ingoing photon flux density (PFD) was measured at 8 different spots inside the reactor with a LI-190SA 2π PAR-sensor, (LI-COR, Lincoln, NE, USA) and an average light intensity of 540 μmol m^{-2} s^{-1} was calculated.

The inocula for these batch experiments were samples taken from a chemostat (D = 0.02 h^{-1}) culture, run under the same pH and temperature as in the experiments and a working volume of 3.5 L. These samples were diluted to a OD_{680} of 0.4 before starting the experiments.

Sparger

The sparger for the lab scale bubble column was either a perforated plate with 16 holes with an internal diameter (d_i) of 1.05 mm each or it was a piece of silicon in which needles were inserted. The number and internal diameter of the needles varied in different experiments as described in Table 3.1. The sparger of the pilot plant bubble column was made of stainless steel and had 21 nozzles with d_i = 1.7 mm (Table 3.1).

Superficial gas velocity

The superficial gas velocity (U_g) was varied in different experiments as described in Table 3.1.

For the bench-scale bubble columns, superficial gas velocity was calculated according to Eq 3.2 and for the pilot plant bubble column it was calculated according to Eq 5.3, which corresponds to the height averaged superficial gas velocity.

$$U_g = \frac{F_g}{\pi \cdot r^2} \qquad \text{Eq 3.2}$$

where F_g is the volumetric gas flow rate ($m^3\ s^{-1}$) and r is the column radius (m)

$$U_g = \frac{Q_m \cdot R \cdot T}{h_d \cdot A \cdot \rho \cdot g} \cdot \ln\left(1 + \frac{\rho \cdot g \cdot h_d}{P_h}\right) \qquad \text{Eq 3.3}$$

where Q_m is the molar flow rate of the gas, h_d is the static height of the gas free liquid, R is the gas constant, T is the absolute temperature, A is the cross-sectional area of the column and P_h is the pressure in the head zone. Eq. 3.3 assumes ideal gas behaviour.

Cell concentration

Dunaliella and *Chlamydomonas* cells were counted and measured with the coulter counter Multisizer II (Beckman Coulter, The Netherlands) and the automatic cell counter Casy® (Schärfe system GmbH, Germany), respectively.

The optical density of the algal suspensions was measured at an absorbance of 680 and 530 nm on a spectrophotometer (Spectronic® 20 Genesys, Spectronic Instruments, UK) against a reference of artificial sea water (ASW).

Viability

Cell viability was determined by staining the culture with fluorescein diacetate (FDA) and analysing it in a flow cytometer (FACScan; Becton Dickison BV, The Netherlands). On the basis of green and red fluorescence viable and dead cells, respectively could be discriminated.

Results and Discussion

Bubble break -up

According to the cell damage model proposed by Tramper et al. (1988) and further elaborated by Jobses et al. (1991), if the bubble break up at the liquid surface is the cause for cell damage, the death rate will be proportional to the gas flow rate per unit volume.

High superficial gas velocities are desirable in microalgae cultivations in order to create a high degree of turbulence allowing a fast circulation of the cells from the dark to the light zone of the reactor. These fast liquid circulation times (on a µ-ms scale) have been shown to give rise to considerable higher photosynthetic efficiency (Kok, 1953; Matthijs et al., 1996) than longer cycles which can even lead to a decrease in the photosynthetic efficiency (Janssen et al., 2000a; 2000b; 2001). Janssen et al. (2003) reported that the average liquid circulation time in vertical bubble columns will be between 0.5 and 2 s at superficial gas velocities of 0.05 m s^{-1} or higher. These calculations were based on the model of Joshi and Sharma (1979). Very high superficial gas velocities are thus required in order to achieve high productivities in bubble columns.

The effect of superficial gas velocities in continuous cultures of the strains *Dunaliella tertiolecta*, *Chlamydomonas reinhardtii* wild type and cell wall lacking mutant was studied. The growth rates and percentage of viable cells of *D. tertiolecta* cultivated under different superficial gas velocities are depicted in Figure 3.1. There is no effect of superficial gas velocities up to 0.076 m s^{-1} in the growth of *D. tertiolecta* and viability was always above 94%. These results are in contradiction with the findings of Suzuki et al. (1995) who reported an increase in death rate for superficial gas velocity values above 0.017 m s^{-1}. However, these experiments were performed in the dark making it impossible to discriminate between growth limiting and damaging conditions, the duration of each experiment and cultivation mode were not described, which makes the interpretation and comparison of these results with the present work very difficult. Another possible reason for this discrepancy might be due to the differences in the gas velocity at the sparger site, which is dependent on the gas flow rate and on the number and diameter of the nozzles. This hypothesis will be discussed further on in this paper.

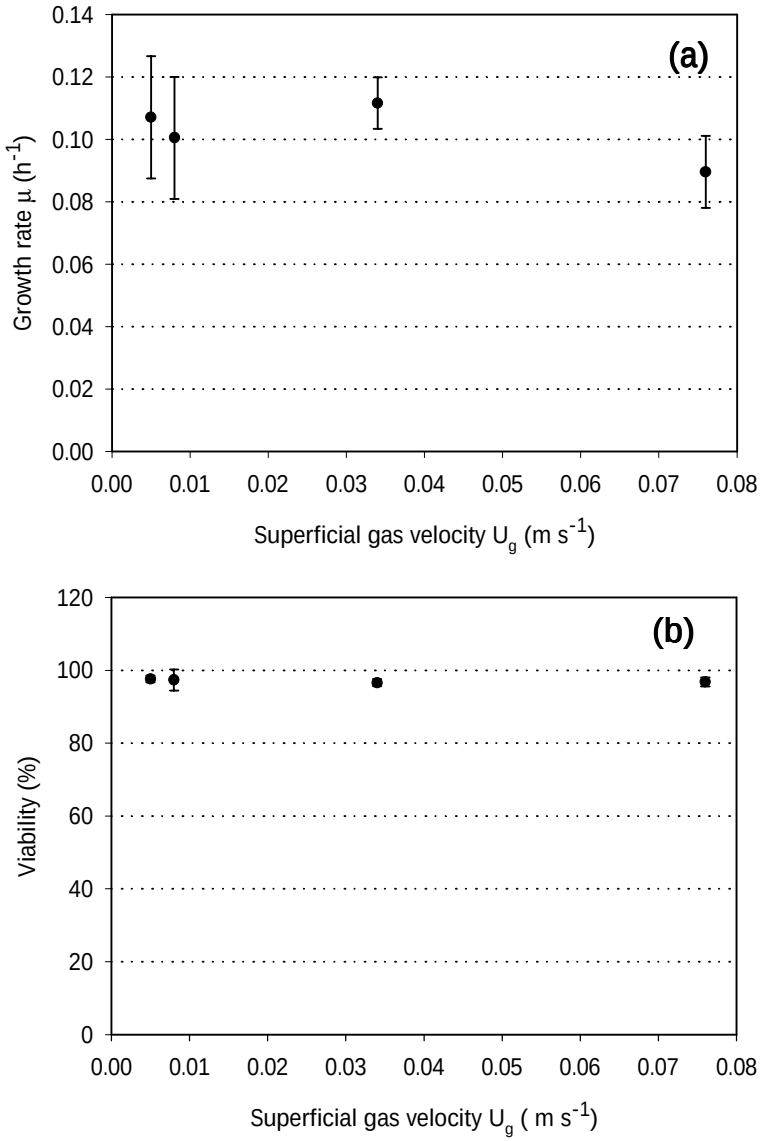

Figure 3.1. (a) Growth rate (μ) and (b) Viability of *D. tertiolecta* grown under different superficial gas velocities (U_g). Experiments were done in bench-scale bubble columns, run as a turbidostat. Error bars represent 95% confidence intervals calculated from four independent measurements.

The effect of high superficial gas velocities on the growth of *C. reinhardtii* wild type and mutant is depicted in Figure 3.2. Superficial gas velocities up to 0.084 ms^{-1} did not affect the growth rate of *C. reinhardtii* wild type while the cell wall deficient mutant could not grow at superficial gas velocities equal or higher than 0.076 m s^{-1}. These results stand for the protective role of the cell wall against hydrodynamic stress. Bronnemeier and Markl (1982) have also reported a protective role of the cell wall of *C. reinhardtii* after performing free jet and stirring experiments with a wild type and a cell wall deficient mutant.

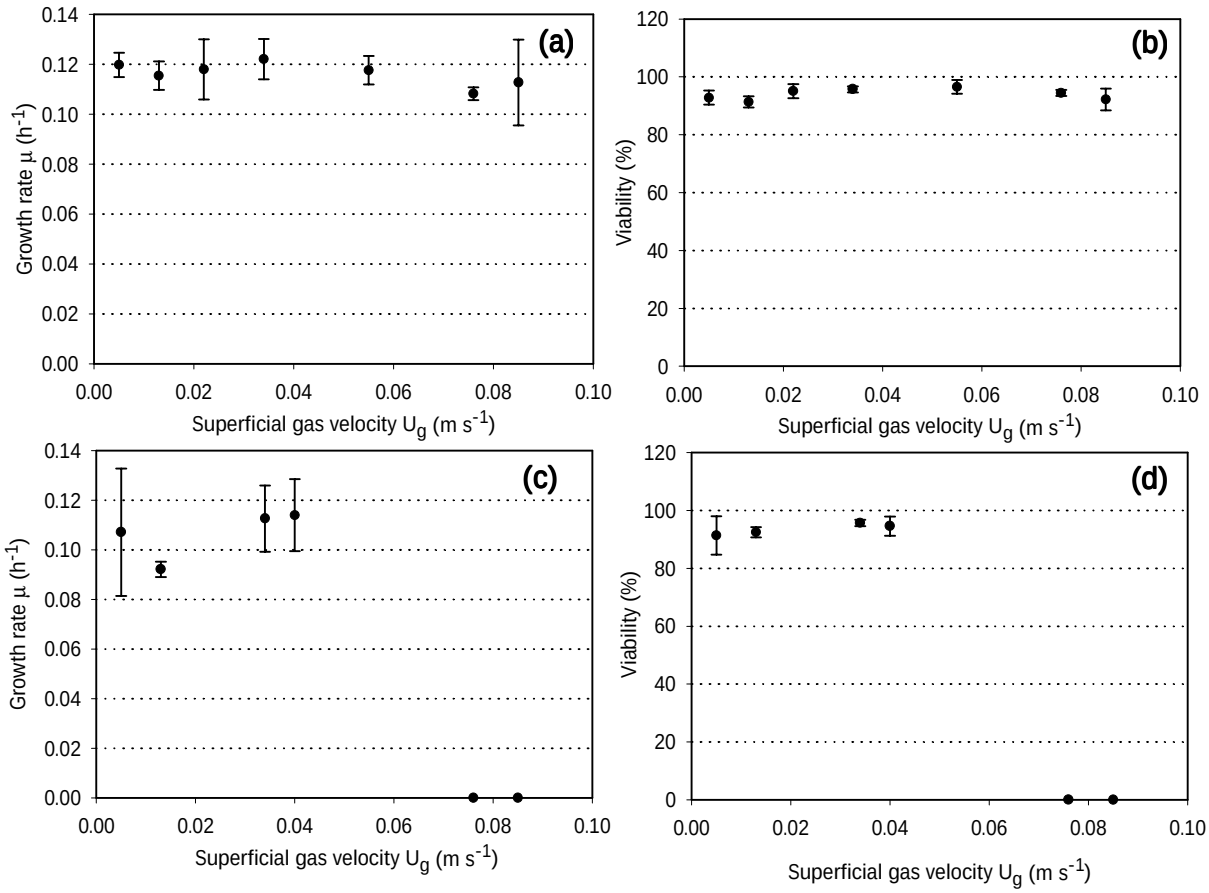

Figure 3.2. Growth rate and viability of *C. reinhardtii* wild type (a) and (b) and cell wall deficient mutant (c) and (d) grown under different superficial gas velocities (U_g). Experiments were done in bench-scale bubble columns, operated as a turbidostat. Error bars represent 95% confidence intervals calculated from four independent measurements.

Cell damage was measured by the decrease in viable cells. The cell death rate constant, k_d, was estimated by linear regression based on Eq 3.1 as it can be seen on Figure 3.3. The cell death rate constant of *C. reinhardtii* cell wall deficient mutant was estimated at 0.46 ± 0.08 h^{-1} for U_g = 0.076 m s^{-1} and increased to 1.01 ± 0.29 h^{-1} with increasing superficial gas velocity to 0.085 m s^{-1}. This might be due to the increased frequency of bubble burst at the culture surface as suggested by Camacho et al. (2001), but it can also be due to an increase in the gas entrance velocity at the sparger as a consequence of increasing the gas flow rate without changing the number and diameter of the nozzles (Eq 3.4). This possibility was further analysed and is discussed below.

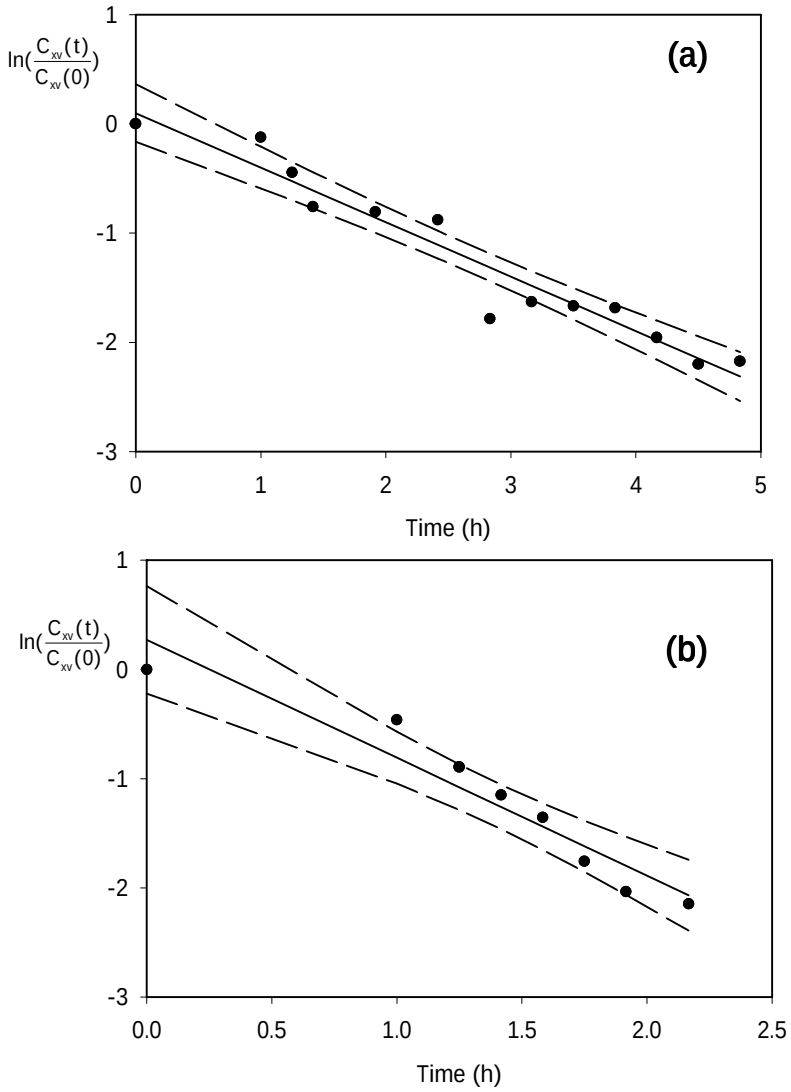

Figure 3.3. Death rate constants (k_d) estimated for *C. reinhardtii* mutant according to Eq. 3.1, at 2 different superficial gas velocities (a) 0.075 m s^{-1} and (b) 0.085 m s^{-1}. Experimental conditions and reactor set up was the same in both experiments. Experiments were done in bench-scale bubble columns, operated as a turbidostat. The parameter k_d is estimated as 0.46 ± 0.08 h^{-1} and 1.01 ± 0.29 h^{-1}: (●) experimental data; (solid line) relationship estimated by linear regression; (broken lines) 95% confidence interval.

Sparger

One possible cause for cell death at the sparger might be the hydrodynamic forces associated with the flow of fluid around a growing and detaching bubble. The maximum velocity with which the bubble penetrates into the liquid may be calculated from

$$v = \frac{F_g}{n \cdot \frac{1}{4} \cdot \pi \cdot d_i^2} \qquad \text{Eq 3.4}$$

where F_g is the volumetric gas flow rate ($m^3\ s^{-1}$), n is the number of nozzles and d_i (m) is the diameter of a nozzle. Assuming the flow around the bubble is laminar, shear stresses associated with these flows may be estimated from:

$$\tau = \eta \cdot \frac{dv}{dx} \qquad \text{Eq 3.5}$$

where η is the dynamic viscosity, and dv/dx is the velocity gradient. For the velocity gradient dv is given by the maximum injector velocity, dv. It is more difficult to estimate dx, which depends on the thickness of the boundary layer around the bubble. Tramper et al. (1986) used the diameter of a cell for dx.

Damage at the sparger site has never been considered as an important cause of cell damage in sparged bioreactors. Increasing the number of aeration nozzles from 1 to 3 (i.e., decreasing the gas jet velocity) caused a marginal reduction in the specific death rate of *D. tertiolecta*. This led to the conclusion that the events at the gas sparger had a minimal contribution to cell damage (Suzuki et al., 1995).

As already described, we tested the same and much higher superficial gas velocities (0.017 - 0.085 m s^{-1}) and no cell damage occurred (Figure 3.1) which indicates that bubble bursting alone can not be responsible for cell damage. One possible explanation for these differences could be the different gas entrance velocities. Even though the superficial gas velocities in the present work were equal or higher than the ones studied by Suzuki et al. (1995), the gas entrance velocities at the sparger in the present work (0.4–5.4 m s^{-1}) were always lower than the gas entrance velocities calculated for the work of Suzuki et al. (1995) (13–125 m s^{-1}). This is due to the higher number of nozzles used in the present work (Eq 3.4).

In order to study the possibility of significant cell damage at the sparger site, batch experiments were conducted in identical reactors, under the same superficial gas velocity (0.034 m s^{-1}) and different number of nozzles (9 and 1) (Table 3.1). In Figure 3.4 it can be seen that *D. tertiolecta* was not able to grow when 1 nozzle was used and a death rate of $0.047 \pm 0.016\ h^{-1}$ was estimated. These results clearly show that the sparger site has a significant role on cell death in sparged bioreactors and therefore should not be neglected.

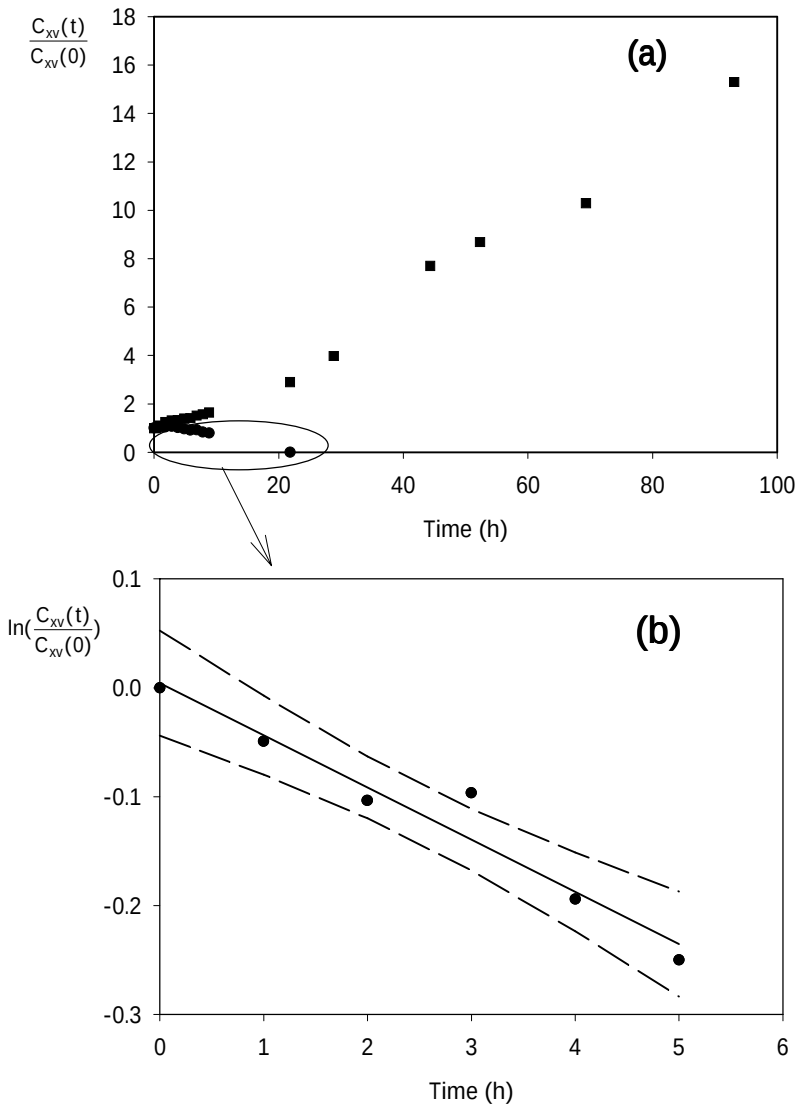

Figure 3.4. (a) Growth curves depicted as the variation in the number of viable cells of *D. tertiolecta* cultivated batch wise in a lab scale bubble column with different number of nozzles in the sparger: (●) 1 and (■) 9. Superficial gas velocity was 0.034 m s^{-1}. (b) The parameter k_d is estimated for the experiment with 1 nozzle as 0.047 ± 0.016 h^{-1}: (•) experimental data; (solid line) relationship estimated by linear regression; (broken lines) 95% confidence interval.

Table 3.1. Reactor dimensions, cultivation mode and gas entrance velocities calculated for the present work and literature studies

Strain & Data source	Reactor scale	Cultivation mode	Column diameter (m)	Column height (m)	Number of nozzles	d_i nozzles (m)	U_g (m s^{-1})	v_l (m s^{-1})	Death rate (h^{-1})
D. tertioleta	Pilot plant	Repeated batch	0.2100	2.5	21	0.00170	0.006	4.7	0
							0.016	12.7	0
							0.025	19.9	0
	Lab	Turbidostat	0.0354	0.4	16	0.00105	0.005	0.4	0
							0.008	0.6	0
							0.034	2.4	0
							0.076	5.4	0
	Lab	Batch	0.0354	0.4	9	0.00080	0.034	7.4	0
					1	0.00080	0.034	66.3	0.047±0.016[a]
C. reinhardtii (wild type)	Lab	Turbidostat	0.0354	0.4	9	0.00080	0.005	1.1	0
							0.013	2.8	0
							0.022	4.8	0
							0.034	7.4	0
							0.055	12.0	0
							0.076	16.6	0
							0.085	18.4	0
C. reinhardtii (mutant)	Lab	Turbisdostat	0.0354	0.4	9	0.00080	0.005	1.1	0
							0.013	2.8	0
							0.034	7.4	0
							0.055	12.0	0
							0.076	16.6	0.460±0.080[a]
							0.085	18.4	1.010±0.290[a]
Phaeodactylum[b]	Lab	Batch	0.080	0.5	24	0.00100	0.010	2.7	0
							0.020	5.3	0
							0.050	13.3	0
Phaeodactylum[b]	Pilot plant	Chemostat	0.193	2.1	17	0.00100	0.010	24.0	0
							0.020	47.8	[c]

[a] Values ± 95% confidence interval
[b] Data from Camacho et al. (2001)
[c] No death rates were calculated but a decrease in steady state biomass concentration was reported due to destruction of the cells

Bubble rising and Scale up

Different results have been reported regarding scale-up and shear. Camacho et al. (2000) reported an increase in death rate with increasing culture height due to more attachment of cells to the bubbles, which eventually will break up leading to the death of the attached cells. This result suggests that at large scale minimization of sparging-related death means minimizing reactor height. This is in direct conflict with the design recommendations of Tramper and Vlak (1988) who recommended maximisation of reactor height for optimal large scale reactors and is supported by the results found by Suzuki et al. (1995) where an increase in death rate of *D. tertiolecta* was observed with decreasing reactor height. It is still unclear if bubble rising contributes to cell damage. How to scale up minimizing sparging-related death is still controversial for microalgae cultivations.

D. tertiolecta was grown in a pilot plant bubble column under 3 different superficial gas velocities (0.006, 0.016 and 0.026 m s^{-1}). The results obtained with repeated batch cultivations are depicted in Figure 3.5a. Viability was always above 95% and no cell damage was observed. The volumetric productivity obtained was highest at the highest superficial gas velocity (0.026 m s^{-1}) (Figure 3.5b), which might have been due to a decrease in the liquid cycle time leading to a better light supply and utilisation by the algae.

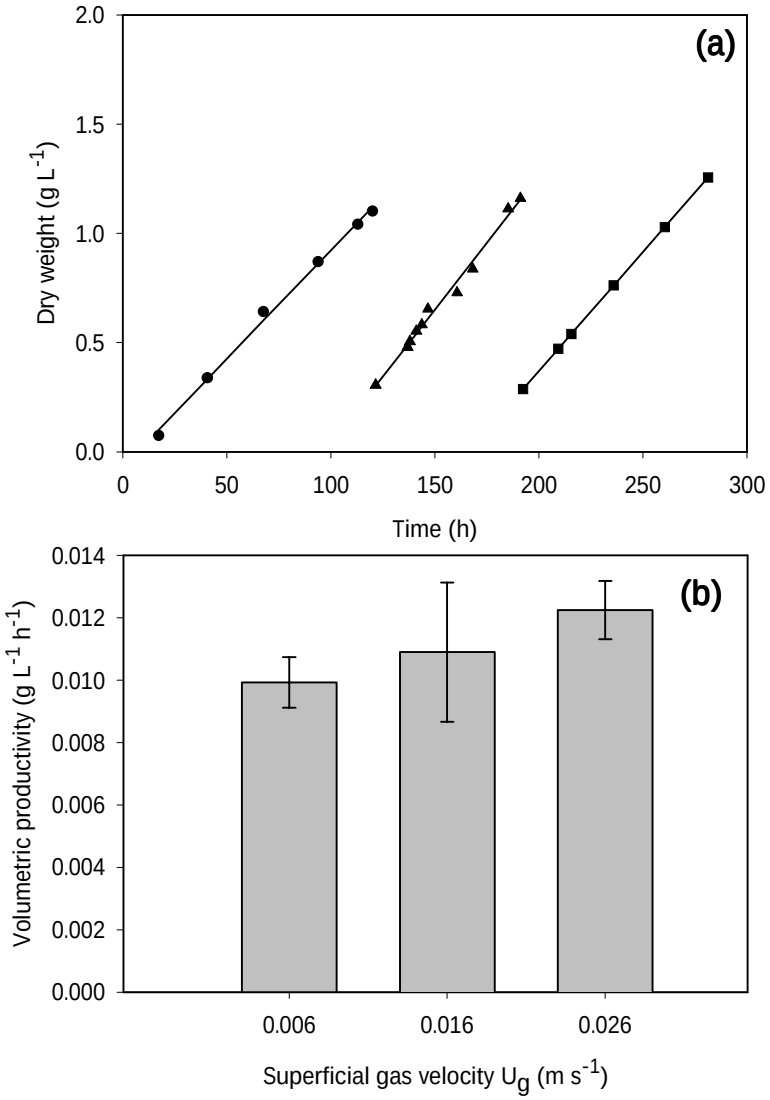

Figure 3.5. (a) Increase in viable cells of *D. tertiolecta* cultivated in repeated batch mode in the pilot plant bubble column under different superficial gas velocities: (●) 0.006 m s^{-1}; (■) 0.016 m s^{-1}; (▲) 0.026 m s^{-1}; (solid line) relationship estimated by linear regression and (b) volumetric productivity calculated for each superficial gas velocity, error bars represent 95% confidence interval.

Camacho et al. (2001) obtained different results for lab and large bubble columns experiments while using similar spargers and superficial gas velocities. In Table 3.1 the entrance gas velocities at the sparger calculated (Eq 3.4) for both lab and pilot plant bubble columns used by Camacho et al. (2001) can be found. The small difference in the number of nozzles at the spargers (24 nozzles in the lab bubble column in comparison to the 17 nozzles in the pilot plant bubble column), the same nozzle diameter and a much higher gas flow rate in the pilot plant bubble column lead to large differences in the gas entrance velocities (Table 3.1). The gas entrance velocity at the sparger of the lab bubble column was maximal at a superficial gas velocity of 0.05 m s^{-1} (ν = 13.3

m s^{-1}) but it was still 2 times lower than the gas velocity at the sparger of the pilot plant with a superficial gas velocity of 0.02 m s^{-1} (47.8 m s^{-1}). This could be a reason for the discrepancy found between lab experiments, where no cell damage was found up to a superficial gas velocity of 0.05 m s^{-1}, and pilot plant scale experiments with cell damage at a superficial gas velocity of 0.02 m s^{-1}.
In the present work the gas entrance velocities at the sparger of the pilot plant bubble column were lower than the one that caused cell damage in lab scale and no cell death was observed in the pilot plant experiments. In the only experiment where cell damage of *D. tertiolecta* occurred (Figure 3.4) only one nozzle was used and the gas velocity at the sparger was 3 times higher than the highest used in all other experiments (66.3 in comparison to 19.9 m s^{-1}).
These results show that cell damage in sparged bioreactors can occur at the sparger site and gas entrance velocity may become an important parameter for photobioreactor design and scale-up for microalgae cultivation. Increasing the number or the internal diameter of nozzles could be a simple solution for cell damage in sparged bioreactors, whenever high superficial gas velocities need to be used. This can be easily deducted from Figure 3.6 where the effect of diameter and number of nozzles in the gas entrance velocity at the sparger can be seen for a certain reactor configuration.

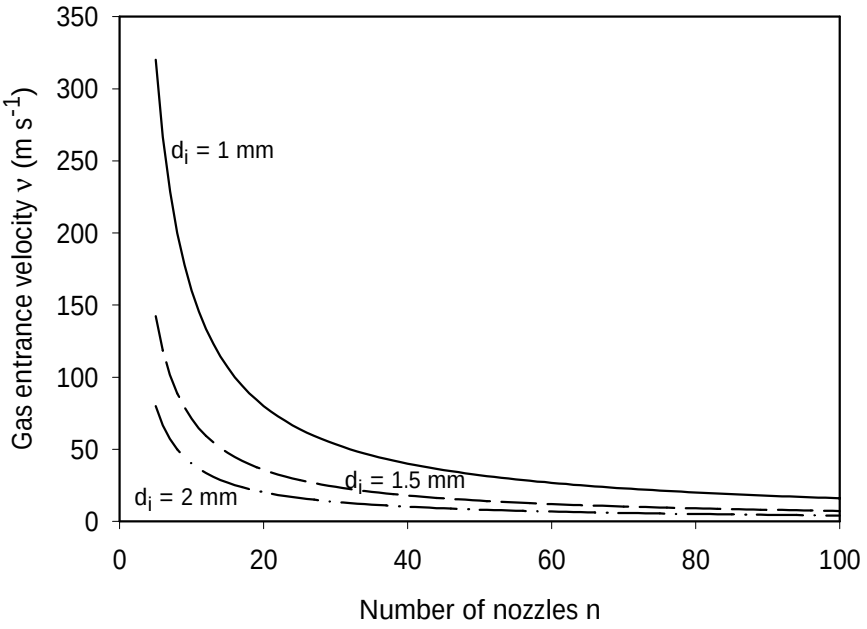

Figure 3.6. Effect of diameter and number of nozzles on the gas entrance velocity at the sparger, calculated with Eq 3.4: (dash-dot line) d_i = 0.002 m; (short dash); d_i = 0.0015 m; (thin solid line) d_i = 0.001 m. The superficial gas velocity (U_g) was assumed 0.04 m s^{-1} and the reactor radius (r) was 0.1 m.

Conclusions

Cell damage in gas sparged photobioreactors was proven to be strain dependent and the cell wall was confirmed to provide protection against hydrodynamic shear.

Superficial gas velocity alone cannot be used to estimate cell damage in sparged microalgae cultures, which means that bubble bursting is not the only factor and might not even be the most important factor leading to cell death. The sparger site was proven to have a major effect on cell damage and the gas entrance velocity should be considered as a possible indication of cell death. More work still needs to be done in order to clarify the influence of this parameter on cell death and its applicability as a reactor-design and scale-up tool for different microalgae strains.

Nomenclature

A	column cross sectional area	[m]
C_{xv}	viable cell concentration	[cells m^{-3}]
d_b	bubble diameter	[m]
d_i	nozzle internal diameter	[m]
F_g	gas flow rate	[m^3 s^{-1}]
g	gravitational acceleration	[m s^{-2}]
h_d	liquid dispersion height	[m]
K_d	cell death rate	[h^{-1}]
n	number of nozzles	[-]
P_h	pressure in the headspace	[Pa]
Q_m	molar gas flow rate	[mol s^{-1}]
R	gas constant	[J K^{-1} mol^{-1})
r	column radius	[m]
T	absolute temperature	[K]
t	time	[h]
U_g	superficial gas velocity	[m s^{-1}]
V_k	hypothetical killing volume	[m^3]
V	culture volume	[m^3]
µ	specific growth rate	[h^{-1}]
ρ	liquid density	[Kg m^{-3}]
v	bubble velocity at the sparger	[m s^{-1}]

η	dynamic viscosity	[N s m^{-2}]
τ	shear stress	[N m^{-2}]

4 Overcoming shear stress of microalgae cultures in sparged photobioreactors

Abstract

In the present work we identified and quantified the effect of hydrodynamic stress on 2 different microalgae strains, *D. tertiolecta* and *D. salina*, cultivated in bench-scale bubble columns. The cell-death rate constant increased with increasing gas-entrance velocity at the sparger. *D. salina* was slightly more sensitive than *D. tertiolecta*. The critical gas-entrance velocities were approximately 50 and 30 m s^{-1} for *D. tertiolecta* and *D. salina*, respectively.

The effects of gas-flow rate, culture height and nozzle diameter on the death-rate constant were also studied. From these results it was concluded that bubble rising and bubble bursting are not responsible for cell death. Regarding nozzle diameter, small nozzles were more detrimental to cells.

The bubble formation at the sparger was found to be the main event leading to cell death.

This chapter has been accepted for publication in Biotechnology & Bioengineering as: Maria J. Barbosa, Hadyianto and René H. Wijffels. Overcoming shear stress of microalgae cultures in sparged photobioreactors.

Introduction

Power input is necessary in sparged photobioreactors, such as bubble columns and flat panels, for mixing, heat elimination and mass and light transfer. Its importance increases with scale-up. However, it can also lead to shear, which can have as consequence impaired cell growth, cell damage and eventually cell death.

High superficial-gas velocities are desirable in microalgae cultivations in order to create a high degree of turbulence allowing a fast circulation of the cells from the dark to the light zone of the reactor. These fast liquid-circulation times (on a µ-ms scale) have been shown to give rise to considerable higher photosynthetic efficiency (Kok, 1953; Matthijs et al., 1996) than longer cycles which can even lead to a decrease in the photosynthetic efficiency (Janssen et al., 2000a; 2001). Janssen et al. (2003) reported that the average liquid circulation time in vertical bubble columns will be between 0.5 and 2 s at superficial-gas velocities of 0.05 m s^{-1} or higher. These calculations were based on the model of Joshi and Sharma (1979). Very high superficial-gas velocities are thus required in order to achieve high productivities in bubble columns.

According to Gudin and Chaumont (1991), the key problem of microalgae cultivation in photobioreactors is cell damage due to shear stress. However, few quantitative studies have been done to characterise algal cells with respect to their shear sensitivity and within these few works, very different types of equipment, methodology and reactor configurations have been used (Bronnemeier and Markl, 1982; Silva et al., 1987).

The growth rates of some microalgae have been reported to increase initially with increasing turbulence, probably due to the improved supply of CO_2 or light. But upon an optimum level of turbulence, the growth decreases sharply with further increase of the superficial-gas velocity (Silva et al., 1987; Suzuki et al., 1995; Merchuk et al., 2000). These results, i.e. an increase in cell damage with increasing superficial-gas velocity, led to the conclusion that algae death was mainly due to the bursting of the bubbles at the surface. But in reality, it could also have been due to the bubble formation, as it will be further explained and discussed.

The effect of hydrodynamic forces generated by air bubbles on animal cells in suspension has been extensively studied (Tramper et al., 1988; Chalmers, 1996). Tramper et al. (1986) distinguished 3 regions in a bubble column where cell death might occur: (1) at the sparger where the bubbles are formed, (2) in the region where the bubbles rise, and (3) at the surface where bubble disengagement occurs.

Cell-death rate can be described by first order kinetics as described by Eq 4.1, provided that the cell-growth rate is zero or negligible compared to the cell-death rate.

$$\ln\left(\frac{C_{Xv}(t)}{C_{Xv}(0)}\right) = -k_d \cdot t \qquad \text{Eq 4.1}$$

where $C_{xv}(t)$ and C_{xv} (0) are the viable-cell concentration (cell m^{-3}) at time t = t and t = 0 (h) respectively, k_d is the first-order death-rate constant (h^{-1}) and t is the time (h).

Tramper et al. (1988) proposed a model for cell damage caused by sparging, in which a hypothetical-killing volume is associated with each air bubble during its live time. This model has been validated for insect cells and hybridomas in bench-scale bubble columns (Jobses et al., 1991; Tramper et al., 1988). Jobses et al. (1991) further elaborated the model by specifying it for each event (bubble formation, bubble rising and bubble break-up) to yield verifiable correlations between the cell-death rate and particular culture parameters. It was found the specific death-rate constant will be independent of culture height if bubble rising is the cause of cell death (at a constant reactor cross sectional area and a constant bubble size). If the bubble formation at the sparger is the cause, the specific death rate will increase with decreasing number of nozzles, i.e. with increasing gas-entrances velocities (provided that the total gas-flow rate, bubble size, orifice diameters and culture volumes are constant). Finally, if bubble break up at the liquid surface is the cause the death rate will be proportional to the gas- flow rate per unit volume (at constant fluid viscosity, surface tension and bubble size).

In order to scale-up photobioreactors minimising cell damage it is also necessary to have knowledge on the effect of culture height on cell damage. Suzuki et al. (1995) found a linear correlation between the specific death rate and the inverse of culture height while Camacho et al. (2000) reported the inverse behaviour: an increase in culture height resulted in an increase in death rate. The authors related the effect of fluid height to cell attachment to bubbles: a greater culture height means that more cells can be captured by the rising bubbles and carried to the surface where cells die as the bubbles rupture. Camacho et al. (2001) reported that the microalgae *Phaeodactylum tricornutum* is sensitive to hydrodynamic stress in bubble columns and that the break-up of small bubbles on the liquid surface seems to be the cause of cell damage ($0.01 < U_g < 0.05$ m s^{-1}). The same authors found that hydrodynamic conditions, which do not promote cell damage in the laboratory-scale, could not be extrapolated to pilot-scale, while using similar spargers and superficial-gas velocities. These results show that there is still a lack of knowledge on how to minimise cell damage when scaling up.

In our previous work, the effect of high superficial-gas velocities (0.06 – 0.085 m s^{-1}) on *Dunaliella tertiolecta*, *Chlamydomonas reinhardtii* wild type and cell-wall lacking mutant, cultivated in bench-scale and pilot plant bubble columns was studied (Barbosa et al., 2003b). The range of superficial-

gas velocities studied included values that are thought to lead to higher photosynthetic efficiencies due to the fast liquid-circulation times that they originate (Janssen et al., 2003). The increase of superficial-gas velocity had no effect on the growth rate and viability of *D. tertiolecta* and *C. reinhardtii* wild type. These results and literature analysis indicated that the main parameter causing cell death was the gas-entrance velocity at the sparger.

In the present work we identified and quantified the effect of hydrodynamic stress on 2 different microalgae strains, *D. tertiolecta* and *D. salina*, cultivated in bench-scale bubble columns. After reaching a certain critical gas-entrance velocity, which was strain dependent, a further increase of the gas-entrance velocity led to an increase in the cell-death rate.

The effect of superficial-gas velocity, culture height and nozzle diameter on the death-rate constant was also studied. From these results it was concluded that bubble rising and bubble bursting are not responsible for cell death. Regarding nozzle diameter, small nozzles were more detrimental to cells.

The bubble formation at the sparger was found to be the main event leading to cell death.

Materials and Methods

Organism and culture medium

Dunaliella tertiolecta CCAP 19/6B was obtained from the Culture Collection of Algae and Protozoa (Oban, UK). *D. tertiolecta* was cultivated in artificial seawater medium (ASW) composed of (quantities in g L^{-1}): NaCl, 24.5; $MgCl_2 \cdot 6H_2O$, 9.8; $CaCl_2 \cdot 2H_2O$, 0.53: Na_2SO_4, 3.2; K_2SO_4, 0.85. The following nutrients were added (quantities in mmol L^{-1}): KNO_3, 16.0; $NaH_2PO_4 \cdot 2H_2O$, 1.0; $NaHCO_3$, 5.0. Also the following trace elements were added (quantities in µmol L^{-1}): $Na_2EDTA \cdot 2H_2O$, 61.6; $FeCl_3 \cdot 6H_2O$, 23.3; $CuSO_4 \cdot 7H_2O$, 0.210; $ZnSO_4 \cdot 7H_2O$, 0.303; $CoCl_2 \cdot 6H_2O$, 0.085; $MnCl_2 \cdot 4H_2O$, 1.83; Na_2MoO_4, 0.052.

Dunaliella salina CCAP 19/18 was obtained from the Culture Collection of Algae and Protozoa (Oban, UK). *D. salina* was cultivated in the same medium composition as *D. tertiolecta* with only a higher salinity (58.6 g L^{-1} NaCl).

D. tertiolecta and *D. salina* were maintained as pure suspended culture in 250 mL-Erlenmeyer flasks containing 50 mL of medium. The cultures were kept at 20ºC, under a light intensity of 50 - 70 µmol m^{-2} s^{-1} and a 16/8 h light/dark cycle. Every three weeks 0.5 mL of a culture was transferred to a new flask containing fresh medium. The 3 week old cultures were used to

inoculate the bubble columns that ran as chemostats. The inoculums for the sparging experiments were samples taken from the chemostat culture.

Cultivation system

D. tertiolecta and *D. salina* were cultivated in identical lab scale bubble columns with an inner diameter of 0.0358 m and a height of 0.725 m (top and bottom not included).

The bubble columns were equipped with a water jacket connected to a temperature-controlled water bath operated at 30ºC for *D. tertiolecta* and 25ºC for *D. salina*. pH was maintained between 7.70 - 7.85 by adding pulses of carbon dioxide to the air. The air flow rate was controlled with a mass flow controller (5850E, Brooks Instrument BV, The Netherlands).

Light was continuously provided by 10 fluorescent light tubes (LYNX LE, 55W, Sylvania, Germany) placed at one side of the reactor and a mirror placed at the opposite side. The ingoing photon-flux density (PFD) was measured at 8 different spots inside the reactor with a LI-190SA 2π PAR-sensor, (LI-COR, Lincoln, NE, USA) and an average light intensity of 240 μmol m^{-2} s^{-1} was calculated from 8 different measurements along the column.

The inoculums for these batch experiments were samples taken from a chemostat culture (dilution rate was 0.030 h^{-1} and 0.015 h^{-1} for *D. tertiolecta* and *D. salina*, respectively), run under the same pH and temperature as in the experiments of the corresponding strain. The working volume was 3.5 L, the average incident light intensity was 77 μmol m^{-2} s^{-1} and the gas flow rate was 1.76 L min^{-1}. These samples were diluted to an OD_{530} of 0.4 – 0.5 before starting the experiments.

The sparger was a piece of silicon in which needles were inserted. The number (1 to 9) and internal diameter of the needles (0.4, 0.8 and 1.2 mm) varied in different experiments according to Table 4.1.

The superficial-gas velocity (U_g) was varied in different experiments by varying the gas flow rate (F_g) (Table 4.1) and it was calculated according to Eq 4.2.

$$U_g = \frac{F_g}{\pi \cdot r^2} \qquad \text{Eq 4.2}$$

where F_g is the volumetric gas flow rate (m^3 s^{-1}) and r is the column radius (m).

Different gas-entrance velocities (v) were obtained by varying the nozzle diameter, number of nozzles or gas flow rate (Table 4.1). Gas-entrance velocity was calculated according to Eq 4.3.

$$\nu = \frac{F_g}{n \cdot \frac{1}{4} \cdot \pi \cdot d_i^2} \qquad \text{Eq 4.3}$$

where F_g is the volumetric gas flow rate ($m^3\ s^{-1}$), n is the number of nozzles and d_i (m) is the diameter of a nozzle.

The culture height was varied by changing the culture volume (0.25, 0.35 and 0.5 L). The correspondent culture heights can be seen in Table 4.1.

Measurements

Cell concentration

Cells were counted and measured with the coulter counter Multisizer II (Beckman Coulter, The Netherlands)

The optical density of the algal suspensions was measured at an absorbance of 680 and 530 nm on a spectrophotometer (Spectronic® 20 Genesys, Spectronic Instruments, UK) against a reference of artificial seawater (ASW).

Viability

Cell viability was determined by staining the culture with fluorescein diacetate (FDA) and analysing it in a flow cytometer (FACScan; Becton Dickinson BV, The Netherlands). On the basis of green and red fluorescence viable and dead cells, respectively could be discriminated.

Results and Discussion

Experiments were performed with cells obtained from a steady-state chemostat culture with a viability of 90-100%, to ensure that their physiological state was equal at the start of every shear-stress experiment. Each experiment was performed within a time span of 6 hours to avoid interference of nutritional limitations or cell growth. In all experiments where cell death occurred, viable-cell loss was accompanied with cell lysis, which made reliable dead-cell count not possible. Therefore, cell damage was measured by the decrease in viable cells. The cell-death rate constant, k_d, was estimated by linear regression based on Eq 4.1.

Superficial-gas velocity

The effect of superficial-gas velocities in batch cultures of the strains *Dunaliella tertiolecta* and *Dunaliella salina* cultivated in bubble columns was studied. The cell death rate constants of both strains cultivated under different superficial-gas velocities are depicted in Figure 4.1. The cell death rate constant, k_d, increased from 0.33 ± 0.06 to 1.05 ± 0.09 h^{-1} and from 0.34 ± 0.05 to 1.62 ± 0.29 h^{-1} for *D. tertioleca* and *D. salina*, respectively with increasing superficial-gas velocity from 0.029 to 0.052 m s^{-1}. This could represent a limitation to achieve high photosynthetic efficiencies in bubble columns, as superficial-gas velocities equal or higher than 0.05 m s^{-1} are desirable in order to attain short light dark cycles (Janssen et al., 2003).

This might have been due to the increased frequency of bubble burst at the culture surface as suggested by Camacho et al. (2001), but it can also be due to an increase in the gas-entrance velocity at the sparger as a consequence of increasing the gas flow rate without changing the number and diameter of the nozzles (Eq 4.3), as previously indicated by Barbosa et al. (2003). This possibility was further analysed and is discussed below.

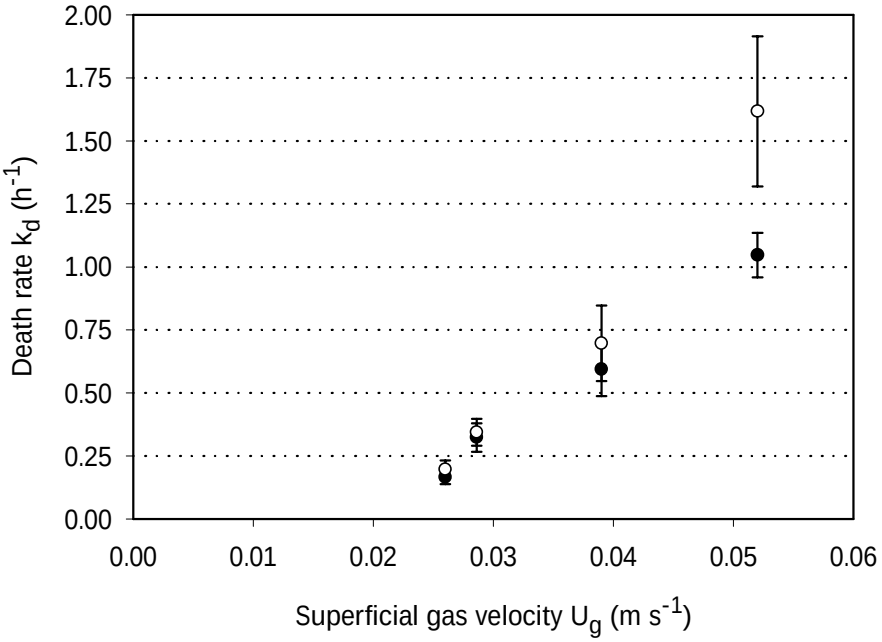

Figure 4.1. First-order death-rate constant, k_d, of (●) *D. tertiolecta* and (○) *D. salina* as a function of superficial-gas velocity (U_g). Experiments were done in bench-scale bubble columns, run batch wise. One nozzle with an internal diameter of 0.8 mm was used and culture height was 0.35 m. Error bars represent 95% confidence intervals.

Gas-entrance velocity at the sparger

The bubble-formation process at the sparger can be separated into two stages. In the first stage the bubble expands, while staying attached to the nozzle. In the second stage the buoyancy forces

cause the bubble to move away from the nozzle. Bubble growth continues through a narrowing neck connecting the bubble to the nozzle. When this neck closes and the bubble detaches from the nozzle, fluid rushes in to the region of the bubble neck. Cell death at the sparger may have two causes: the direct contact of the cell with a rapid expanding bubble surface or due to the local liquid flows around a growing and detaching bubble. The maximum velocity with which the bubble penetrates into the liquid may be calculated from Eq 4.3.

Damage at the sparger site has never been considered by other authors as an important cause of cell damage in sparged bioreactor for microalgae cultures. It has been assumed until now that the main cause for cell damage was the bubble bursting at the liquid surface (Suzuki et al., 1995; Camacho et al. 2001).

In order to study the possibility of significant cell damage at the sparger site, batch experiments were conducted in identical reactors, at the same superficial-gas velocity (0.052 m s^{-1}) and different gas-entrance velocities (20.9 to 104.4 m s^{-1}), obtained by varying the number of nozzles (Table 4.1). In Figure 4.2 the cell death rate constants for both *D. tertiolecta* and *D. salina* are depicted as a function of gas-entrance velocity. The cell death rate constant clearly increased with increasing the gas-entrance velocity for both strains.

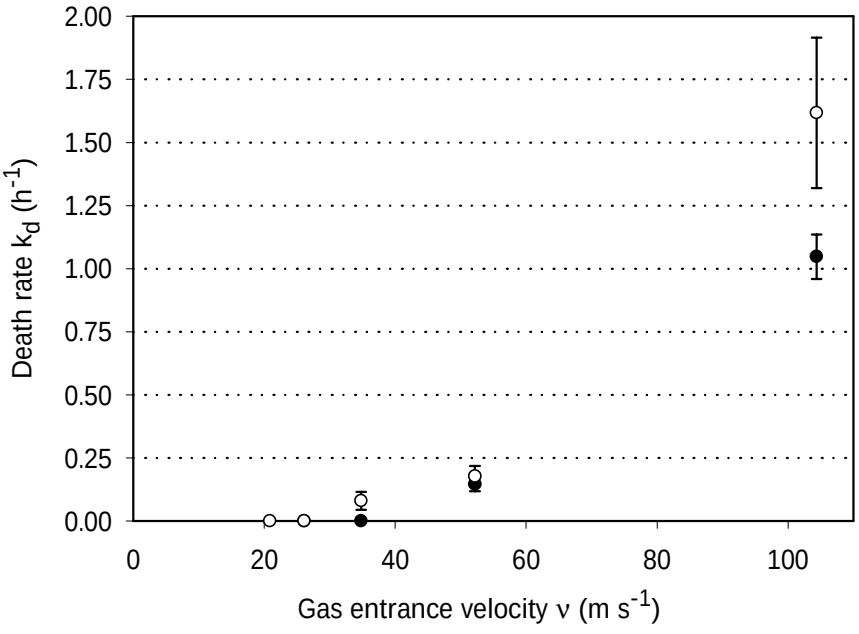

Figure 4.2. First-order death-rate constant, k_d, of (●) *D. tertiolecta* and (○) *D. salina* as a function of gas-entrance velocity (ν). Experiments were done in bench-scale bubble columns, run batch wise. Superficial-gas velocity was 0.052 m s^{-1}, the nozzles had an internal diameter of 0.8 mm and culture height was 0.35 m.. Error bars represent 95% confidence intervals.

Table 4.1. Experimental design and death rate constants obtained at each experiment for the strains *D. tertiolecta* and *D. salina*.

Number of nozzles n (-)	Nozzle diameter d_i (mm)	Culture heigh H (m)	Superficial gas velocity U_g (m s^{-1})	Gas-entrance velocity ν (m s^{-1})	***D. tertiolecta*** Death rate k_d (h^{-1}) [b]	***D. salina*** Death rate k_d (h^{-1}) [b]
1	0.8	0.35	0.029	57.4	0.33 ± 0.06	0.34 ± 0.05
			0.039	78.3	0.59 ± 0.11	0.70 ± 0.15
			0.052	104.4	1.05 ± 0.09	1.62 ± 0.30
			0.026	52.2	0.17 ± 0.03	0.20 ± 0.04
	0.8	0.50	0.039	78.3	0.34 ± 0.04	- [a]
	0.8	0.25	0.039	78.3	0.88 ± 0.10	- [a]
	0.4	0.35	0.010	78.3	0.76 ± 0.02	- [a]
	1.2	0.35	0.088	78.3	0.51 ± 0.05	- [a]
2	0.8	0.35	0.029	28.7	0 [c]	0.05 ± 0.01
			0.039	39.1	0 [c]	0.09 ± 0.01
			0.052	52.2	0.14 ± 0.03	0.18 ± 0.04
			0.078	78.3	0.70 ± 0.03	0.76 ± 0.13
			0.057	57.4	0.31 ± 0.04	0.42 ± 0.04
3	0.8	0.35	0.029	19.1	0	- [a]
			0.039	26.1	0	- [a]
			0.052	34.8	0 [c]	0.08 ± 0.04
			0.078	52.2	0.25 ± 0.05	0.26 ± 0.08
4	0.8	0.35	0.029	14.4	0	- [a]
			0.039	19.6	0	0
			0.052	26.1	0	- [a]
5	0.8	0.35	0.052	20.9	- [a]	0
9	0.8	0.35	0.012	2.6	0 [c]	- [a]

[a] Experiment not performed

[b] k_d ± 95 % confidence interval

[c] Growth rates were calculated (Figure 4.5)

To further verify the effect of gas-entrance velocity on cell-death rate, experiments were conducted, maintaining the gas-entrance velocity constant (52.18 m s^{-1}) and varying the superficial-gas velocity between 0.026 and 0.078 m s^{-1}. It can be seen in Figure 4.3 that the cell-death rate remained almost constant with increasing superficial-gas velocity, which proves that the gas-entrance velocity is the main cause for cell damage and that bubble bursting is not

responsible for cell death. This means that high superficial-gas velocities could be used in bubble columns in order to obtain short circulation times, without leading to cell damage.

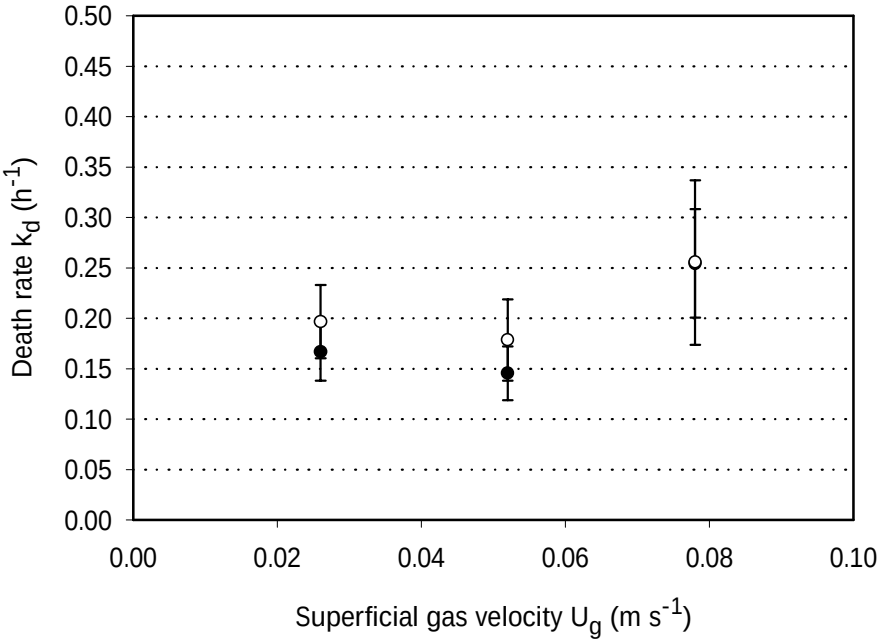

Figure 4.3. First-order death-rate constant, k_d, of (●) *D. tertiolecta* and (O) *D. salina* as a function of superficial-gas velocity (U_g), determined at a constant gas-entrance velocity (v = 52.2 m s^{-1}). Experiments were done in bench-scale bubble columns, run batch wise. The nozzles had an internal diameter of 0.8 mm and culture height was 0.35 m. Error bars represent 95% confidence intervals.

The death rate constants, k_d, obtained in all experiments are plotted in Figure 4.4 as a function of gas-entrance velocity. For both strains, the cell death rate constant increased with increasing gas-entrance velocity. It seems to be a critical gas-entrance velocity above which cell death occurs. This critical value was strain dependent, approximately 50 m s^{-1} for *D. tertiolecta* and 30 m s^{-1} for *D. salina,* which shows that cell damage in gas sparged photobioreactors is strain dependent and *D. salina* is more shear sensitive than *D. tertiolecta.* The differences in sensitiveness between these two strains might be due to differences in fluid viscosity (due to differences in salt concentration), morphology (e.g. cell size, shape) and physiology. Shear stress can be avoided, if the critical value for the strain of interest is known, by properly designing the sparger in order to keep the gas entrance velocity below the critical value.

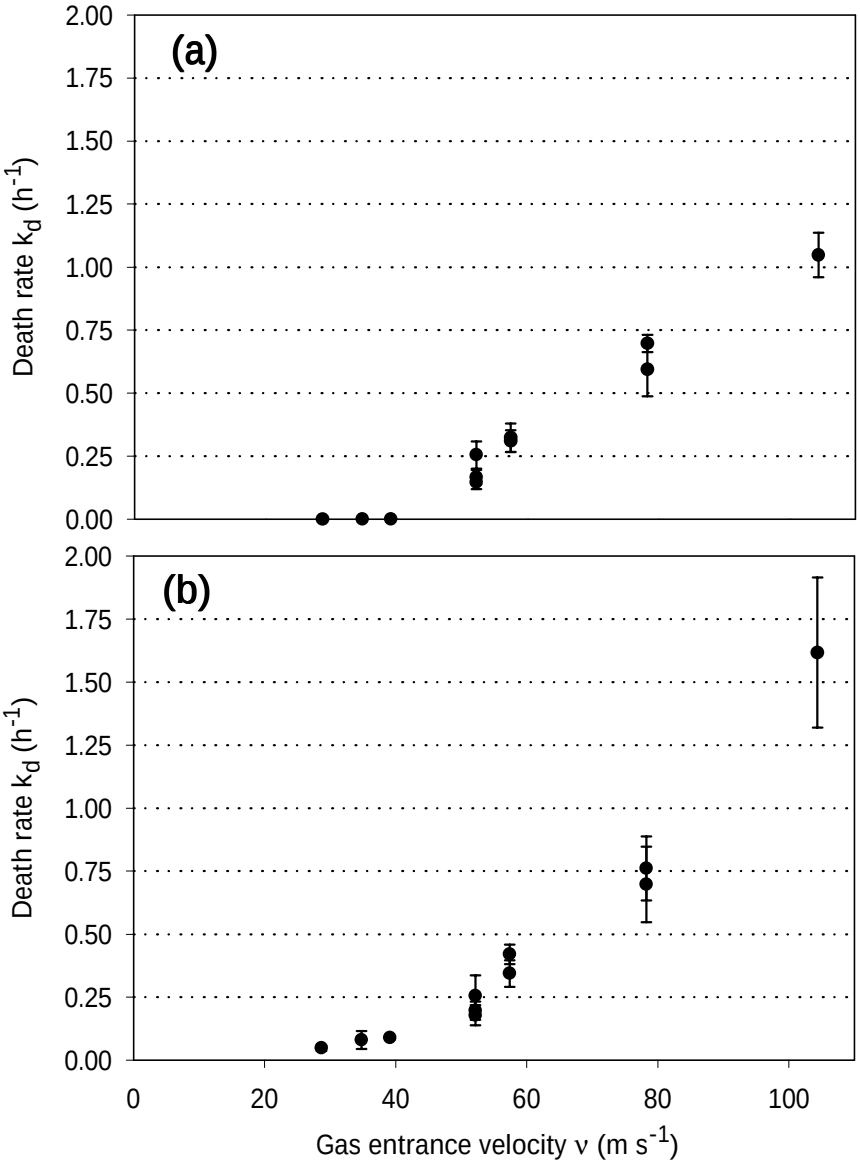

Figure 4.4. First-order death-rate constant, k_d, of (a) *D. tertiolecta* and (b) *D. salina* as a function of the gas-entrance velocity (ν). The superficial-gas velocity (U_g) and number of nozzles (n) varied between 0.010 - 0.078 m s^{-1} and 1-9, respectively. Experiments were done in bench-scale bubble columns, run batch wise. The nozzles had an internal diameter of 0.8 mm and culture height was 0.35 m. Error bars represent 95% confidence intervals.

The growth rates and viability of *D. tertiolecta* at the four lowest gas-entrance velocities at which no cell death occurred (2.56, 28.7, 34.8 and 39.1 m s^{-1}) were measured and are plotted in Figure 4.5. A slight and apparently not significant decrease of growth rate can be seen, while viability was still high (> 70%). This means that an increase in gas-entrance velocity may lead to a slight decrease in growth rate before reaching the critical value at which cell death started to occur.

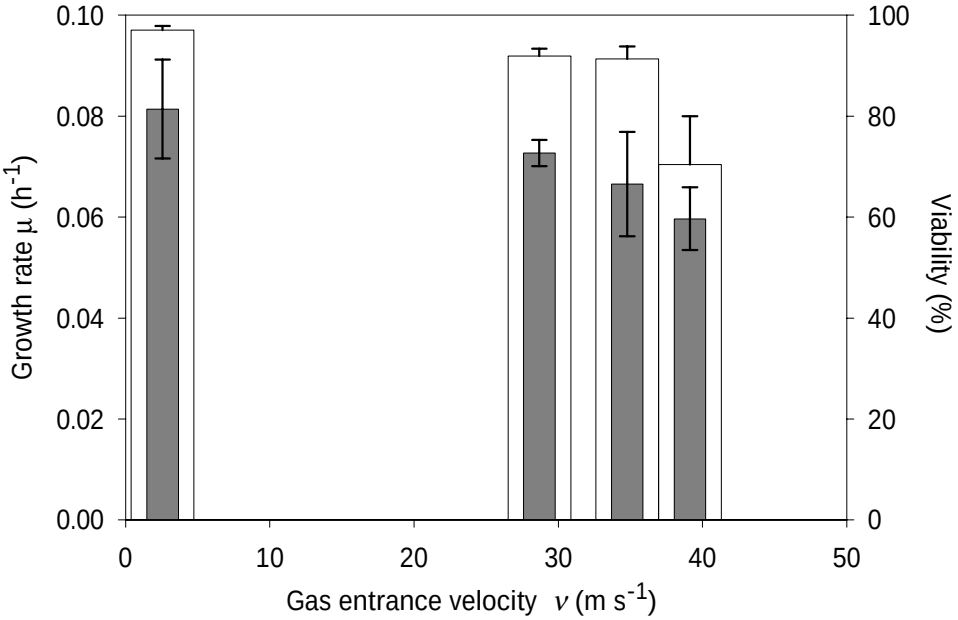

Figure 4.5. Growth rate, μ (grey bars) and viability (white bars) of *D. tertiolecta* as a function of gas-entrance velocity. Error bars represent 95% confidence intervals.

Culture height

Different results have been reported regarding scale-up by increasing culture height and shear. Camacho et al. (2000) reported an increase in death rate with increasing culture height due to more attachment of cells to the bubbles, which eventually will break up leading to the death of the attached cells. This result suggests that at large scale minimization of sparging-related death means minimizing reactor height. This is in direct conflict with the design recommendations of Tramper and Vlak (1988) who recommended maximisation of reactor height for optimal large-scale reactors for animal cells cultivation and is supported by the results found by Suzuki et al. (1995) where an increase in death rate of the microalgae *D. tertiolecta* was observed with decreasing reactor height. Our results are in agreement with Suzuki et al. (1995) and support the design recommendations of Tramper and Vlak (1988). A decrease in the specific death rate was observed with increasing culture height for *D. tertiolecta* (Figure 4.6). As described by Jobses et al. (1991), this means that bubble rising is not the cause for cell damage and that high photobioreactors should be used to minimise cell death.

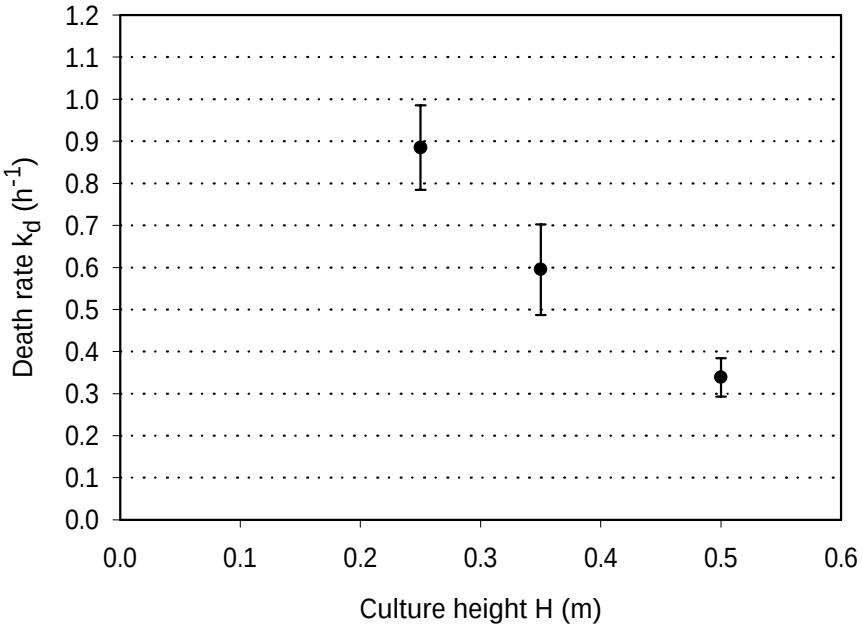

Figure 4.6. First-order death-rate constant, k_d, of *D. tertiolecta* as a function of culture height (H), determined at a constant gas-entrance velocity (v = 78.3 m s^{-1}) and superficial-gas velocity (U_g = 0.039 m s^{-1}). Experiments were done in bench-scale bubble columns, run batch wise. The nozzles had an internal diameter of 0.8 mm. Error bars represent 95% confidence intervals.

Nozzle diameter

Varying the internal diameter of nozzles may lead to differences in bubble sizes, which have been shown to affect the cell death rate of animal cells (Wu and Goosen, 1995; Handa et al., 1985). Wu and Goosen (1995) showed that the killing volume associated to one bubble is proportional to the bubble surface area for bubble diameters ranging from 0.5-4.5 mm, which means that big bubbles are more detrimental to cells. This differs from the findings of Handa et al. (1985) who reported that smaller bubbles (below 2 mm in diameter) were more hazardous on a per bubble basis, which can be explained by the fact that the forces associated with the bubble rupture at the liquid surface increase exponentially with decreasing bubble size (Wu, 1995). These studies and consequent explanations of the results were made assuming that cell death occurs at the liquid surface, which has been proven to be the main cause for animal-cell death in bioreactors. However, for microalgae cells, we have shown that cell death takes place at the sparger and the effect of bubble size on cell death has never been related to the bubble formation at the sparger.

The effect of nozzle diameter, which varied between 0.4 and 1.2 mm, at a constant gas-entrance velocity (78.3 m s^{-1}), on the cell death rate of *D. tertiolecta* can be seen in Figure 4.7. Bubble size was not measured but visual observation clearly showed that the bubbles formed from the nozzles with a smaller diameter (0.4 mm) were smaller than the ones formed from the larger nozzles (0.8

and 1.2 mm). No clear differences could be seen between the bubbles formed from the nozzles with diameters of 0.8 and 1.2 mm. From Figure 4.7 it can be seen that the smallest bubbles led to the highest specific death rate. Whether this is due to the small bubble size or due to the small diameter of the orifice itself is not known. This could also be due to an increase in the frequency of bubbles generated per nozzle. The frequency of bubble generation (f) increases with increasing gas-flow rate and decreasing bubble diameter as can be seen in Eq 4.4.

$$f = \frac{6 \cdot F_g}{\pi \cdot d_b^{\,3}} \qquad \text{Eq 4.4}$$

The gas-flow rate was lowest during the experiments with the smallest nozzle (Table 4.1) but the decrease in the frequency of bubble generation due to the low gas-flow rate can be easily compensated with the decrease in the bubble size, resulting in a net increase of bubble frequency per nozzle (Eq 4.4).

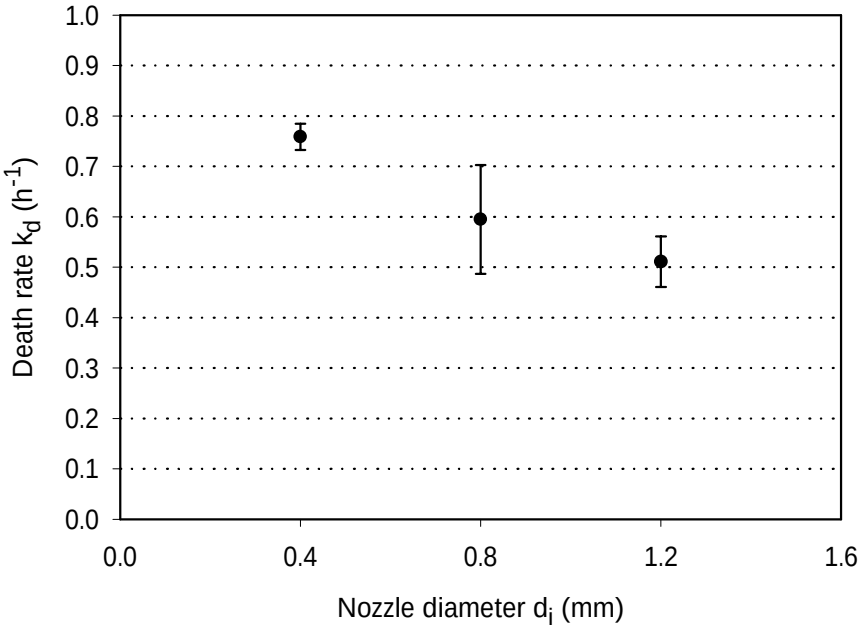

Figure 4.7. First-order death-rate constant, k_d, of *D. tertiolecta* as a function of nozzle diameter (d_i), determined at a constant gas-entrance velocity (v = 78.3 m s^{-1}) and superficial-gas velocity (U_g = 0.039 m s^{-1}). Experiments were done in bench-scale bubble columns, run batch wise. Culture height was 0.35 m. Error bars represent 95% confidence intervals.

Conclusions

It can be concluded that bubble formation is the main cause for cell death in gas-sparged photobioreactors and that gas-entrance velocity could be used as a tool for reactor design. Bubble bursting and bubble rising were proven not to contribute to cell death. Cell damage was strain dependent and each strain had a critical gas-entrance velocity above which cell death occurred.

These findings contribute to optimal design, operation and scale-up of photobioreactors in terms of minimising shear-related cell death. Based on these results, the strategy to follow, whenever a reactor needs to be scaled-up and/or high superficial-gas velocities need to be used, is to determine the critical gas velocity at the sparger for the strain of interest and to keep the gas velocity at the sparger lower than the critical value by increasing the number of nozzles or/and increasing the nozzle diameter. Nevertheless, knowledge on the flow patterns and hydrodynamic forces at the sparger as well as on the formation of a new bubble surface in combination with adsorption of cells would be of great importance for understanding events at the sparger and for a proper sparger design.

With the present work more insight was gained in cell death of microalgae grown in sparged photobioreactors. The mechanisms responsible for cell death at the sparger still need to be clarified. Study of the effect of cell concentration and viscosity on cell death rate of microalgae cells is also of great interest for high-density cultures, where a high mixing rate is a requisite to achieve high light efficiencies.

Nomenclature

C_{xv}	viable cell concentration	[cells m^{-3}]
d_i	nozzle internal diameter	[m]
d_b	bubble diameter	[m]
F_g	gas flow rate	[m^3 s^{-1}]
f	bubble generation frequency	[s^{-1}]
H	culture height	[m]
k_d	cell death rate	[h^{-1}]
n	number of nozzles	[-]
r	column radius	[m]
t	time	[h]
U_g	superficial-gas velocity	[m s^{-1}]

μ	growth rate	[h^{-1}]
ν	bubble velocity at the sparger	[m s^{-1}]

5 Optimisation of cultivation parameters in photobioreactors for microalgae cultivation using the A-stat technique

Abstract

Light availability inside the reactor is often the bottleneck in microalgal cultivation and for this reason much attention is being given to light limited growth kinetics of microalgae, aiming at the increase of productivity in photobioreactors.

Steady-state culture characteristics are commonly used for productivity optimisation and for cell physiology studies in continuous cultures, and are normally achieved using chemostat cultivations. In the present study, we investigated the applicability of a new and dynamic cultivation method called acceleration-stat (A-stat) to microalgae cultivations where light is the limiting substrate. In the A-stat the dilution rate is increased at a constant rate. This acceleration rate should be a compromise between a short cultivation time, in order to make it a fast process, and the metabolic adaptation rate of the microorganism to changes in the environment. Simulations of the A-stat were done with different acceleration rates to have an indication of the best rate to use. An A-stat was performed in a pilot plant bubble column (65 L) with *D. tertiolecta* as a model organism, and results showed that a pseudo steady state was maintained throughout the experiment. From this work, it was concluded that the A-stat can be used as a fast and accurate tool to determine kinetic parameters and to optimise any specific type of photobioreactor.

This chapter will be published as: Maria J. Barbosa, Jeroen Hoogakker and René H. Wijffels. 2003. Optimisation of cultivation parameters in photobioreactors for microalgae cultivation using the A-stat technique. Biomolecular Engineering (in press)..

Introduction

Microalgae are a natural source of high-value compounds for the pharmaceutical and food industry, such as bioactive compounds, vitamins, pigments and fatty acids. The maximisation of biomass productivity in photobioreactors is an important step for the development of microalgae biotechnology, and it implies the optimization of cultivation parameters and knowledge of the growth characteristics of the microorganism.

Light availability inside the reactor is often the bottleneck in microalgal cultivation. The light falling on the reactor surface is the only energy source for these photoautotropic microorganisms. The incident light intensity, light path and biomass concentration determine the degree of self-shading, which leads to a light gradient inside the reactor. The light gradient and the frequency at which the cells cycle from the light zone to the dark zone determine the reactor productivity.

For the above reasons, much attention is being given to light limited growth kinetics of microalgae, aiming at the increase of productivity in photobioreactors (Grima et al., 1999a; Wu and Merchuk, 2001).

Several models have been developed to predict growth and volumetric productivities in photobioreactors (Cornet et al., 1992; Fernandez et al., 1998; Wu and Merchuk, 2002). In all these models, experimental data, obtained under quasi steady-state conditions was generated and fitted to a growth model in order to obtain kinetic parameters.

Such models can provide important insight into the dependence of mass productivity on certain variables of a photobioreactor. However, these models generate only qualitative information and cannot be extrapolated to other photobioreactor configurations, other strains or even to different cultivation conditions. To be able to extrapolate so far, further knowledge on the metabolic response to fluctuations in the light regime is required.

Therefore, each time the model is to be used with different conditions (reactor type, strain, cultivation conditions) new experimental data needs to be generated.

Steady-state culture characteristics are commonly used for productivity optimisation, and for cell physiology studies in continuous cultures, and are normally achieved by using the conventional chemostat cultivation.

In chemostat cultivations, a sequence of step-wise changes in dilution rate or medium composition is applied. After each change, at least three residence times are required for the culture to reach steady-state. This method is time consuming, especially when a large number of steady states points are necessary. A faster cultivation technique, the acceleration–stat (A-stat) has been recently developed by Paalme et al. (1995).

The A-stat is defined as a continuous culture with smooth controlled change (acceleration rate) of a cultivation parameter. The acceleration rate should be small enough to keep the system in steady-state, resulting in an unlimited number of steady-state points and as high as possible in order to make the A-stat cultivation a fast process. Therefore it is essential to find a compromise between the highest acceleration rate (i.e. the fastest A-stat), and an acceptable approximation of steady-state conditions (Sluis et al., 2001).

The A-stat technique has been previously used at lab-scale to study physiological and kinetic characteristics of heterotrophic microorganisms such as yeasts (Paalme et al., 1997b; Albergaria et al., 2000; Sluis et al., 2001), and some bacteria (Paalme et al., 1995; 1997a; Kask et al., 1999) where the substrate is evenly diluted inside the reactor. However, given that in microalgae cultures the only energy source is the light falling on the reactor surface, the system studied in this work is very different from the ones in which the A-stat has been previously used.

In the present study, we aimed at investigating the applicability of the A-stat to microalgae cultivations, and to optimise productivity in a large-scale bubble column using the microalga *Dunaliella tertiolecta* as a model organism. Simulations of the A-stat were done with different acceleration rates in order to have an indication of the best rate to use to have the system in pseudo steady state. An A-stat was performed in a pilot plant bubble column where the dilution rate was smoothly increased at the rate estimated to be the best. As predicted, the growth rate stayed most of the time above 90% of the dilution rate. During the experiment the A-stat was changed to a chemostat to determine if the behaviour of the culture characteristics in the A-stat was comparable to that in the chemostat. Results showed that the culture characteristics in these two systems were approximately the same and that the A-stat can be used as a fast and accurate tool to optimise the productivity of a photobioreactor and determine kinetic parameters whenever new data is required for model simulations.

Materials and methods

Strain and culture medium

Dunaliella tertiolecta CCAP 19/6B was obtained from the Culture Collection of Algae and Protozoa (Oban, UK). *D. tertiolecta* was cultivated in artificial seawater medium (ASW) composed of (quantities in g L^{-1}): NaCl, 24.5; $MgCl_2 \cdot 6H_2O$, 9.8; $CaCl_2 \cdot 2H_2O$, 0.53: Na_2SO_4, 3.2; K_2SO_4, 0.85. The following nutrients were added (quantities in mmol L^{-1}): KNO_3, 16.0; $NaH_2PO_4 \cdot 2H_2O$, 1.0; $NaHCO_3$, 5.0. Also the following trace elements were added (quantities in µmol L^{-1}): $Na_2EDTA \cdot 2H_2O$, 61.6;

$FeCl_3 \cdot 6H_2O$, 23.3; $CuSO_4 \cdot 7H_2O$, 0.210; $ZnSO_4 \cdot 7H_2O$, 0.303; $CoCl_2 \cdot 6H_2O$, 0.085; $MnCl_2 \cdot 4H_2O$, 1.83; Na_2MoO_4, 0.052.

D. tertiolecta was maintained as a pure suspended culture in 250 mL-Erlenmeyer flasks containing 50 mL of medium. The cultures were kept at 20ºC, under a light intensity of 50-70 µmol m^{-2} s^{-1} and a 16/8 h day/night cycle. Every three weeks, 0.5 mL of a culture was transferred to a new flask containing fresh medium. Four flasks containing 50 ml of 3 week old cultures were brought into four sterile 3 L-Erlenmeyer flasks each one containing 1 L of fresh medium. After 10 days the reactor was inoculated with 4 L of inoculum.

Cultivation system

The A-stat was carried out in a pilot plant bubble column with a working height and diameter of respectively 1.91 and 0.21 m. The working and culture volume were 66 and 65 L, respectively. The reactor was surrounded by 62 fluorescent tubes (Britegro 2023, Sylvania, Germany) and the incident light intensity was 193 µmol m^{-2} s^{-1}, which was continuously provided. The cultivation ran batch wise until the OD_{530} was equal to 1 (0.45 g L^{-1}), and then a constant dilution rate of 0.025 h^{-1} was started. This dilution rate was kept constant for one week, which corresponded to 3 residence times. Steady-state conditions were ascertained by constant biomass concentration, which was measured daily, and by constant oxygen production and carbon dioxide supply of the system, which was measured on line through all the cultivation time.

After 1 week of chemostat cultivation, a smooth and constant increase in dilution rate (D) was started according to Eq 5.1:

$$D = D_0 + a \cdot t \qquad \text{Eq 5.1}$$

The acceleration rate (a) was 0.00011 h^{-2}. The A-stat ran for 400 h, until a dilution rate of 0.072 h^{-1} and then it was turned into a chemostat where this dilution was kept constant for more 140 hours.

During all cultivations, a Bio controller (Applikon, The Netherlands) controlled the cultivation parameters (pH and Temperature) and a Bioexpert (Applikon, The Netherlands) acquired the on-line data, which were the temperature, pH, oxygen tension in the broth, medium flow rate, air and carbon dioxide flow rate and their concentration in the headspace of the reactor. The reactor was equipped with a water jacket connected to a water bath, which allowed controlling the temperature at 30ºC. The pH was controlled at 7.8 by adding carbon dioxide to the air flow and the superficial gas velocity was 0.006 m s^{-1} (gas flow rate = 13.5 L min^{-1}). The concentration of carbon dioxide in the outgoing air was measured on-line with a Servomex 1440 Gas Analyser (The Netherlands).

Photon flux density

The photon flux density (PFD) was measured as PAR (Photosynthetic Active Radiation, 400-700 nm). To verify if the PFD on the reactor walls was constant during cultivation time, the PFD was weekly measured with a LI-190SA 2π PAR-sensor, (LI-COR, Lincoln, NE, USA) at 3 different spots of the illuminated area. The PFD was also measured inside the reactor (every 0.5-cm starting at the reactor wall) during cultivation with a LI-192SA underwater 2π PAR-sensor (LI-COR, Lincoln, NE, USA).

Sampling

The reactor had two sampling ports, in the top and in the bottom of the column. 100 mL of culture was daily collected from each sampling port. The optical density was measured and the volume of culture suspension (V) required for further analysis was calculated according to Eq 5.2:

$$V = 80 \cdot \frac{1.4}{OD_{680}} \qquad \text{Eq 5.2}$$

Where 80 is the necessary culture volume with an optical density (OD_{680}) of 1.4 to do all the analysis.

The suspension collected from the reactor was centrifuged at 5000 *g*, 4ºC, for 5 min (Beckman J2-MC centrifuge with a JA-20 rotor). The supernatant was centrifuged again. Both pellets were resuspended in 80 mL of ASW to a final OD_{680} of 1.4. This washed suspension was used for the determination of dry weight, protein, chlorophyll and the average spectral absorption coefficient. This procedure was done in separate for the two samples from the top and bottom of the column to verify the existence of any gradients in the column. As there were no gradients, from half of the run on only one sample was taken from the bottom port.

Analysis

Dry weight

Dry weight content was determined in triplicate when 1 sample was taken and in duplicate when 2 samples were taken. A volume of 20 mL of the washed suspension was filtered through a pre-combusted (550ºC, 2 h) and pre-weighted glass fiber filter (Whatman GF/F). The culture was washed with ammonium formate 0.5 M as described by Zhu and Lee (1997). The filters with biomass were dried at 105ºC and allowed to cool in a dessicator, and subsequently reweighed.

Chlorophyll

The chlorophyll concentration was determined in triplicate when 1 sample was taken and in duplicate when 2 samples were taken. A volume of 2.5 mL of the washed suspension (containing

24-98 μg of chlorophyll-a) was filtered through a glass fiber filter (Whatman GF/F) coated with a thin layer of $CaCO_3$. The extraction was done with 10 mL of 90% v/v ethanol and was facilitated by heating the solution for 3 min (78ºC). The solution was stored in the dark at 4ºC to complete extraction overnight. After filtration through the same filters as mentioned before the chlorophyll-a concentration was determined according to Nusch (1980).
The standard errors of the calculated chlorophyll concentrations were based on the error in the biomass and chlorophyll estimates.

Optical density
The optical density of the algal suspensions (OD_{680} and OD_{530}) was measured at a wavelength of 680 and 530nm on a spectrophotometer (Spectronic® 20 Genesys, Spectronic Instruments, UK) against a reference of ASW.

Spectral absorption coefficient
The washed suspension was used to determine the average spectral absorption coefficient (Janssen et al., 2000a; 2000b). The absorbance was measured in duplicate in a Beckman DU-640 spectrophotometer equipped with an RSA-BE-65 integrating sphere (Labsphere, UK). Forward-scattered light was measured from 400 to 700 nm with a 0.5 nm interval. Absorbance from 720 to 750 nm was also measured and its average was subtracted from the absorbance between 400 and 700 nm assuming this was residual scattering.
From the absorbance scans the average spectral absorption coefficient per amount of protein (a_{prot}) or dry weight (a_{dw}) was calculated according to Dubinsky et al. (1986). The relative spectral distribution of the lamps required for these calculations was measured from 400 to 700 nm on a S2000 spectroradiometer (Ocean Optics Inc, USA) calibrated with a HL-2000-CAL halogen light source (Top Sensor Systems, The Netherlands).
The standard errors of the calculated absorption coefficients were based on the error in the biomass estimates.

Calculations

Growth rate
As the dilution rate (D) varied linearly during the A-stat and the volume (V) remained constant, the specific growth rate was derived from the experimental biomass concentration according to equations 5.3 and 5.4. At each experimental time point (t), the specific growth rate was calculated by averaging μ_{t-1} (Eq 5.3) and μ_{t+1} (Eq 5.4), according to Eq 5.5:

$$\mu_{t-1} = \frac{C_{x,t} - C_{x,t-1}}{(t_t - t_{t-1}) \cdot C_{x,t}} + D_t \qquad \mu_{t+1} = \frac{C_{x,t} - C_{x,t+1}}{(t_t - t_{t+1}) \cdot C_{x,t}} + D_t \qquad \text{Eq 5.3 and 5.4}$$

$$\mu_t = \frac{\mu_{t-1} + \mu_{t+1}}{2} \qquad \text{Eq 5.5}$$

where $C_{x,t}$, $C_{x,t-1}$ and $C_{x,t+1}$ are the biomass concentrations at time t_t, t_{t-1} and t_{t+1}, respectively.
The standard errors were calculated based on the error in the biomass estimates.

Simulations

The effect of the acceleration rate on the steady-state characteristics of *D. tertiolecta* was simulated using Mathcad 2000. The simulations were made using a modified model of Evers (1991) as proposed by Janssen et al. (2003) for the calculation of the average light intensity inside the reactor and a light-limited growth kinetic model of Grima et al. (1994).

Kinetic parameters for simulations

The growth kinetic parameters were obtained by fitting the experimental data acquired during the linear phase (light-limited phase) of a batch cultivation of *D. tertiolecta* under the same conditions and in the same reactor as in the A-stat, to the growth model of Grima et al. (1994) (Eq. 5.9, Appendix I). The biomass concentration was measured daily and the growth rate was determined by direct use of Equations 5.3 to 5.5, with D = 0.

The average light intensity (PFD_{ave}) inside the reactor was calculated with the modified model of Evers (1991) (Eq 5.6 – 5.8, Appendix I). For this calculation, the experimental biomass concentrations (C_x), a $PFD_{in,}$ of 193 µmol m^{-2} s^{-1} and a constant absorption coefficient (a_c) of 200 m^2 kg^{-1} (value obtained in a previous work, data not shown) were used. The growth rates and the average light intensities calculated were fitted to the model of Grima et al. (1994) in order to estimate the kinetic parameters. The fit of the growth model is expressed by the coefficient of determination, r^2, which was calculated to be 0.995 and the kinetic parameters are presented on Table 5.1. These values were used for the A-stat simulations at different acceleration rates.

Table 5.1. Values of model parameters and conditions used for simulations of A-stat cultivations under different acceleration rates with the strain *D. tertiolecta.*

Parameter	Value	Condition	Value
μ_{max}	0.09 h^{-1}	$C_{x,0}$	1 g L^{-1}
K	69.86 µmol m^{-2} s^{-1}	D_0	0.019 h^{-1}
m	2.04	D_f	0.075 h^{-1}
		PFD_{in}	193 µmol m^{-2} s^{-1}
		a_c	200 m^2 kg^{-1}

Results and Discussion

Simulations

A model (Appendix I) was developed to simulate light limited continuous fermentations in order to be able to estimate the best acceleration to use during the A-stat. This model incorporates a light limited kinetic model of Grima et al. (1994) (Eq 5.9, appendix I) where photoinhibition is not considered, and it is based on the assumption that cells adapt to an average light intensity inside the reactor. The reason to have chosen this model was the low light intensity used in the present work (193 µmol m^{-2} s^{-1}), which does not lead to photoinhibition. The average light intensity inside the reactor was calculated by using a modified model of Evers (1991) as proposed by Janssen et al. (2003) (Eq 5.6 – 5.8, Appendix I) and the absorption coefficient was assumed to be constant. In the original model of Evers (1991), the light absorbing surface was taken as a cylindrical surface. In the modified version of Janssen et al. (2003), the light exposed surface is a flat surface facing the reactor. This modification was used in the present work to allow a comparison between the model and the experimental results that were obtained with a 2π PAR sensor. It can be seen in Figure 5.1 that the modified model of Evers gives a good simulation of the light gradient inside the bubble column.

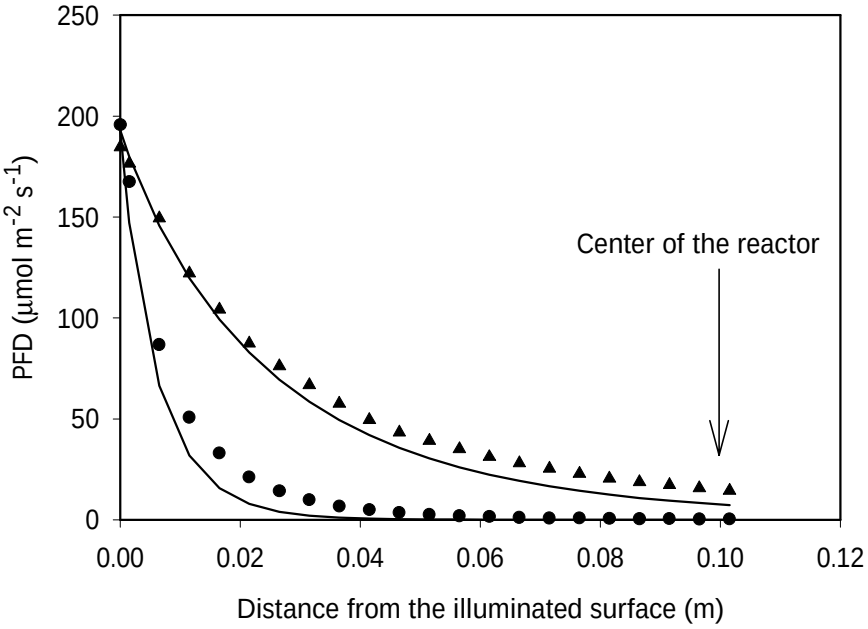

Figure 5.1. Light gradient inside the reactor at two different biomass concentrations (C_x = 0.52 g L^{-1} (●) and C_x = 0.15 g L^{-1} (▲) calculated with the modified model of Evers (1991) (solid line) and measured (discrete points).

The model parameters and the starting values used for the A-stat simulation can be found in Table 5.1.

The choice of the acceleration rate is very important, as it determines if the system will be in a pseudo-steady state. The acceleration rate should be fast enough in order to make it a fast process, but at the same time it should be slow enough to allow the microorganism to adapt its metabolism to the new conditions imposed by the change in the dilution rate. This technique has never been used with photosynthetic microorganisms, so the acceleration rate had to be carefully selected. The results from the simulations of three different acceleration rates, 0.001, 0.0001 and 0.00001 h^{-2} which correspond to A-stats of 2, 20 and 200 days, respectively, are depicted in Figure 5.2. It can be seen that an increase in the acceleration rate leads to bigger differences between growth and dilution rates, i.e. non steady state conditions. The worst case is at the fastest dilution rate (0.001 h^{-2}) where the growth rate drops until 60% of the dilution rate.

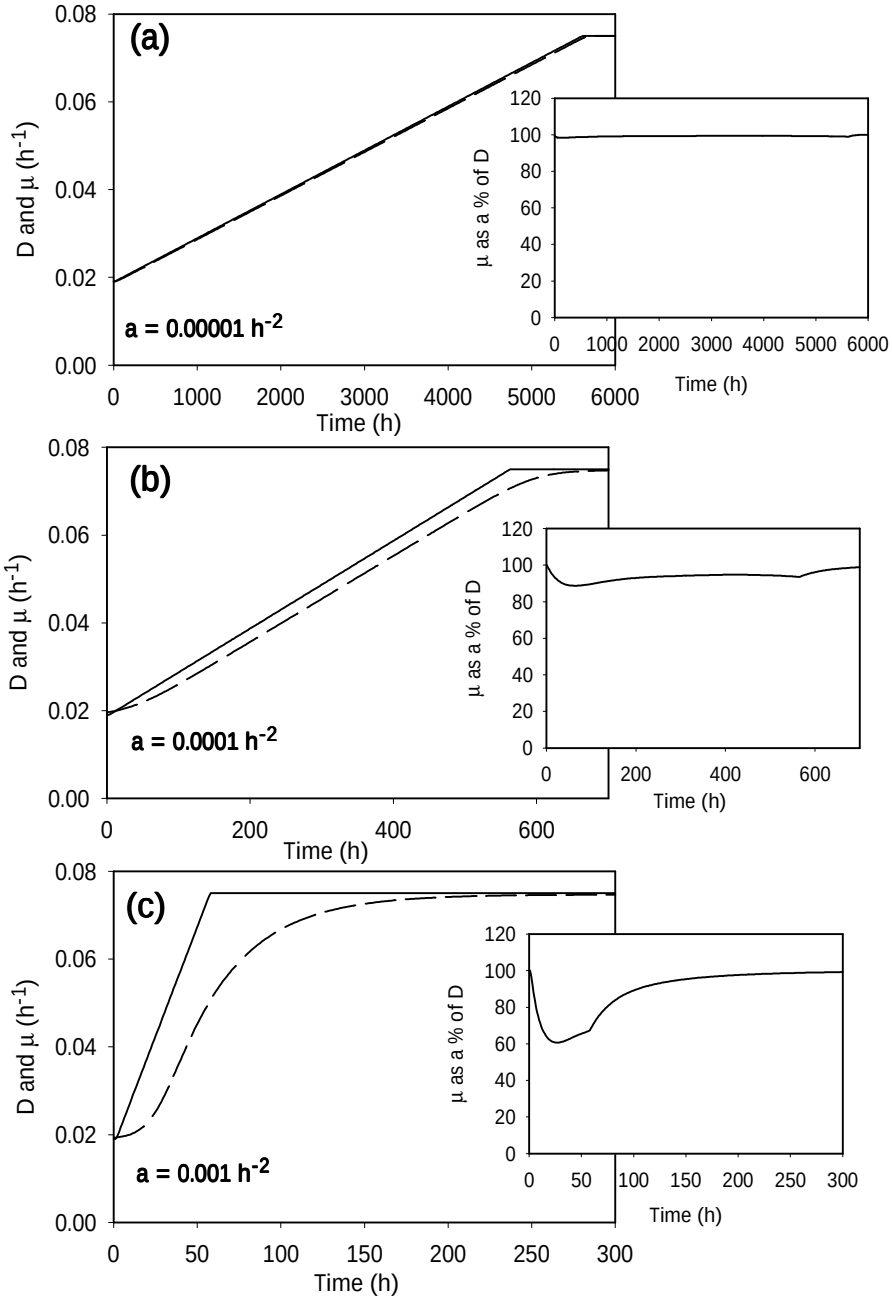

Figure 5.2. Simulation of the A-stat cultivation of *D. tertiolecta* cultivated in a pilot plant bubble column. Effect of acceleration rate: (a) 0.00001 h^{-2}, (b) 0.0001 h^{-2}, (c) 0.001 h^{-2} on the dilution rate (solid lines) and growth rate (dashed lined) profile.
In the small figures the growth rate is given as a percentage of the dilution rate.

Pseudo steady state

The A-stat was carried out in a pilot plant bubble column to optimise biomass productivity as a function of the dilution rate in this system, and to test the applicability of this technique to photosynthetic microorganisms. The dilution rate was smoothly increased, at a constant acceleration rate of 0.00011 h^{-2}, from 0.025 until 0.072 h^{-1}, which corresponds to ca. 25 and 75 %,

respectively of the expected maximum specific growth rate (Table 5.1). The acceleration rate was chosen based on the simulations (Figure 5.2) and on an arbitrary criterion that the system is considered to be in pseudo steady state when the growth rate is higher than 80% of the dilution rate.

The specific growth rate (μ) was derived from the experimental biomass concentration (Eq. 5.3-3.5) and is depicted in Figure 5.3 with the dilution rate. According to the initial predictions, the μ dropped to maximally 80% of the dilution rate, but during most of the cultivation time it was higher than 90% of the dilution rate (Figure 5.3). These results show that cell growth could keep up with the dilution rate and that pseudo steady state was maintained throughout the experiment.

At the end of the experiment, the A-stat was changed to a chemostat and the dilution rate was kept at 0.072 h^{-1} for 140 hours, and it can be seen in Figure 5.3 that the growth rate could still follow the dilution rate. It can be concluded that there was not a deviation between the A-stat and chemostat and the results obtained in this experiment can be used for the characterization of steady –state culture conditions in this system.

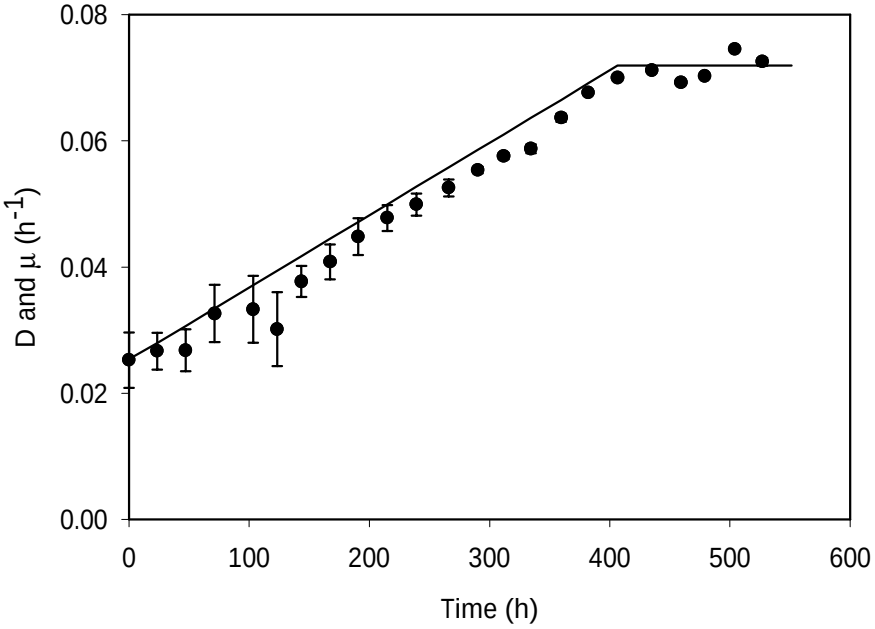

Figure 5.3 Steady state conditions during the A-stat. Dilution rate (solid line) and experimental growth rates (●) of the A-stat performed in a pilot plant bubble column at an acceleration rate of 0.00011 h^{-2}. Error bars represent standard errors.

These results are different from the ones obtained in heterotrophic fermentations where a big deviation was found between the A-stat and the chemostat culture characteristics obtained at the same dilution rate. These differences were proven to be dependent on both the delay of the concentrations of the medium components in the A-stat compared to the chemostat, and the

limitation in the metabolic adaptation rate of the microorganism. These differences increased with increasing acceleration rate (Sluis et al., 2001).

Regarding the delay of the concentration of the medium substrates during an A-stat cultivation, the uncommon substrate 'light' seems to bring an advantage in this respect when compared to conventional substrates such as glucose. The average light intensity inside the reactor will be directly dependent on the cell concentration, and on its specific absorption coefficient. An increase in dilution rate will cause a decrease in the biomass concentration (Figure 5.4), but the dilution rate itself does not have a direct effect on the light intensity, which means that the delay of substrate concentration in the medium did not play an important role in this system.

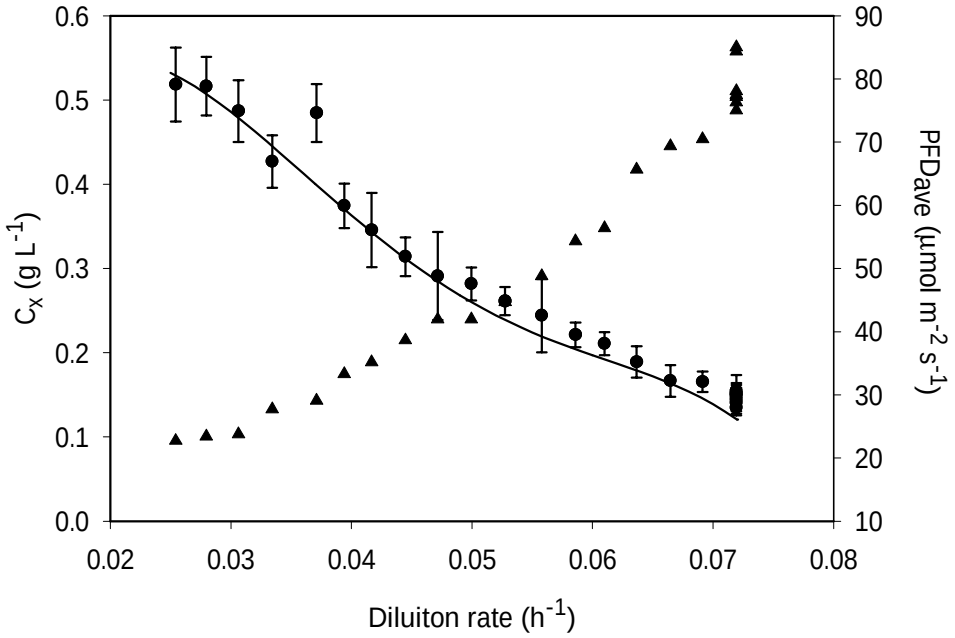

Figure 5.4. Experimental biomass concentrations (C_x) (●), model fit (solid line) to the experimental biomass concentration and average light intensity (PFD_{ave}) (▲) as a function of dilution rate during the A-stat cultivation. Error bars represent standard errors. Initial conditions and fit parameters are given on Table 5.2, respectively.

What concerns metabolic adaptation of microalgae to changes in the environment, these microorganisms have to adapt their photosynthetic apparatus to changes in the light intensity. When cultivated under a certain light intensity, they will exhibit a corresponding size of the cellular light-absorbing surface, consisting of pigment molecules arranged in antenna complexes inside the photosystem. The specific surface, i.e the absorption coefficient, decreases if the light intensity increases and this process is called photoacclimation (Falkowski and LaRoche, 1991).

In Figure 5.5a and 5.5b, a small decrease of both absorption coefficient and chlorophyll content, respectively, can be seen with increasing average light intensity. The changes were not very large due the small range of average light intensities (22 – 85 μmol m^{-2} s^{-1}) and low incident light intensity (193 μmol m^{-2} s^{-1}). This explains the fact that a possible slow rate of acclimation did not influence the A-stat results. For this reason, the simulations were accurate, and a good fit of the model to the experimental data can be see in Figure 5.4, even neglecting adaptation times and assuming a constant absorption coefficient. The fitted kinetic parameters to the experimental data are presented in Table 5.2, as well as the model conditions. Especially the parameters m and μ_{max} fitted from the A-stat experimental data (Table 5.2) are quite different from the ones obtained with the batch experiment (Table 5.1). This result shows that the A-stat can be used to further specify kinetic parameters.

Table 5.2. Values of model parameters obtained from the fit of the experimental data acquired during the A-stat to the model described on appendix I and model conditions.

Parameter	Value	Condition	Value
μ_{max}	0.11 h^{-1}	$C_{x,0}$ [(1)]	0.52 g L^{-1}
k	60.45 μmol m^{-2} s^{-1}	D_0 [(1)]	0.025 h^{-1}
M	1.35	Df [(1)]	0.072 h^{-1}
		PFD_{in} [(1)]	193 μmol m^{-2} s^{-1}
		a_c [(2)]	228 m^2 kg^{-1}
		a [(1)]	0.00011 h^{-2}

[(1)] These values correspond to experimental conditions.

[(2)] This value corresponds to the average of all experimental absorption coefficients obtained during the A-stat.

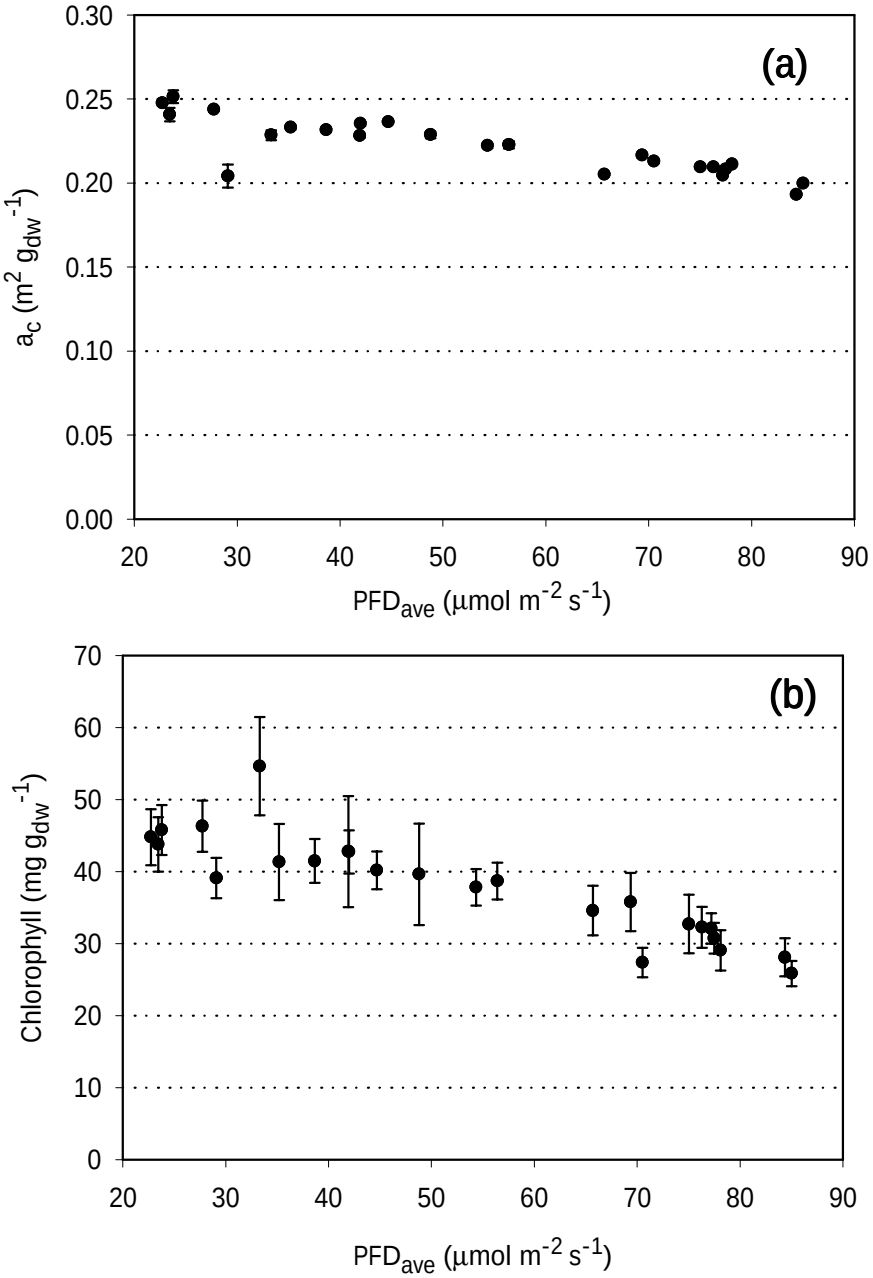

Figure 5.5. Photoacclimation during the A-stat: (a) Spectral absorption coefficient (a_c) and (b) chlorophyll concentration (C_{chlo}) as a function of average light intensity (PFD_{ave}).
The average light intensity was calculated using the modified model of Evers (Appendix I) with PFD_{in} =193 µmol m^{-2} s^{-1} and experimental biomass concentrations (C_X) and absorption coefficients (a_c).

Productivity

An increase in dilution rate resulted in a decrease in biomass concentration (Figure 5.5) as expected. The limiting substrate, light, cannot be stored in the culture medium, an increase in dilution rate will directly lead to a decrease in biomass concentration, which will result in a higher

average light intensity inside the reactor and a consequent increase of the growth rate (Figure 5.5).

There is a clear plateau where the volumetric productivity is close to maximal. At dilution rates from 0.025 to 0.060 h^{-1}, the productivity is rather constant, and for values higher than 0.060 h^{-1} it starts to decrease (Figure 5.6). The maximal volumetric productivity was 0.36 g L^{-1} d^{-1} at a dilution rate of 0.030 h^{-1}, but a clear peak cannot be seen (neglecting the 5th data point which seems to be a measurement error) (Figure 5.6). Such a plateau has been previously reported (Cornet et al., 1992), and it can be explained by the fact that during this range of dilution rates the PFD_{ave} is low (Figure 5.5) and apparently the culture can utilise the light with the same efficiency within this range.

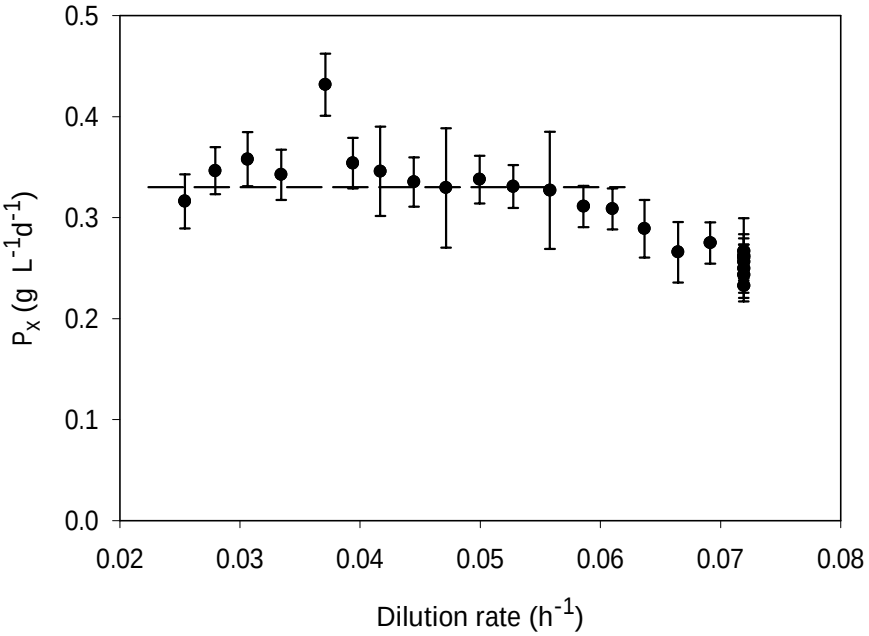

Figure 5.6. Volumetric productivity (P_x) as a function of dilution rate. Error bars represent standard errors. Horizontal dashed line corresponds to the range of dilution rates at which productivity is constant.

Conclusions

The robustness of every model predicting volumetric productivities in microalgae grown in photobioreactors depends on both the accuracy of the kinetic parameters used and on the light transfer model. The results presented show that the A-stat can be used as a fast and accurate tool to determine kinetic parameters in continuous cultivations and to optimise cultivation parameters

in a specific photobioreactor. Its applicability to other photobioreactors and other light regimes is presently being studied.

Appendix I

The model presented below was used to describe the growth of *D. tertiolecta* during A-stat cultivations at different acceleration rates.

Average light intensity and light gradient inside the reactor

Modified model of Evers (1991) according to Janssen et al. (2003)

The light intensity at a distance s from the reactor wall can be calculated by:

$$PFD(s) = \frac{PFD_{in}}{\int_{0.5\cdot\pi}^{1.5\cdot\pi} \cos(\Theta+\pi)\cdot d\Theta} \cdot \left[\int_{0.5\cdot\pi}^{1.5\cdot\pi} \cos(\Theta+\pi)\cdot \exp[-a_c \cdot C_x \cdot b]\cdot d\Theta\right] \quad \text{Eq 5.6}$$

where b is the light path from the reactor surface until the point s, and can be calculated by the following equation:

$$b = (r-s)\cdot\cos\Theta + \left[r^2 - (r-s)^2\cdot\sin\Theta^2\right]^{0.5} \quad \text{Eq 5.7}$$

The average light intensity, PFD_{ave}, can now be calculated by:

$$PFD_{ave} = \frac{\int_0^r 2\cdot\pi\cdot(r-s)\cdot PFD(s)\cdot ds}{\pi\cdot r^2} \quad \text{Eq 5.8}$$

Light-limited growth rate

Light-limited growth kinetic model proposed by Grima et al. (1994):

$$\mu = \frac{\mu_{max}\cdot PFD_{ave}{}^m}{K^m + PFD_{ave}{}^m} \quad \text{Eq 5.9}$$

The balance for biomass during the A-stat

$$\frac{dC_x}{dt} = C_x\cdot(\mu - D) \quad \text{Eq 5.10}$$

and

$$\frac{dD}{dt} = a \quad \text{Eq 5.11}$$

Nomenclature

a	acceleration rate	[h^{-2}]
a_c	spectral averaged absorption coefficient on a dry weight basis	[m^2 g^{-1}]
b	light path	[m]
C_x	biomass concentration	[g L^{-1}]
C_{chlo}	chlorophyll concentration on a dry weight basis	[mg g^{-1}]
$C_{x,0}$	initial biomass concentration	[g L^{-1}]
D	dilution rate	[h^{-1}]
D_0	initial dilution rate	[h^{-1}]
K	affinity of algae to light	[µmol m^{-2} s^{-1}]
m	exponent in Eq 5.4	[-]
PFD	photon flux density	[µmol m^{-2} s^{-1}]
PFD_{in}	photon flux density falling on the reactor surface in the inside part	[µmol m^{-2} s^{-1}]
PFD_{ave}	average photon flux density	[µmol m^{-2} s^{-1}]
P_x	biomass volumetric productivity	[g L^{-1} d^{-1}]
r	reactor radius	[m]
s	distance from the vessel surface	[m]
µ	specific growth rate	[h^{-1}]
μ_{max}	maximum specific growth rate	[h^{-1}]
Θ	angle of light path with line through reactor center	[-]

6 Optimisation of biomass, vitamins and carotenoid yield on light energy in a flat panel reactor using the A-stat technique

Abstract

Steady-state culture characteristics are usually determined in chemostat cultivations, which are very time consuming. Acceleration-stat (A-stat) cultivations in which the dilution rate is continuously changed at a constant acceleration rate, leading to different average light intensities inside the photobioreactor, can supply more information and reduce experimental time. The acceleration rate should be small enough to keep the system in steady state and as high as possible in order to reduce experimental time. Four different accelerations were studied, a pseudo steady state was maintained at acceleration rates of 0.00016 and 0.00029 h^{-2} and results were similar to those of the chemostat. An increase in the acceleration rate led to an increase in the deviation between the results obtained in the A-stat and those in the chemostats obtained at the same dilution rate. From this work it was concluded that it is advantageous to use the A-stat instead of chemostats to determine culture characteristics and optimize a certain photobioreactor. For the above reasons, the A-stat was used to optimize the biomass and product yield of continuous cultures of the microalgae *D. tertiolecta* in a flat panel. The effect of the average light intensity inside the photobioreactor on the production of vitamin C and E, lutein and β-carotene was studied using the A-stat. The highest concentration of these products were 3.48 ± 0.46, 0.33 ± 0.06, 5.65 ± 0.24 and 2.36 ± 0.38 mg g^{-1}, respectively. These results were obtained at different average light intensities, showing the importance of optimizing each product on light intensity.

This chapter has been submitted for publication as: Maria J. Barbosa, Jan Willem Zijffers, Adrian Nisworo, Wouter Vaes, Jan van Schoonhoven and René H. Wijffels. Optimisation of biomass, vitamins and carotenoid yield on light energy in a flat panel reactor using the A-stat technique.

Introduction

Microalgae are a natural source of specific and attractive compounds for the pharmaceutical cosmetic and food industry.

The efficiency of microalgal cultivation systems can be characterized by volumetric productivity and efficiency of light utilisation. In photobioreactors light energy is the growth limiting substrate and should be efficiently used for growth and production of the desired compounds. Optimisation of the biomass and product yields on light energy is thus essential to attain cost-effective photobioreactors.

Steady-state culture characteristics are generally used to study growth and production kinetics as well as physiological characteristics of microorganisms. Usually these characteristics are determined in chemostat cultivations, which are very time consuming especially when a large number of steady-state points are necessary. In contrast, acceleration–stat (A-stat) cultivations in which a cultivation parameter is continuously changed with a controlled and constant acceleration rate are not so time consuming and a wider range of steady states can be studied (Paalme et al., 1995). The acceleration rate should be small enough to keep the system in steady state resulting in an unlimited number of steady-state points and as high as possible in order to make the A-stat cultivation a fast process. Therefore it is essential to find a compromise between the highest acceleration rate (i.e. the fastest A-stat) and an acceptable approximation of steady-state conditions (Sluis et al., 2001).

This technique was previously used with the microalgae *Dunaliella tertiolecta* grown in a pilot plant bubble column, by continuously increasing the dilution rate at a constant rate, leading to a continuous change in the average light intensity inside the reactor (Barbosa et al. 2003c). It was shown that the A-stat was an accurate and fast tool to optimise productivity of a continuous culture of *D. tertiolecta* in a pilot plant bubble column (Barbosa et al. 2003c).

In the present work we studied the applicability of this technique to optimize product and biomass yield on light energy in a flat-panel photobioreactor with a different light regime.

The microalgae *Dunaliella tertiolecta* was cultivated in a flat-panel reactor and the A-stat technique was used by continuously varying the dilution rate, leading to a continuous change in the light gradient inside the reactor. Four different acceleration rates were tested in order to accurately determine the highest acceleration rate (i.e., the fastest A-stat) at which pseudo-steady-state conditions were still maintained.

The A-stat results were compared to results obtained with three chemostat runs at different dilution rates, in order to validate the technique and to prove the advantage of the A-stat compared to the chemostat.

D. tertiolecta is one of the few organisms which simultaneously produces antioxidant vitamins such as carotenoids (β-carotene, lutein), vitamins C (ascorbic-acid) and E (β-tocopherol) (Abalde and Fabregas, 1991; Takeyama et al., 1997). The anti-oxidant properties of these molecules have received much attention due to their application in clinical and nutritional fields (Takeyama et al. 1997).

The production of these molecules by microalgae cells is dependent on the light intensity (main substrate in phototrophic cultivations) (Phillips et al., 1995; Abe et al., 1999; Kusmic et al., 1999). However, the effect of a wide range of light intensities and light regimes on the production of these products in continuous cultivations of *D. tertiolecta* has never been studied.

For the above reasons, Vit C, Vit E, lutein and β-carotenoid yield on light energy were optimised using the A-stat technique. The effect of the average light intensity inside the photobioreactor on the production of vitamin C and E, lutein and β-carotene was studied using the A-stat.

Materials and methods

Strain and culture medium

Dunaliella tertiolecta CCAP 19/6B was obtained from the Culture Collection of Algae and Protozoa (Oban, UK). *D. tertiolecta* was cultivated in artificial seawater medium (ASW) composed of (quantities in g L^{-1}): NaCl, 24.5; $MgCl_2 \cdot 6H_2O$, 9.8; $CaCl_2 \cdot 2H_2O$, 0.53: Na_2SO_4, 3.2; K_2SO_4, 0.85. The following nutrients were added (quantities in mmol L^{-1}): KNO_3, 32.0; $NaH_2PO_4 \cdot 2H_2O$, 2.0; $NaHCO_3$, 10.0. Also the following trace elements were added (quantities in µmol L^{-1}): $Na_2EDTA \cdot 2H_2O$, 61.6; $FeCl_3 \cdot 6H_2O$, 23.3; $CuSO_4 \cdot 7H_2O$, 0.210; $ZnSO_4 \cdot 7H_2O$, 0.303; $CoCl_2 \cdot 6H_2O$, 0.085; $MnCl_2 \cdot 4H_2O$, 1.83; Na_2MoO_4, 0.052.

D. tertiolecta was maintained as pure suspended culture in 250 mL-Erlenmeyer flasks containing 50 mL of medium. The cultures were kept at 20ºC, under a light intensity of 50-70 µmol m^{-2} s^{-1} and a 16/8 h day/night cycle. Every three weeks 0.5 mL of a culture was transferred to a new flask containing fresh medium. The reactor was inoculated with 100 mL of pure inoculum.

Cultivation system

The A-stats were carried out in a flat panel built up from lexan (polycarbonate) plates held together in a stainless steel frame, with a height, diameter and depth of respectively, 0.60, 0.20 and 0.03 m (Figure 6.1) and a culture volume of 3.4 L.

The reactor was continuously illuminated at one surface by 10 fluorescent tubes (LYNX LE, Sylvania, Germany) and the incident light intensity was around 1000 µmol m^{-2} s^{-1} for each experiment.

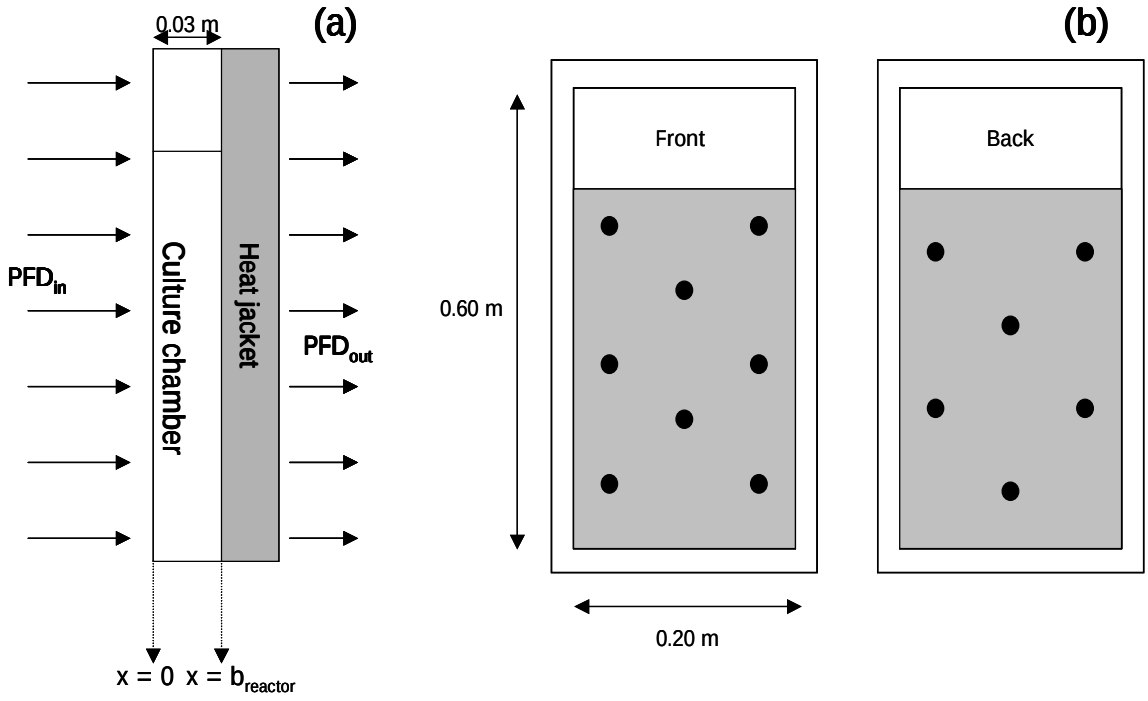

Figure 6.1. Scheme of the flat panel reactor: (a) side and (b) front view, black dots represent measuring points for light intensity at the back and in the front (illuminated surface) of the reactor.

During all cultivations a Bio controller (Applikon, The Netherlands) controlled the cultivation parameters (pH and temperature) and the BioXpert program (Applikon, The Netherlands) acquired the on-line data, which were the temperature, pH, medium flow rate, air and carbon dioxide flow rate and weight of the medium vessel. The medium was pumped by a Watson and Marlow 205U tube pump, which was controlled by the Bioxpert program. Due to possible tube alterations of the pump tube in time, the real medium flow rate was calculated at the end of each experiment as the decrease in weight of the medium vessel in time, which was monitored with a Sartorius BP 34000-P balance also connected to the Bioxpert program. The reactor was equipped with a water jacket (Figure 6.1) connected to a cryostat, which controlled the temperature at 30ºC. The pH was controlled at 7.8 by adding carbon dioxide to the air flow and the gas flow rate was 3.0 L min^{-1}. The air was sparged through 17 needles with a diameter of 0.8 mm and a length of 40 mm. The needles were pinched through a piece of silicon, which was positioned at the bottom of the reactor.

Cultivations

Before each experiment, the cultivation ran batch wise until the biomass concentration was approximately 2.5 g L^{-1} and then a constant dilution rate was started. This dilution rate was kept constant for 3 residence times in order to reach steady-state. Steady-state conditions were ascertained by constant biomass concentration, constant ratio between OD_{680} / OD_{530} which were daily measured, and by constant carbon dioxide supply of the system, which was measured on-line during all cultivation time.

A-stats

After steady state was achieved during chemostat, a smooth and constant increase in dilution rate (D) was started according to Eq 6.1:

$$D = D_0 + a \cdot t \qquad \text{Eq 6.1}$$

Four acceleration rates (a) were studied 0.00016, 0.00029, 0.00107 and 0.00809 h^{-2}, which corresponded to A-stat cultivation times of 27.4, 11.8, 3.35 and 0.48 days, respectively. A scheme of the experiments performed in time, with the values for the initial and final dilution rates for each A-stat is depicted on Figure 6.2.

The first A-stat ran until wash out of the cells. For this reason a new inoculation was made before starting the other experiments (Figure 6.2).

A duplicate of the first A-stat was performed to optimise product yield. Due to practical reasons (tubing deformation in time during cultivation) the acceleration rate was slightly lower, 0.00015 instead of 0.00016 h^{-2}.

Chemostats

Three different chemostats were carried out at three different dilution rates: 0.0455, 0.0603 and 0.1016 h^{-1} under the same condition as during the A-stat.

Photon flux density

The photon flux density (PFD) was measured as PAR (Photosynthetic Active Radiation, 400-700 nm) with a LI-190SA 2π PAR-sensor, (LI-COR, Lincoln, NE, USA). The PFD falling on the reactor surface (PFD_{in}) was measured at the beginning and at the end of each experiment to verify if the PFD_{in} was constant during cultivation time. The PFD_{in} is the average of different measurements at 8 different locations of the illuminated area (Figure 6.1). The PFD coming through the reactor was daily measured at the back of the reactor during cultivation (PFD_{out}). The PFD_{out} is the average of different measurements at 6 different locations (Figure 6.1).

Sample standardization

A sample of culture was daily collected. The optical density was measured at ($OD_{680,sample}$) and the volume of culture suspension (V_{sample}) required for further analysis was calculated according to Eq 6.2:

$$V_{sample} = V_{standard} \cdot \frac{OD_{680,standard}}{OD_{680,sample}} \qquad \text{Eq 6.2}$$

Where $V_{standard}$ is the necessary culture volume with an optical density of $OD_{680,standard}$ to do all the analysis.

The suspension collected from the reactor was centrifuged at 5000 *g*, 4ºC, for 5 min (Beckman J2-MC centrifuge with a JA-20 rotor). The supernatant was centrifuged again. Both pellets were resuspended in a certain volume ($V_{standard}$) of ASW (this volume depends on which analysis were going to be done) to a final optical density of $OD_{680,standard}$ = 1.4. This washed suspension was used for the determination of dry weight, protein, chlorophyll and the average spectral absorption coefficient.

Vitamins and carotenoids

The principle used to standardize the sample was also used to prepare the sample to be analysed for vitamin and carotenoid content. For the determination of the vitamin content a total volume of $V_{standard}$ = 65 mL with an $OD_{680,standard}$ = 2 was needed. The sample volume (V_{sample}) that had to be collected was calculated using Eq 6..2.

This sample was centrifuged twice, using the same conditions as mentioned above, and the pellets were re-suspended in 65 mL of a solution of sodium erythorbate (isoascorbic acid) 0.01% w/v in ammonium formate 0.5 M.

Two tubes were filled with 30 mL of the re-suspended algae and were centrifuged again under the same conditions. The supernatant was discarded and the pellets were frozen at –20°C until vitamin and carotenoid analysis.

Analysis

Dry weight

Dry weight content was determined in triplicate, according to (Zhu and Lee, 1997).

Chlorophyll

Chlorophyll concentration was determined in triplicate, according to (Nusch, 1980).

Optical density

The optical density of the algal suspensions (OD_{680} and OD_{530}) was measured at a wavelength of 680 and 530 nm on a spectrophotometer (Spectronic® 20 Genesys, Spectronic Instruments, UK) against a reference of ASW.

Spectral absorption coefficient

The washed suspension was used to determine the average spectral absorption coefficient (Janssen et al., 2000a; 2000b). The absorbance was measured in duplicate in a Beckman DU-640 spectrophotometer equipped with an RSA-BE-65 integrating sphere (Labsphere, UK). Forward-scattered light was measured from 400 to 700 nm with a 0.5 nm interval. Absorbance from 720 to 750 nm was also measured and its average was subtracted from the absorbance between 400 and 700 nm assuming this was residual scattering.

From the absorbance scans the average spectral absorption coefficient per dry weight (a_c) was calculated according to Dubinsky et al. (1986). The relative spectral distribution of the lamps required for these calculations was measured from 400 to 700 nm on a S2000 spectroradiometer (Ocean Optics Inc, USA) calibrated with an HL-2000-CAL halogen light source (Top Sensor Systems, The Netherlands).

Vitamins and carotenoids

Vitamin C

Vitamin C was analysed according to Speek et al. (1984). In short, samples were extracted using 5% trichloroacetic acid. The extract thus obtained was adjusted to pH 4.5, after which ascorbic acid was enzymatically oxidized by ascorbate oxidase to dehydroascorbic acid. Dehydroascobic acid was derivatized by 12-diamonibenzene to its quinoxaline derivative, which was analysed using reversed phase high performance liquid chromatography (HPLC) with fluorescence detection (excitation λ 355 nm, emission λ 425 nm).

Carotenoids and tocopherols

Samples were saponified during 30 minutes at 80°C by ethanolic KOH (10%) containing 2% sodium ascorbate. After cooling down at room temperature, the mixture was extracted by iso-propylether. The extract was dried under a gentle flow of nitrogen, and the residue dissolved in hexane. Subsequently, the samples were analysed for tocopherols using straight-phase HPLC with fluorescence detection (excitation λ 296 nm, emission λ 320 nm) as described by Speek et al. (1985), and for carotenoids using reversed phase HPLC with photo-diode-array (PDA) detection as described by Broekmans (2002).

Calculations

Growth rate

As the dilution rate (D) varied linearly during the A-stat and the volume (V) remained constant, the specific growth rate was derived from the experimental biomass concentration according to equations 6.3 and 6.4. At each experimental time point (t), the specific growth rate was calculated by averaging μ_{t-1} (Eq 6.3) and μ_{t+1} (Eq 6.4), according to Eq 6.5:

$$\mu_{t-1} = \frac{C_{x,t} - C_{x,t-1}}{(t_t - t_{t-1}) \cdot C_{x,t}} + D_t \qquad \mu_{t+1} = \frac{C_{x,t} - C_{x,t+1}}{(t_t - t_{t+1}) \cdot C_{x,t}} + D_t \qquad \text{Eq 6.3 and 6.4}$$

$$\mu_t = \frac{\mu_{t-1} + \mu_{t+1}}{2} \qquad \text{Eq 6.5}$$

where $C_{x,t}$, $C_{x,t-1}$ and $C_{x,t+1}$ are the biomass concentrations at time t_t, t_{t-1} and t_{t+1}, respectively

Average light intensity

The average light intensity (PFD_{ave}) and the light gradient inside the reactor were calculated using Beer's Law:

$$PFD_{out}(\lambda) = PFD_{in}(\lambda) \cdot e^{-a_c(\lambda) \cdot C_x \cdot b} \qquad \text{Eq 6.6}$$

The average wavelength dependent light intensity ($PFD_{ave}(\lambda)$) inside the reactor was determined by integrating Eq 6.7 between x = 0 and x = $b_{reactor}$ (Figure 6.1).

$$PFD_{ave}(\lambda) = \frac{\int_0^{b_{reactor}} PFD_{in}(\lambda) \cdot e^{-a_c(\lambda) \cdot C_x \cdot x} dx}{\int_0^{b_{reactor}} 1 \cdot dx} \qquad \text{Eq 6.7}$$

The solution to this integral is given by Eq 6.8:

$$PFD_{ave}(\lambda) = PFD_{in}(\lambda) \cdot \frac{1}{b_{reactor}} \cdot (1 - e^{-a_c(\lambda) \cdot C_x \cdot b_{reactor}}) \cdot \frac{1}{C_x \cdot a_x(\lambda)} \qquad \text{Eq 6.8}$$

and the average light intensity (PFD_{ave}) was calculated with Eq 6.9

$$PFD_{ave} = \sum_{400}^{700} PFD_{ave}(\lambda) \cdot \Delta\lambda \qquad \text{Eq 6.9}$$

Eq 6.9 was numerically solved by taking small steps of 0.5 nm (measurement step of the absorption of the sample and of the spectrum of the lamp), between 400 and 700 nm, which corresponds to the PAR range (Photosynthetic Active Region).

Light gradient and light penetration depth

The light gradient was calculated with Eq 6.6 by replacing the light path (b) for different reactor depths.

The photic volume in the photobioreactor was calculated based on the light gradient and it was arbitrarily defined as the reactor depth at which 90% of the incoming light intensity is absorbed (Richmond and Cheng-Wu, 2001; Janssen et al., 2003).

Biomass and product yield on light energy

The biomass yield on light energy ($Y_{X,E}$) was calculated according to Eq 6.10

$$Y_{x,E} = \frac{P_x \cdot V_{reactor}}{E_a \cdot 10^{-6} \cdot 3600} \qquad \text{Eq 6.10}$$

where P_x is the biomass volumetric productivity (g L^{-1} h^{-1}), 3600 is used to convert seconds to hours, $V_{reactor}$ is the reactor volume (L), E_a is the amount of light absorbed (µmol photons s^{-1}) and 10^{-6} is used to convert µmol to mol of photons. The product yield on light energy was calculated by using the same equation, replacing the biomass volumetric productivity by the product volumetric productivity.

Light absorbed

The amount of light energy absorbed was calculated by subtracting the measured PFD_{out} (corrected by the water jacket – Figure 6.1) to the measured light intensity falling on the reactor surface (PFD_{in}).

Results and Discussion

Effect of acceleration rate on pseudo steady-state conditions

The choice of the acceleration rate during an A-stat cultivation is very important as it determines if the system will be in a pseudo-steady state. The acceleration rate should be fast enough in order to reduce experimental time but at the same time it should be slow enough to allow the microorganism to adapt its metabolism to the new conditions imposed by the change in the dilution rate.

In order to determine the highest acceleration rate for estimating steady-state culture characteristics and optimise the yield on light energy with the A-stat in a flat panel photobioreactor, A-stats with acceleration rates (a) of 0.00016, 0.00029, 0.00107 and 0.00809 h^{-2} (Figure 6.2) as well as chemostats at fixed dilution rates were performed. During the A-stats the

dilution rate increased from ca. 0.017 to 0.100 h^{-1}. At the lowest acceleration rate (a = 0.00016 h^{-2}) the A-stat run until wash out of the culture in order to determine the maximum growth rate (μ_{max} = 0.11 h^{-1}) and to determine until when the growth rate could keep up with the dilution rate, which was 0.1 h^{-1}. From this dilution rate on, the difference between dilution and growth rate increased (Figure 6.3a).

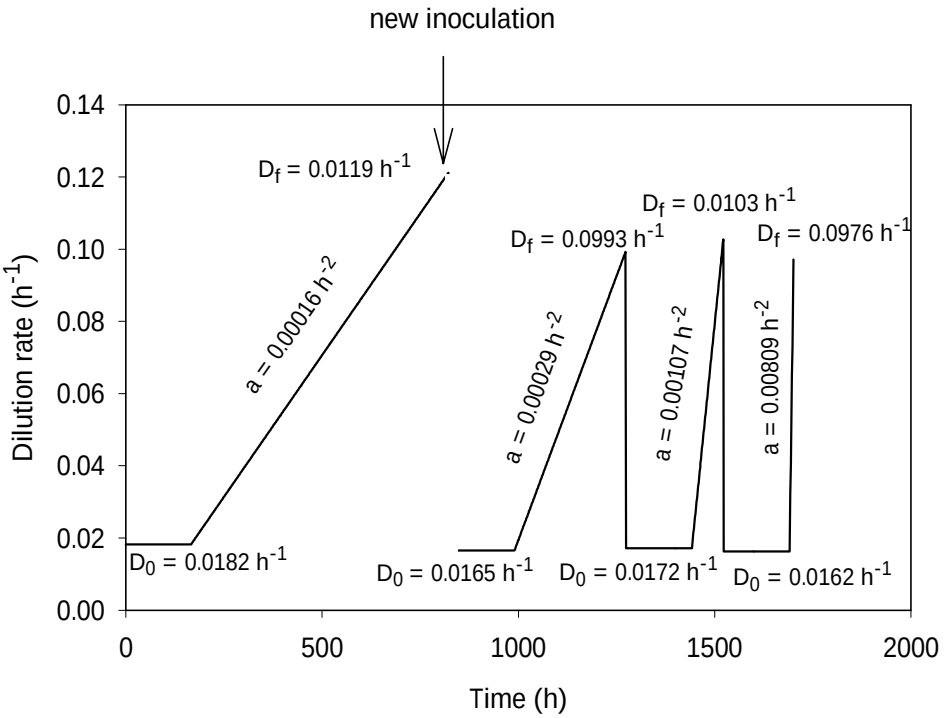

Figure 6.2. Scheme of the dilution rate in time of the experiments conducted to study the effect of acceleration rate on pseudo steady-state culture characteristics. D_0 are initial dilution rates, D_f are the final dilution rates and *a* is the acceleration rate.

The specific growth rate (μ) was derived from the experimental biomass concentration (Eq. 6.3-6.5) and is depicted in Figure 6.3 with the dilution rate, as a function of time. It can be seen that an increase in acceleration rate resulted in an increased deviation between growth and dilution rate. The highest difference between the dilution rate imposed and the growth rate calculated increased from 15 % to 76 % with increasing acceleration rate from 0.00016 to 0.00809 h^{-2}.

At the two lowest dilution rates, 0.00016 (27.4 days) and 0.00029 h^{-2} (11.8 days), the growth rate was always higher than 85 and 78 % of the dilution rate, respectively. For this reason and according to what has been previously defined (Barbosa et al., 2003c), we can conclude that a pseudo steady state was maintained throughout all range of dilution rates at these acceleration rates. At an acceleration of 0.00107 h^{-2} (3.3 days) the growth rate dropped until 70% of the dilution rate and at the fastest A-stat (a = 0.00809 h^{-2}; 0.42 days) the growth rate could clearly not keep up with the dilution rate (Figure 6.3d) and remained almost constant. The acceleration rate should be

a compromise between the required accuracy of the results and the experimental time; therefore it might vary for different experiments with different aims.

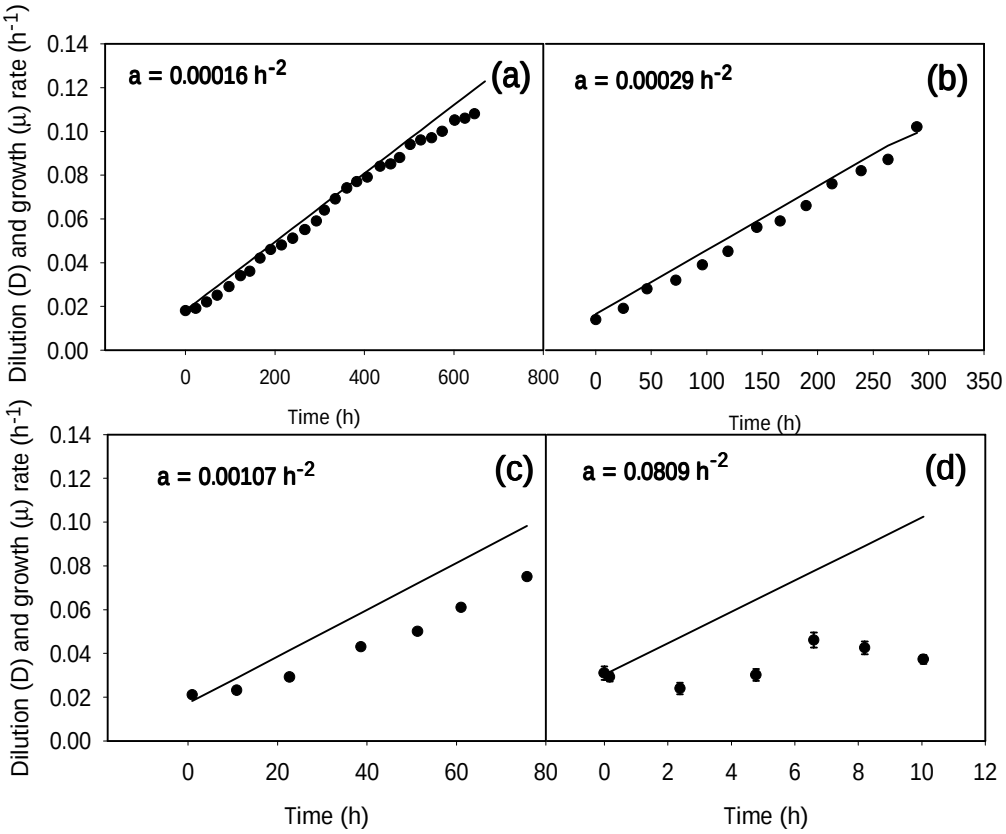

Figure 6.3. Effect of acceleration rate (a) on pseudo steady state during the A-stat cultivation of *D. tertiolecta*. (a) 0.00016 h^{-2}, (b) 0.00029 h^{-2}, (c) 0.00107 h^{-2} (d) 0.00809 h^{-2}. Dilution rate (solid line), growth rate (discrete points). Error bars represent standard errors.

Effect of acceleration rate on culture characteristics

Increasing the dilution rate led to a decrease of the biomass concentration as it can be seen in Figure 6.4a. The steepness of the biomass decrease is strongly dependent on the acceleration rate. In the fastest A-stat (a = 0.0809 h^{-2}) there was a very small decrease in the biomass concentration when compared to the other A-stats.

During these microalgae cultivations, light is the limiting substrate and it cannot be stored in the culture medium. An increase in dilution rate will directly lead to a decrease in biomass concentration, which will result in a higher average light intensity inside the reactor. The dilution rate itself does not have a direct effect on the light intensity, as opposed to heterotrophic fermentations where the substrate concentration in the reactor is directly influenced by the dilution rate.

If we consider the biomass as a substrate at a certain concentration inside the reactor (no growth and no death) we can simulate the effect of the rate of change of the dilution rate on the biomass concentration during A-stats using a mass balance (Eq 6.11):

$$\frac{dC_x}{dt} = -(D_0 + a \cdot t) \cdot C_x \qquad \text{Eq 6.11}$$

In Figure 6.4b the calculated biomass concentrations; assuming biomass as a substrate, i.e., neglecting growth and death, during A-stat cultivations with four different acceleration rates (0.00016, 0.00029, 0.00107 and 0.00809 h^{-2}) are compared and the experimental biomass concentrations obtained from the A-stat run at the highest acceleration rate (0.00809 h^{-2}) is plotted.

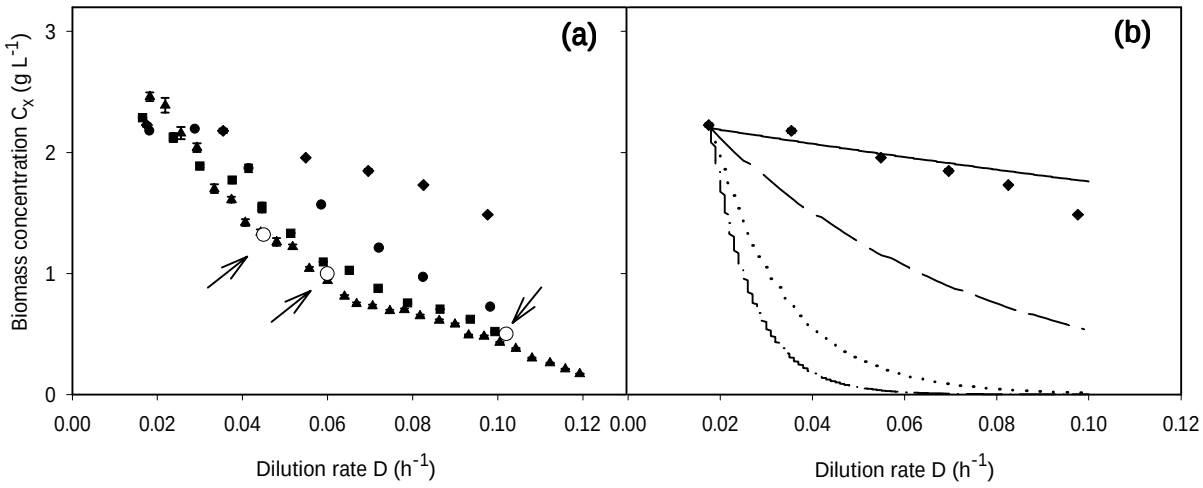

Figure 6.4. (a) Effect of acceleration rate: 0.00809 h^{-2} (◆), 0.00107 h^{-2} (●), 0.00029 h^{-2} (■) and 0.00016 h^{-2} (▲) during A-stat cultivations on biomass concentration and comparison to chemostat experiments (O) performed at three different dilution rates; (b) Simulation of the effect of acceleration rate: 0.00809 h^{-2} (solid line), 0.00107 h^{-2} (long dashed line), 0.00029 h^{-2} (dotted line) and 0.00016 h^{-2} (dashed-dotted line) assuming biomass as a substrate (Eq 6.11), no growth and no death. The discrete points are the experimental biomass concentrations during the A-stat at an acceleration rate of 0.00809 h^{-2} (◆). Error bars represent standard errors for the A-stat data and 95% confidence interval for the chemostat data points.

It can be seen in figure 6.4 that there is a delay in the decrease of biomass concentration at high acceleration rates. If there are no changes in the biomass concentration there will be no changes in the average light inside the reactor and consequently the growth rate will also remain constant (Figure 6.3d and Figure 6.5a)

The average light intensity inside the reactor will be directly dependent on the cell concentration and on light dependent physiological characteristics such as light absorption coefficient and

chlorophyll content. The cells have the capacity to adapt their photosynthetic apparatus to different light intensities in a process called photoacclimation. When cultivated under a certain light intensity they will exhibit a corresponding size of the cellular light-absorbing surface, consisting of pigment molecules arranged in antenna complexes inside the photosystem. The specific surface, i.e the absorption coefficient, decreases if the light intensity increases (Falkowski and LaRoche, 1991).

The average light intensity was calculated based on Beer's law (Eq 6.7) that is based on light absorption. However, light is also scattered by the microalgae cells and especially at high biomass concentrations scattering will increase the light path and as a result, the probability of absorption will increase. In reality, the average light intensity will be smaller than the values presented on Figure 6.5a.

In Figure 6.5b and 6.5c a decrease of both absorption coefficient and chlorophyll content, respectively, can be seen with increasing average light intensity, except at the highest acceleration rate where it remained constant.

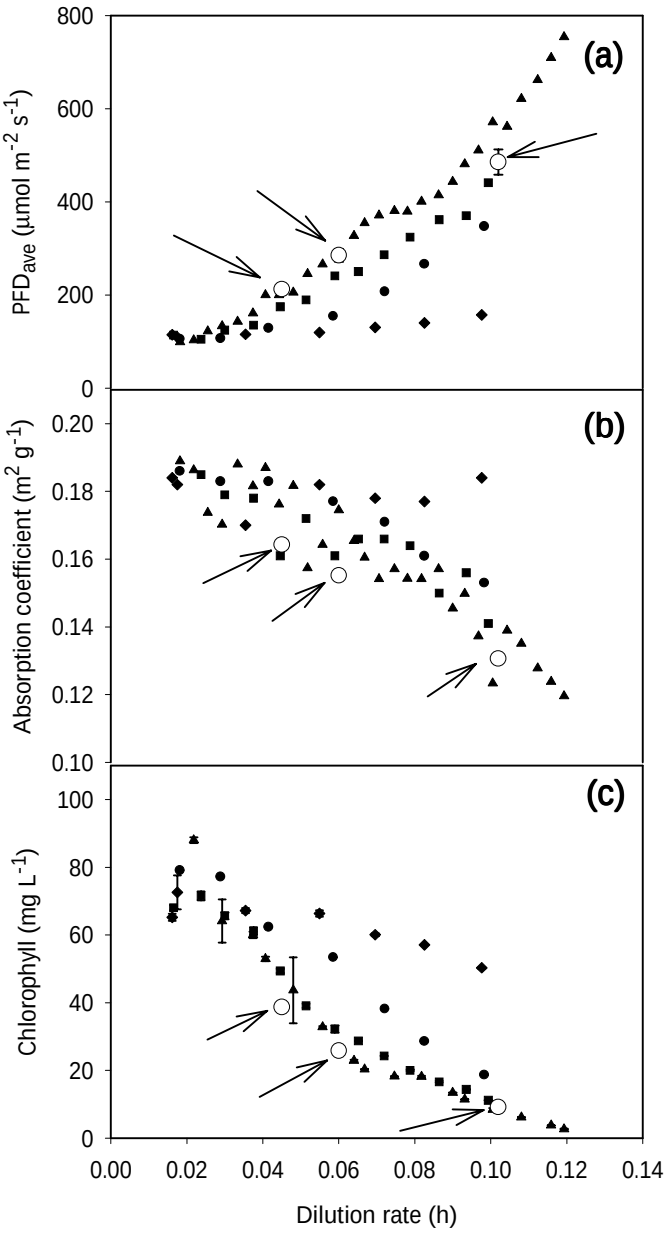

Figure 6.5. Effect of acceleration rate, 0.00809 h^{-2} (◆), 0.00107 h^{-2} (●), 0.00029 h^{-2} (■) and 0.00016 h^{-2} (▲), during A-stat cultivations on the (a) average light intensity inside the reactor (PFD_{ave}), (b) specific absorption coefficient, (c) chlorophyll concentration and comparison to results obtained in chemostats (O) run at different dilution rates. Error bars represent standard errors for the A-stat data and 95% confidence interval for the chemostat data points.

A-stat vs Chemostat

In order to validate the A-stat, the culture characteristics obtained with the A-stat run at different acceleration rates were compared to steady-state characteristics obtained from chemostat cultivations. Figures 6.4a and 6.5 clearly show that especially at low acceleration rates (0.00016

and 0.00029 h^{-2}) the culture characteristics in the A-stat are identical to those in the chemostat obtained at the same dilution rate. An increased acceleration rate generally resulted in an increased deviation between the results from the A-stat and those obtained at the same dilution rate in the chemostat.

The same behaviour has been previously reported by Sluis et al. (2001) for yeast cultivations even though identical culture characteristics obtained with the A-stat and chemostat were not reached. Sluis et al. (2001) proved that these differences were dependent on both the delay of the concentrations of the medium components in the A-stat compared to the chemostat, and the limitation in the metabolic adaptation rate of the microorganism.

In the present work, because light (the limiting substrate) cannot be stored in the medium, there is not a direct delay of the light intensity during the A-stat due to the fast increase in dilution rate. However, there is a delay on the decrease of biomass concentration at high acceleration rates (Figure 6.4), which will end up delaying the changes in light intensity inside the reactor. The reason for this is that the light intensity inside the reactor is directly dependent on biomass concentration.

At the highest acceleration rate (0.00809 h^{-2}), there were no environmental changes; i.e. changes in the light intensity (Figure 6.5a). The agreement between the simulation (assuming no growth and no death) and experimental data at an acceleration rate of 0.00809 h^{-2} (Figure 6.4a) shows that the experimental biomass concentration was only a function of the decrease in biomass concentration in time due to the fast increase of dilution rate. The delay in the change of light intensity inside the reactor led to a clear deviation between the A-stat and chemostat.

An acceleration rate of (0.00108 h^{-2}) led to a small deviation between A-stat and chemostat (Figure 6.4a and 6.5). This was once more due to the delay in the decrease in biomass concentration and not due to a limitation in the metabolic adaptation of the microalgae. This can be deduced from Figure 6.6, where the delay in the decrease of biomass concentration is eliminated by plotting the culture characteristics against the concentration of biomass instead of the dilution rate. There is no deviation between the specific growth rate and chlorophyll concentration in the A-stat (a = 0.00108 h^{-2}) and chemostat at the same dilution rate.

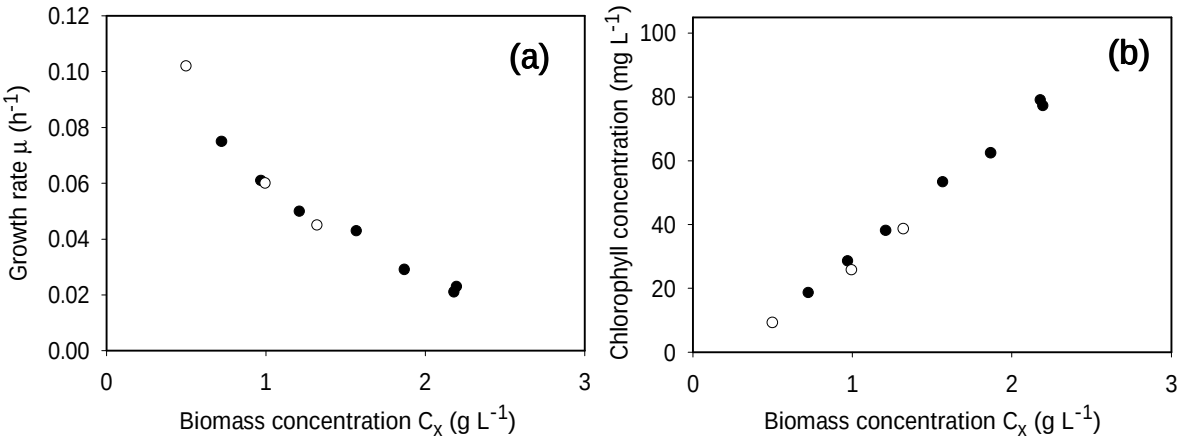

Figure 6.6. Effect of biomass concentration on the (a) growth rate and (b) chlorophyll concentration during the A-stat performed at an acceleration rate of 0.00107 h^{-2} (●) and for the chemostats performed at three different dilution rates (O). Error bars represent standard errors for the A-stat data and 95% confidence interval for the chemostat data points.

Optimisation of biomass yield on light energy

In order to optimise biomass and product yield on light energy and to verify the reproducibility of the A-stat, a duplicate of the first A-stat (a = 0.00016 h^{-2}) was performed by continuously changing the dilution rate from 0.0175 until 0.0963 h^{-1}. Due to practical reasons (tubing deformation during cultivation) the acceleration rate (measured at the end of the experiment with the online measurements of the weight of the medium vessel) was slightly lower than in the first A-stat, 0.00015 instead of 0.00016 h^{-2}. The choice of acceleration rate was based on the previous A-stat carried out at this acceleration rate which led to pseudo steady-state conditions (Figure 6.3a) and to similar results to the ones obtained with chemostats at the same dilution rate (Figure 6.5). Despite the small change in acceleration rate, the results of both A-stats were very similar, showing the reproducibility of the technique (Figure 6.7a).

The predominant factor determining the biomass yield on light energy is the light regime inside the reactor, which is characterised by (1) light intensity at the reactor surface; (2) duration of exposure of individual cells to the photic and dark volumes of the reactors, and (3) the frequency of fluctuation between these volumes. In these experiments both the incident light intensity and the frequency of fluctuation remained constant, only the percentage of photic and dark volumes changed during the A-stat and consequently the relative time that cells spend in the photic and dark zone of the reactor. The volumetric productivity and biomass yield on light energy obtained during the A-stat are shown in Figure 6.7b. It can be seen a plateau over a range of dilution rates (0.03 to 0.05 h^{-1}) where the volumetric productivity and the yield on light energy yield are maximal, 1.5 g L^{-1} d^{-1} and 0.6 g mol^{-1}, respectively. This range of dilution rates corresponds to a range of

average light intensities from 120 to 210 µmol m^{-2} s^{-1} and to a photic zone (zone where 90% of the incoming light is absorbed) of 36 to 68% of the total reactor volume (Figure 6.7b). Apparently the culture can utilise the light with the same efficiency within this range, in this photobioreactor and an incident light intensity of 1000 µmol m^{-2} s^{-1}. Such a plateau has been previously reported by Cornet et al. (1992) and Barbosa et al. (2003c).

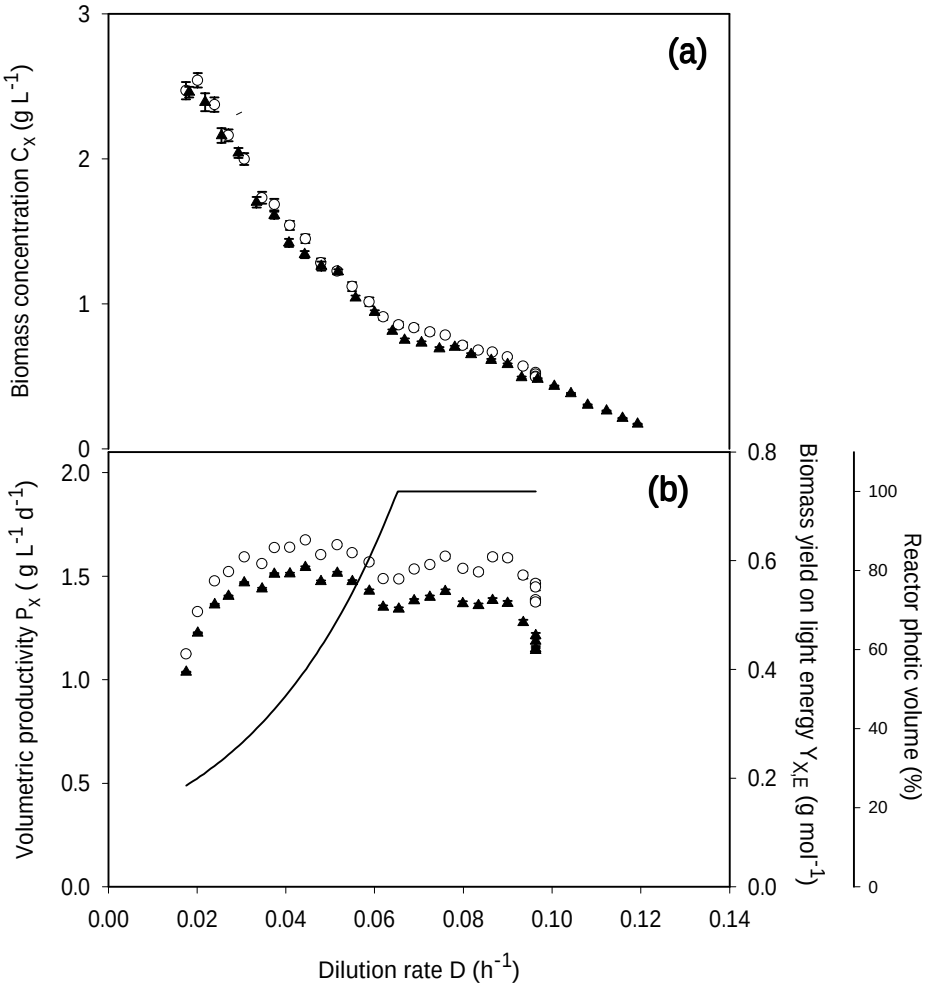

Figure 6.7. (a) Experimental biomass concentrations (C_x) during the A-stat performed at an acceleration rate of 0.00016 h^{-2} (▲) and 0.00015 h^{-2} (O); (b) Effect of dilution rate on volumetric productivity, P_x (●), Biomass yield on light energy, $Y_{X,E}$ (O) and on the photic volume as a percentage of the total reactor volume (solid line). Error bars represent standard errors.

Optimisation of product yield on light energy

Excessive light absorption under high light intensities can cause photo-oxidative damage to the photosynthetic reaction centers, thereby impairing photosynthesis (Casper-Lindley and Björkman, 1998). Photosynthetic organisms have developed mechanisms to safely dissipate excessive energy

as heat, which is called non-photochemical quenching (NPQ) and thus decrease the energy arriving at the reaction centers.

Dunaliella has a light harvesting complex similar to plants, containing chlorophyll a, b, β-carotene, lutein and the β-carotenoid xanthophyll-cycle pigments violaxanthin, anteraxanthin and zeaxanthin (Jansson, 1994). The β-carotenoid xanthophylls cycle pigments have the capacity to dissipate the excess light energy as heat. Lutein, which is a α-carotenoid, has a structural function in the light harvesting complex II (LHC II) monomer and may also have a role in energy quenching (Green and Kühlbrandt 1995). Chlorophylls and β-carotene are responsible for light absorption and β-carotene also works as an antioxidant in the protection against excessive light and as a precursor of the xanthophylls pigments (Phillips et al. 1995; Young et al., 1997)

The vitamins E (α-tocopherol) and C (ascorbic-acid) are also present in *Dunaliella tertiolecta* (Fabregas and Herrero, 1990; Abalde and Fabregas, 1991) and they also have a protective role against photooxidation. β-carotene and vitamin E are known to function together as radical trapping antioxidants (Palozza and Krinsky, 1992).

Vitamin C, besides acting as an antioxidant, it can regenerate vitamin E after it has functioned as a radical trapping antioxidant (Niki, 1987; Doba et al., 1985).

The optimisation of product yield (vitamins C and E, lutein and β-carotene) on light energy was done using the A-stat at an acceleration rate of 0.00015 h^{-2}. Figure 6.8 shows the yield of each product on light energy and the amount of product per amount of chlorophyll, as a function of the average light intensity inside the reactor.

Vitamin E (α-tocopherol) is the most active of the tocopherols and it represented 96 to 80% of the total carotenoids at the beginning and end of the A-stat, respectively.

The yield of vitamin E on light energy is plotted in Figure 6.8a as a function of the average light intensity. A significant negative correlation was found between these two parameters (Spearman Rank correlation coefficient = -0.680).

The few works studying the effect of light intensity on the production of vitamin E were done with the microalga *Euglena* and an increase of the vitamin E cell content with increasing light intensity was observed. Kusmic et al. (1999) observed an enhancement of vitamin E content in *Euglena gracilis* under an incident light intensity of 1000 μmol m^{-2} s^{-1} when compared to dark conditions. Ogbonna et al. (1999) reported a simultaneous increase of α-tocopherol content also in *Euglena gracilis* with a decrease in the chlorophyll content of the cells with increasing light supplied per cell. The author kept the incident light intensity at 300 μmol m^{-2} s^{-1} and increased the biomass concentration. Our results show the opposite trend; besides the decrease in the vitamin E yield on light energy with increasing the average light intensity inside the reactor, it can be seen in Table 6.1 that the vitamin E cell content decreased from 0.33 ± 0.06 to 0.16 ± 0.03 mg g^{-1} (± 95% ci)

with increasing the average light intensity from 84 ± 6 to 430 ± 34 µmol m^{-2} s^{-1} (± 95% ci). The reason for this discrepancy could be the fact that *Dunaliella* and *Euglena* have different xantophyll–cycle pigments and *Dunaliella* possesses high amounts of lutein, up to 5.65 ± 0.2 mg g^{-1} (Table 6.1), which may also have a role in dissipation of excessive light energy while in Euglena this α-carotenoid xanthophyll is absent (Casper-Lindley and Björkman, 1998). These two strains have also different behaviours towards the same light intensity, suggesting that they might have different photoprotective mechanisms, in the case of *Euglena* it could be tocopherols that can compensate at least partially for the lack of non photochemical quenching and/or xantophylls as it has been shown that carotenoid epoxidation does not change in *Euglena* under aerobic conditions (accumulation of de-epoxidized xanthophylls enhances energy quenching) (Krisnky, 1964).

The biosynthesis of vitamin E in the cell is still not fully understood. Different results were obtained from several authors; according to Threlfall and Goodwin (1967), the majority of all tocopherols in light-grown *Euglena* are synthesized inside the chloroplasts, while lesser amounts in mitochondria and microsomes. According to Shigeoka et al. (1986) the majority of tocopherols of *Euglena* are synthesized inside the mitochondria, with lesser amounts in chloroplasts and microsomes, and the least in the cytosol. According to Tani and Tsumura (1989) non-photosynthetic microorganisms do not produce detectable amounts of vitamin E. Kusmic et al. (1999) found indications that the formation of vitamin E occurs equally inside both the mitochondrial and chloroplastic compartment, and that the correlation between light and vitamin E production is not linked to the existence of chlorophyll.

We did not find a correlation between chlorophyll content and vitamin E content of the cells as it can be seen in Figure 6.8e. However, we did find a negative correlation between the amount of vitamin E per cell and the average light intensity inside the reactor. This finding makes vitamin E an interesting compound for high-cell density cultivations, where the average light intensity is always low and consequently the cell content in vitamin E will be high.

A clear increase in the vitamin C yield on light energy with increasing average light intensity can be seen in Figure 6.8b. The vitamin C content of the cells increased from 1.72 ± 0.76 to 3.48 ± 0.46 mg g^{-1} with increasing average light intensity from 84 ± 6 to 430 ± 34 µmol m^{-2} s^{-1} (Table 6.1). The highest content of vitamin C found in the present work (3.48 ± 0.46 mg g^{-1}) is higher than the values previously reported for *Dunaliella tertiolecta* (Fabregas and Herrero, 1990; Abalde and Fabregas, 1991), probably due to the use of higher light intensities in the present work as it was observed that high light intensities enhanced vitamin C production (Figure 6.8b). Brown et al. (2002) did not find any significant effect of light intensity on the vitamin C cellular content of *Isochrysis sp*, however only incident light intensity was considered, which might explain the divergence from our results.

Table 6.1. Vitamin content of *D. tertiolecta* at the beginning and at the end of the A-stat (± 95% ci)

	PFD_{ave} 84 ± 6 μmol m^{-2} s^{-1}	PFD_{ave} 430 ± 34 μmol m^{-2} s^{-1}
Biomass concentration (g L^{-1})	2.46 ± 0.07	0.51 ± 0.02
Dilution rate (h^{-1})	0.0175	0.096
Content per biomass (mg g^{-1})		
Vitamin E	0.33± 0.06	0.16 ± 0.03
Vitamin C	1.72 ± 0.76	3.48 ± 0.46
Lutein	5.65 ± 0.24	4.07 ± 0.13
β-carotene	2.36 ± 0.38	1.36 ± 0.01
Zeaxanthin	< 0.005	< 0.005

The yield of lutein and β-carotene slightly decreased with increasing average light intensity inside the reactor (Figure 6.8c, d). The biomass content of both carotenoids also decreased from 5.65 ± 0.24 to 4.07 ± 0.13 mg g^{-1} for lutein and from 2.36 ± 0.38 to 1.36 ± 0.01 mg g^{-1} for β-carotene with increasing the average light intensity from 84 ± 6 to 430 ± 34 μmol m^{-2} s^{-1} (Table 6.1). These results were not expected as both carotenoids have an anti-oxidative function in the cells and consequently should increase with increasing light intensity. However the amount of lutein per chlorophyll slightly increased (Figure 6.8f) and the amount of β-carotene per chlorophyll remained constant (Figure 6.8h), which is in agreement with the work of Casper-Lindley and Björkman (1998). Casper-Lindley and Björkman (1998) also reported that the amount of zeaxanthin per chlorophyll increased with increasing light intensity from 100 to 400 μmol m^{-2} s^{-1}, which indicated that zeaxanthin has an active role in the non-photochemical quenching of light energy in *D. tertiolecta*. In the present work the amount of zeaxanthin did not increase with increasing light intensity from 84 ± 6 to 430 ± 34 μmol m^{-2} s^{-1} (Table 6.1) which means that little or no light inhibition occurred during the A-stat.

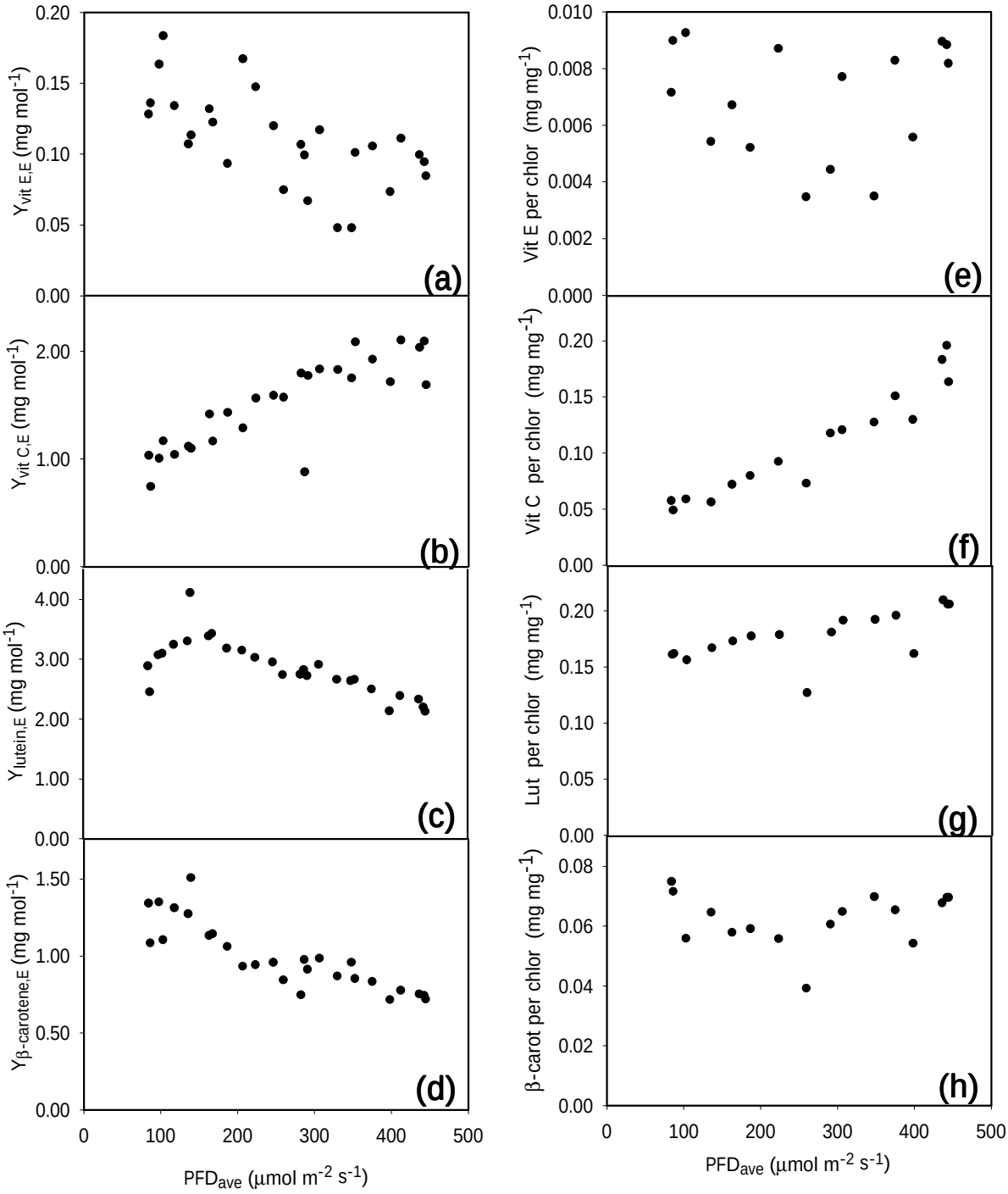

Figure 6.8. Effect of average light intensity (PFD_{ave}) on the yield of: (a) Vitamin E, (b) Vitamin C, (d) lutein, (c) β-carotene, on light energy and on the amount of product per amount of chlorophyll: (e) Vitamin E, (f) Vitamin C, (g) lutein, (h) β-carotene. These results were obtained with an A-stat cultivation performed at an acceleration rate of 0.00015 h^{-2}.

Conclusions

In the study presented here we proved the accuracy and the reproducibility of the A-stat applied to microalgae cultures. We determined the fastest possible A-stat, at which pseudo steady-state culture conditions were achieved. Results showed that pseudo–steady state could be achieved at acceleration rates of 0.00016 and 0.00029 h^{-2}, and if only rough estimated steady-state culture characteristics are required an acceleration rate of 0.00107 h^{-2} could also be used. The results obtained with the A-stat performed at acceleration rates of 0.00016 and 0.00029 h^{-2} were similar to the chemostats at the same dilution rates. Therefore it is clearly advantageous to use A-stat instead of chemostat, because the experimental time is much shorter and more information can be gathered.

Furthermore the A-stat was used to optimise the biomass and product yield on light energy in continuous cultures of *D. tertiolecta* in a flat panel reactor. The effect of the average light intensity on the cell content of vitamin C and E, lutein and β-carotene was studied. There was no correlation between the amount of vitamin E and chlorophyll in the cells. The cell content of vitamin E decreased while the amount of vitamin C increased with increasing average light intensity. This makes vitamin E an interesting compound to produce in high cell-density microalgae cultivations.

Nomenclature

a	acceleration rate	[h^{-2}]
a_c	spectral averaged absorption coefficient on a dry weight basis	[$m^2\ g^{-1}$]
a_c (λ)	wavelength dependent specific absorption coefficient	[$m^2\ g^{-1} nm^{-1}$]
$b_{reactor}$	reactor light path	[m]
C	concentration	[$g\ L^{-1}$]
D	dilution rate	[h^{-1}]
E_a	light absorbed by the culture	[µmol
PFD	photon flux density	[µmol $m^{-2}\ s^{-1}$]
PFD (λ)	wavelength dependent photon flux density	[µmol $m^{-2}\ s^{-1}\ nm^{-1}$]
P_x	biomass volumetric productivity	[$g\ L^{-1}\ d^{-1}$]
t	time	[h]
µ	specific growth rate	[h^{-1}]
μ_{max}	maximum specific growth rate	[h^{-1}]

$V_{reactor}$	reactor volume	[L]
$Y_{i,E}$	yield of component i on light energy	[g mol^{-1}]
$Y_{x,E}$	biomass yield on light energy	[g mol^{-1}]
λ	wavelength	[nm]

Subscripts

X, biomass; 0, initial; f, final; out, outgoing; in, ingoing; ave, average.

Abbreviations

Chlor, chlorophyll; carot, carotene; lut, lutein.

7 High-cell density cultures: design and operational characteristics of photobioreactors

Abstract

High-cell density cultures are required to make microalgae an effective source of high-value compounds. This entails a proper reactor design and process optimisation.

The light regime, mass transfer and hydrodynamic stress in photobioreactors are controlled, in part, by the fluid dynamics. We define here the main operational characteristics: light regime, mass transfer, hydrodynamic stress and mixing rates. Furthermore, information has been gathered concerning the interactions between these characteristics, reactor design (including sparger) and operating variables (e.g. gas input, liquid properties). These variables determine the main flow-dynamics characteristics in microalgae photobioreactors: liquid-circulation time and bubble-size distribution. The aspects that still need to be further developed in microalgae biotechnology are pointed out. Reactors in which high-cell density cultures can be maintained, such as flat panel bioreactors should be in focus. New limiting factors will have to be addressed to further optimise the performance of photobioreactors. We have described here new issues that should be considered for future research such as optimisation of the optical path of flat panels, sparger design, liquid properties (coalescence, viscosity and surface tension), optimal cell density and growth inhibition.

This chapter has been submitted for publication as: Maria J. Barbosa, Marcel Janssen, Amos Richmond and René H. Wijffels. High-cell density cultures offering new perspectives in microalgae biotechnology: design and operational characteristics of photobioreactors.

Introduction

The production of high-value compounds using light and seawater is a unique property of photosynthetic microorganisms.

The basic idea of using sunlight to produce high-value compounds brings along several limitations that are not found in heterotrophic fermentations. In addition to mass transfer, mixing rate and shear stress, one has to consider light regime in the design and scale-up of photobioreactors. Moreover, these operational parameters cannot be controlled independently, as they are closely interrelated. Light regime is often referred to as the key parameter and major constrain for the development of an efficient process (Tredici et al., 1999). The light regime inside a photobioreactor, however, depends on a variety of parameters such as sparger and reactor design, gas-power input and liquid properties. The whole process and the relations between all variables should be understood and considered for optimal design and operating conditions. Presently, the bottleneck for the development of microalgal biotechnology is the lack of cost-effective large-scale cultivation systems. High volumetric productivities are required in order to reduce the size of cultivation systems and, consequently, reduce production and downstream processing costs. This entails high biomass concentrations and a high efficiency of light utilisation.

In this work we will only consider vertical gas-sparged photobioreactors, bubble columns and flat panels, due to their simple construction and operation. Moreover, these configurations show clear advantages: (1) mass transfer rates are high and (2) liquid circulation times are short.

The literature on reactor design and performance is focused on the influence of liquid circulation time and gas input on the light regime and mass transfer. Very few works have been published on hydrodynamic stress (Suzuki et al., 1995; Camacho et al., 2001). The effect of some important operating (superficial gas velocity and liquid properties) and design (sparger and reactor design) variables on the liquid-circulation time and bubble-size distribution have been overlooked in most of the works concerning microalgae biotechnology.

High light intensities are required to attain high biomass concentrations. The only way by which microalgae can efficiently use high light intensities in photobioreactors is by exposing the cells to short cyclic periods of light and darkness (Kok, 1953; Terry, 1986; Richmond, 2000). Because these light/dark cycles should be of high frequencies, short optical paths and high gas inputs are required. On the other hand, one has to keep in mind that the gas input per nozzle should be kept low in order to reduce shear and to avoid cell damage and even death (Barbosa et al., 2003b; 2003 accepted).

We will define the relevant characteristics for the performance of photobioreactors, i.e. light regime, mass transfer, hydrodynamic stress, liquid circulation time and bubble size distribution as well as the most important interactions between them. The general guidelines for a thorough process design and optimisation of microalgae cultivations will be discussed as well as future issues to be considered in autotrophic cultivation of microalgae, namely optimisation of the optical path of flat panels, sparger design, liquid properties (coalescence, viscosity and surface tension) and growth inhibition.

The need for high-cell densities in photobioreactors

Phototrophic cultivations should approach the general features of the successful heterotrophic systems in order to be a cost-effective source of high-value compounds for the pharmaceutical, cosmetic and food industry. This entails fast growing cultures of high cell densities, arbitrarily set as biomass concentrations higher than 10 g L^{-1}. The technology for high –cell density cultures of microalgae has not yet been developed. Presently, most researchers and companies in microalgae biotechnology (the latter using mostly open raceway ponds) work with very low biomass concentrations, < 1 g L^{-1}, which are less interesting for mass cultivation of microorganisms.
In the ideal photobioreactor both areal and volumetric productivity should be maximal. We should aim at bringing as much light as possible to the reactor to increase photosynthetic productivity and at “diluting” light over a large as possible photosynthetic surface to increase photosynthetic efficiency. A large photosynthetic surface can be obtained by a large reactor illuminated area and a high cell absorbance surface. This should be done by using a small as possible optical path and high cell densities in order to expose the individual cells to low light doses and high light/dark cycle frequencies. High photosynthetic efficiencies should be obtained in this mode, as will be later discussed in this work.

Light regime

Light regime is characterised by the mode individual cells receive light and the amount of light received. One common characteristic to all photobioreactors operated at high biomass concentrations, is the existence of a steep light gradient due to light absorption by the cells and mutual shading. In dense systems there are dark and light zones and cells will circulate from one zone to the other, receiving light intermittently. Cycle time and the ratio between light and dark periods in the cycle will determine the photosynthetic efficiency (biochemical energy stored in

biomass per light energy absorbed by the cells). Light/dark cycles of several seconds to tens of seconds do not lead to an improvement in the photosynthetic efficiency. Indeed, such long cycles lead to a decrease in the photosynthetic efficiency in comparison to the efficiency under continuous light (Janssen et al., 2000a, 2000b, 2001; Barbosa et al., 2003). In addition, photodamage during long high-light periods leads to a decrease in the photosynthetic efficiency (Grima et al., 1996).

Light/dark cycles of tens of seconds are observed in airlift reactors (Table 7.1). The long cycles even at high gas superficial gas velocities make them less efficient for the cultivation of microalgae (Barbosa et al., 2003a).

In constrast, short light/dark cycles (in the order of milliseconds and microseconds) can enhance the photosynthetic efficiency (Kok, 1953; Phillips and Myers, 1954; Matthijs, et al., 1996; Nedbal, et al., 1996) and avoid photoinhibition (damage of the photosynthetic apparatus) under high light intensities (Grima et al., 1996). Hu et al. (1998) reported a maximal productivity at a light intensity of 4000 μmol m^{-2} s^{-1} (i.e. 2 times the solar flux at midday in summer) in comparison to lower light intensities.

To attain maximal photosynthetic efficiencies, the light/dark cycle period should approach the photosynthetic unit turnover time, (Dubinsky et al., 1986; Richmond et al., 2003), which is in effect equal to the dark-reaction time, which is of the order of 1-15 ms. Because the light-reaction time is an instantaneous process, of the order of nsec to μsec, cells should be shortly exposed to high light intensity, followed by a longer exposure to a dark period. Optimally, in reactors with short optical paths and high biomass concentrations, the light zone corresponds to only 5 to 7% of the reactor's volume if light is applied on one side only (Richmond et al., 2003).

Table 7.1. Liquid circulation times (t_c) estimated for different reactor configurations. All calculations are explained by Janssen et al. (2003)

Reactor type	Reactor dimensions	U_g (m s^{-1})	t_c (ms)
Flat panel	OP = 1.3 cm	-	87 – 130
	OP = 2.6 cm	-	173 – 260
Bubble column	T_v = 20 cm	0.05	960
Air-lift	A_d / A_r = 0.5	0.05	28600
	T_v = 20 cm		
	h_l = 500 cm		
	C_b = 11.8 cm		

OP - optical path; T_v – vessel diameter; A_d-cross sectional area downcomer; A_r- cross sectional area riser; h_l- non-aerated liquid height, C_b - bottom clearance; U_g – superficial gas velocity.

Short light/dark cycles can be found in flat panels and bubbles columns (Table 7.1), but for each reactor design, the optical path (for flat panels) and diameter (for bubble columns) and the gas flow rate will determine the average circulation time. The estimations of the cycle times in the flat panel (Table 7.1) were based on the liquid flow measured as the rate of dispersion of a dye inside the reactor (Hu et al., 1996; Hu and Richmond, 1996) and assuming that the liquid moves with the same velocity alongside the light-path axis. Whether this assumption is valid for all optical paths is not known.

Photosynthetic efficiencies obtained in different systems therefore greatly differ from each other, the flat panel yielding highest efficiencies closer to the theoretical maximum (33%). This value was calculated considering that 8 moles of photons with a corresponding energy of 0.175 MJ (at 680 nm) are necessary to fix one molecule of carbon dioxide. An efficiency of 16% has been reported by Hu and Richmond (1998) in a flat panel with an optical path of 2.6 cm and an incident light intensity of 1800 μmol m^{-2} s^{-1}, while for a 20 cm bubble column and an incident light intensity of 300 μmol m^{-2} s^{-1}, we have calculated a maximum efficiency of ca. 8% (unpublished data).

Richmond (2000) has explained the increasing complexity of the limitation to cell growth as culture density increases until no net growth is possible. Assuming all other conditions to be optimal, the sole limitation to photosynthetic activity and cell growth in optically thin cultures is the intensity of the light source. As cell concentration rises and the cells receive light intermittently, cell density becomes the major factor in productivity as it determines the light availability per cell. Further up on the cell concentration scale, provided nutrient limitation is barred by maintaining nutrient-sufficiency, the rate of mixing becomes increasingly effective in controlling culture growth. Thereafter, when the rate of mixing cannot lead to a further increase in productivity (Figure 7.1a) either due to shear or to reactor design limitations, the length of the optical path becomes most important in determining the light regime for individual cells. Decreasing the optical path facilitates maintenance of ultra-high cell concentrations thereby increasing the illuminated surface-to-volume ratio (S/V ratio) and the frequency of the light/dark cycles. As cell concentration rises further, growth-inhibition curtails culture growth. Despite the fact that evidence for growth inhibition has been shown, the phenomena responsible for it are still not understood. Several possibilities have been suggested and shall be discussed.

Considering only high-cell densities, let us begin at the level at which the degree of mixing determines culture productivity. The higher the intensity of the light source, the higher (potentially) becomes the optimal cell density (OCD) - cell density which yields maximal productivity per culture volume under the given circumstances (Figure 7.1b), and the more significant the degree to which the extent of mixing may exert on the output rate (Hu and Richmond, 1996; Richmond, 1996) (Figure 7.1a).

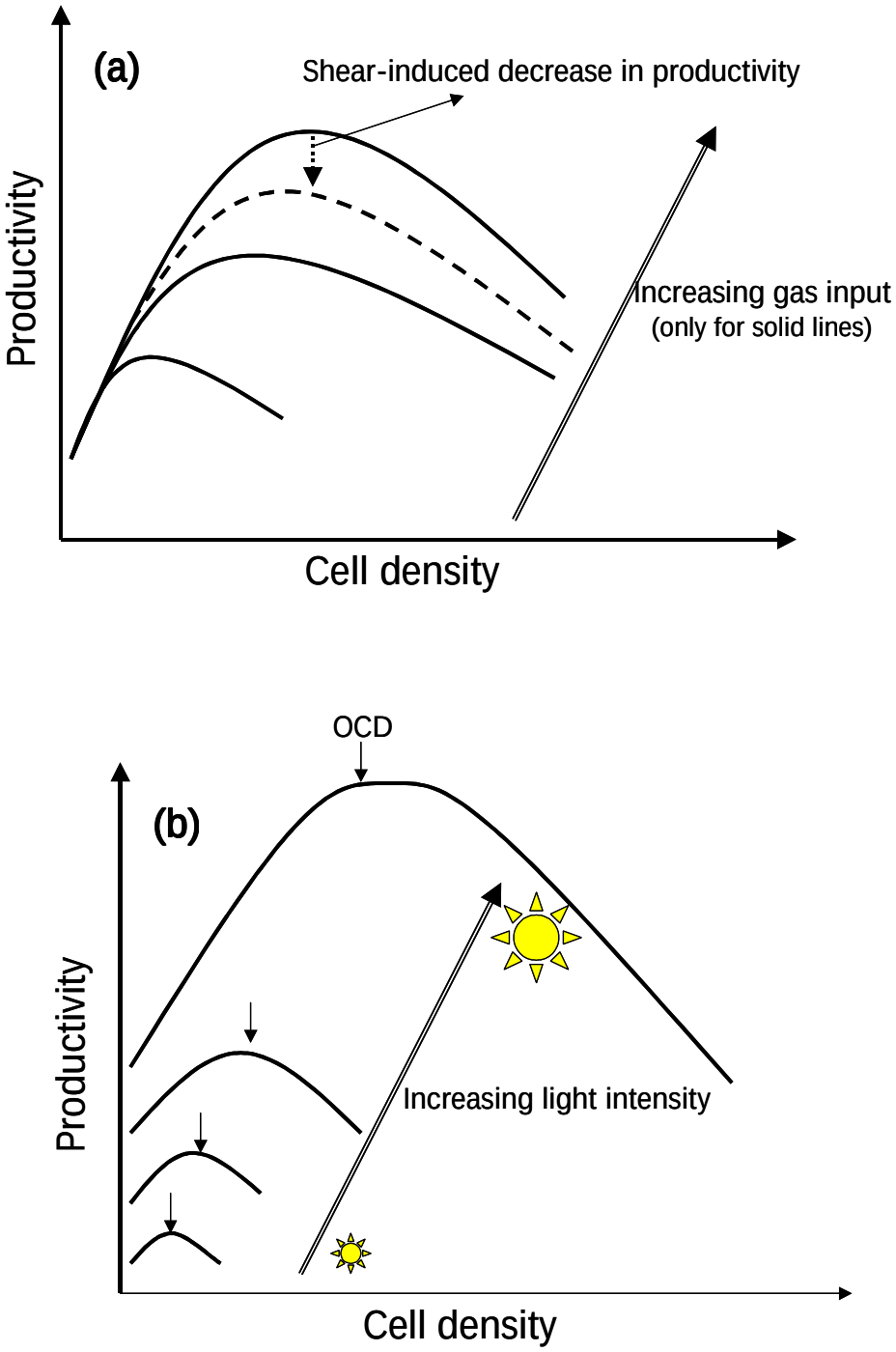

Figure 7.1. Effect of (a) gas input and (b) light intensity on optimal-cell density (OCD) and productivity (based on results from Hu and Richmond, 1996 and Hu et al., 1998). Incident light intensity and mixing rate are assumed constant in (a) and (b), respectively.

For a certain optical path, the effect of mixing rate on productivity can be seen in Figure 7.1a; increasing the mixing rate until a certain value will lead to an improvement of the light regime and a consequent increase in the optimal cell density and productivity. At this point, a further increase

of the gas flow rate can lead to two different situations (Figure 7.1a): (1) cell damage, leading to a decrease in productivity; (2) no further increase of productivity takes place due to light limitation; after a certain superficial-gas velocity (> 0.06 m s^{-1}), a further increase will not lead to an additional increase in the mean liquid velocity, instead the additional energy input leads to increased fluctuation velocities and to an increased turbulent dissipation (Michele and Hempel, 2002). At this level, improving fluid dynamics by increasing the gas input no longer results in higher productivities and therefore other options to improve fluid dynamics have to be considered. Richmond and co-workers have explored the reduction in the optical path as a means to decrease liquid circulation times inside the reactor in order to achieve higher productivities (Hu et al., 1998; Hu et al., 1996; Zou and Richmond, 2000). Reducing 27-fold the light-path, from 20 to 0.75 cm led to ca. 50% increase in areal productivity in *Spirulina platensis* (Hu et al., 1998).
The most promising photobioreactor is the flat panel with a short optical path (< 2.6 cm), as the highest biomass concentrations and photosynthetic efficiencies have been reached in this system (Janssen et al., 2003; Richmond, 1996). This is mainly due to the small optical path, which allows a fast liquid circulation in the order of tens of milliseconds (Table 7.1) and high light/dark frequency.

Gas bubbles may also affect the light regime. Gas bubbles can lead to light dispersion and light transmission through the bubbles, allowing a further penetration of light along the reactor optical path (Sánchez Mirón et al., 1999). The exact effect will depend on bubble size, light path and cell density.
Reactor and sparger design, gas input and liquid properties, all affecting the optimal cell density, are therefore the main parameters determining the light regime in photobioreactors.

Liquid circulation rate

The mechanically simple set-up of flat panels and bubble columns stands in clear contrast with the complex flow patterns, which are developed in these systems (Figure 7.4a). It is difficult therefore to fully understand and control the liquid-circulation time and bubble-size distribution in these systems.
In bubble columns and flat panels, the gas phase exists as a dispersed bubble phase in a continuous liquid phase. The gas phase moves in one of three characteristic regimes, depending upon the nature of dispersion, as follows: (1) Homogeneous bubbly flow regime at superficial gas velocities lower than 0.04 m s^{-1}, where bubbles are relatively small and of uniform diameter and concentration, and turbulence is low; (2) Heterogeneous regime, at superficial gas velocities higher than 0.075 m s^{-1}, where a wide range of bubble sizes coexists within a very turbulent liquid,

and (3) slug-flow, which is observed in columns with smaller diameters (≤ 0.1 m), at superficial gas velocities higher than 0.04 m s^{-1} and is characterised by large bubbles bridging over most of the column diameter (Figure 7.2) (Merchuk et al., 1994).

It is important to note that for media containing a large amount of dissolved salts, such as seawater, the flow transition occurs at slightly higher superficial gas velocities, due to the anti-coalescence properties of the salts (Chisti, 1989).

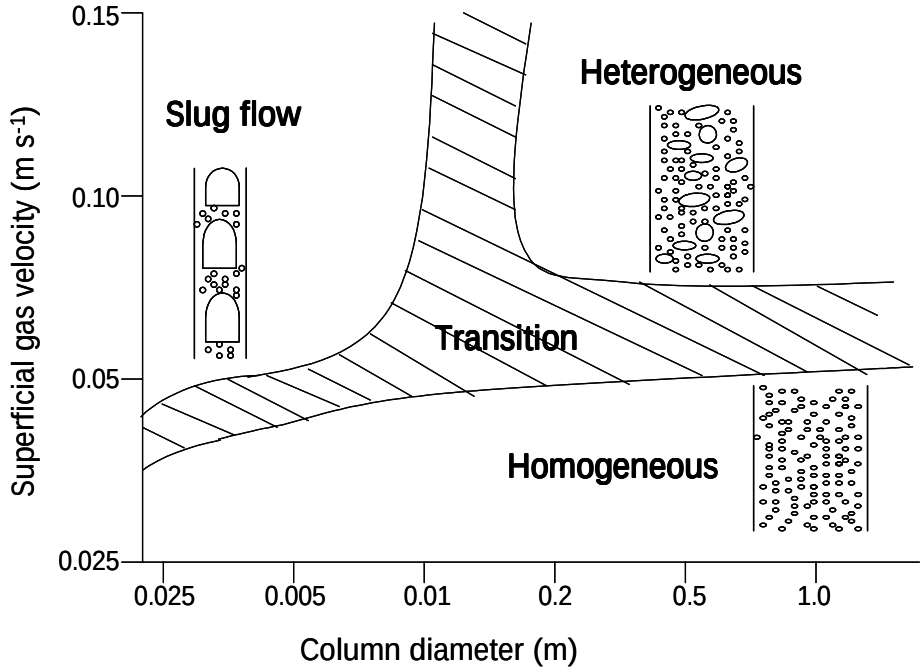

Figure 7.2. Flow regimes in bubble columns as a function of column diameter and superficial-gas velocity (Adapted from Deckwer et al., 1980).

The effect of superficial gas velocity (0.02 – 0.09 m s^{-1}) on the axial liquid velocity at different radial positions of the column and on the centerline axial liquid velocity along the column has been well described by Michele and Hempel (2002) for a pilot plant bubble column. Formation of large bubbles at high superficial gas velocities was found to be the most important effect influencing liquid velocity profiles. At superficial gas velocities of 0.02-0.04 m s^{-1}, the bubble column is operated in the homogeneous to transition flow regime where liquid backmixing is mainly due to backflow of liquid around the simple rising bubbles. Radial gradients of axial liquid velocity are rather small, and an increase of superficial gas velocity to 0.06 m s^{-1} yields a significant increase of mean liquid velocity marking the onset of the heterogeneous flow regime. Further increase of the superficial gas velocity to 0.08 and 0.09 m s^{-1} does not yield an additional increase in mean liquid velocity, instead the additional energy input leads to increased fluctuation velocities and to an increased turbulent dissipation (Michele and Hempel, 2002)

The underlying physics of flow and hence the quantitative relationship between the reactor parameters (design and operating) and the performance objectives are still not fully understood (Joshi et al., 2002).

Hydrodynamic stress

A high degree of turbulence is desirable in high cell density microalgae cultures in order to promote a high light/dark cycle frequency and improve mass transfer, as already discussed. In Table 7.1 it can be see that only at high superficial gas velocities (≥ 0.05 m s^{-1}) the average cycle time in bubble columns ($\varnothing = 0.2$ m) will be shorter than 2 s (Janssen et al., 2003). Therefore, bubble columns should be operated at the highest feasible aeration rates consistent with the shear tolerance of the microalgae strain, in order to reduce liquid circulation times (high light/dark cycle frequency).

In flat panels, lower superficial gas velocities, between 0.03 and 0.035 m s^{-1}, are required to create a high degree of turbulence (Richmond, 1996; Hu and Richmonds, 1996), with estimated liquid circulation times in the order of tens of milliseconds (80 – 240 ms) (Table 7.1).

The growth rates of some microalgae have been reported to increase initially with increasing turbulence, probably due to the improved supply of light or CO_2. As soon as the optimum level of turbulence has been reached, however, growth decreases sharply with further increase of the superficial-gas velocity (Silva et al., 1987; Suzuki et al., 1995; Hu and Richmond, 1996; Merchuk et al., 2000). This is believed to be due to cell damage, but only recently effects of hydrodynamic stress on microalgae cultures have been identified and quantified (Barbosa et al., 2003b; 2003 accepted).

Cell damage can take place during bubble formation, bubble rising or bubble break-up. Very few quantitative studies have been done regarding hydrodynamic stress in microalgae cultures grown in gas-sparged photobioreactors (Suzuki et al., 1995; Camacho et al., 2001). It has been assumed until recently that the main cause for cell damage was the bubble bursting at the liquid surface (Suzuki et al., 1995, Camacho et al., 2001). However, we have found that bubble formation is responsible for cell damage and that cell death increases with increasing gas entrance velocity beyond a certain critical value, which is strain dependent (Barbosa et al., 2003b; 2003 accepted). We concluded that the gas velocity at the sparger is an important parameter for reactor design and operation (Barbosa et al., 2003; 2003a).

These findings are supported by Tramper et al. (1987) who estimated that shear stress produced by the detaching bubbles from the sparger surface could be an order of magnitude higher than

that by the bursting bubbles and still higher than that by the rising bubbles. Murhammer and Goochee (1990) noticed a significant effect of sparger type on the survival of insect cells in air-lift bioreactors, which appeared to be correlated inversely with the pressure drop across the sparger. They proposed that the oscillation of newly formed bubbles on the sparger surface, and the sudden liquid flux to fill the space vacated by the detaching bubbles, may be responsible for cell damage in the sparger region. Knowledge on the flow patterns and hydrodynamic forces at the sparger as well as on the formation of a new bubble surface in combination with adsorption of cells would be of great importance for understanding events at the sparger and for a proper sparger design.

The best strategy presently available to follow when a reactor needs to be scaled-up and/or high superficial-gas velocities need to be used is to determine the critical gas velocity at the sparger for the strain of interest and keep gas velocity at the sparger lower than the critical value by increasing the number of nozzles or/and increasing the nozzle diameter.

At a constant gas entrance velocity, the sparger with a nozzle diameter of 0.4 mm, which led to the formation of smaller bubbles, was more detrimental to cells than the ones with nozzle diameters of 0.8 and 1.2 mm (Barbosa et al., 2003 accepted). The same behaviour has been shown for animal cells by Wu and Goosen (1995), who reported that an increase in the internal diameter of the nozzle and consequent increase of the bubble size led to a decrease in the cell death rate. In order to avoid cell death at the sparger, nozzle diameter and therefore bubble size should not be smaller than a certain value, which will be strain dependent. However, it should also not be too large due to the consequent decrease in mass transfer rate and the possibility of leading to a decrease in the light efficiency in very short-optical path flat panel reactors, as discussed further in the manuscript.

Besides a well-conceived sparger, also protective additives can be used to avoid shear-related cell damage. This is frequently used in animal cell culture in order to avoid cell death (Wu, 1995). These additives, strongly affect the physical properties of culture fluids, e.g. surface tension and viscosity. Surface-active polymers such as pluronic polyols and polyethylene glycols usually reduce the surface tension. On the other hand, cellulose derivatives and dextrans elevate the liquid viscosity (reviewed by Wu, 1995). The detrimental effect of hydrodynamic forces on microalgae cells of *Phaeodactylum tricornutum* has been reduced by adding a cellulose derivative (CMC) (Camacho et al., 2001). This additive however, enhances viscosity, which may be disadvantageous to microalgae cultures. For this reason it would be interesting to test surface-active polymers, such as pluronic, that only decrease the surface tension.

The surfactants, which may be adsorbed to the bubble film, can influence oxygen and carbon dioxide transfer rate from the bubble to the liquid medium as shall be discussed later in this

manuscript. The effects of viscosity and surface tension on mass transfer, liquid circulation and bubble size are discussed under liquid properties.

Mass transfer

Photosynthetic production of algae is always accompanied with production of oxygen and consumption of carbon dioxide. Oxygen levels above air saturation can inhibit photosynthesis in some microalgal species (Aiba, 1982) and the carbon dioxide concentration should not fall below a critical value, or the availability of the carbon source will limit growth.

The volumetric mass transfer coefficient (k_la) of the system should therefore be high enough to avoid inhibitory oxygen levels and carbon dioxide limitation in the culture medium. It is important to note that growth rate of some strains seem not to be affected by high concentrations of oxygen.

The volumetric mass transfer coefficient (k_la) is the product of two terms: (1) the mass transfer coefficient (k_l) and (2) the interfacial area per unit volume of the aerated reactor (a). The k_la is affected primarily by superficial gas velocity, sparger design and medium properties.

In the homogeneous regime, the volumetric mass-transfer coefficient increases linearly with increasing superficial gas velocity due to the larger number of bubbles formed. Under these conditions, there are no interactions between bubbles. A further increase in the superficial gas velocity results in a less than linear increase in the volumetric mass transfer coefficient, as a result of coalescence, which changes the interfacial area per unit volume of gas (Merchuck et al., 1994).

Mass transfer is substantially greater in pneumatically agitated vertical reactors, such as bubble columns and flat panels, than in horizontal tubular reactors (Hu et al., 1996; Camacho et al., 1999; Sanchez Miron et al., 1999). The poor mass-transfer capacity of horizontal tubular reactors makes them unattractive for the cultivation of photosynthetic organisms that are sensitive to high oxygen concentrations (Babcock et al., 2002).

Presently, mass transfer is not an issue in vertical gas-sparged photobioreactors. Nevertheless, as biomass concentration increases and liquid properties change, as discussed later, the mass transfer coefficient may also change.

It is possible to estimate the theoretically required mass transfer coefficients to attain a certain photosynthetic efficiency at a certain light intensity in a flat-panel reactor. At steady state the oxygen-production rate (OPR) will be equal to the oxygen-transfer rate (OTR). By knowing the OPR, the needed k_la can be calculated by means of Eq 7.1.

$$OPR = OTR = kla \cdot (C_{ol}^{*} - C_{ol}) \qquad \text{Eq 7.1}$$

where C_{ol}* is the concentration of O_2 in the liquid phase at equilibrium conditions with the gas phase and C_{ol} is the concentration of O_2 in the bulk of the liquid phase.

In order to calculate the OPR for a given incident light intensity and reactor surface to volume ratio (S/V) at the desired photosynthetic efficiency we only need to know: (1) the energy of a mol of photons (in these calculations we considered only photons with a wavelength of 680 nm, and a corresponding energy of ca. 0.175 MJ/mol photons) and (2) the energy stored in carbohydrate during photosynthesis, which is ca. 0.477 MJ/mol of O_2 produced (Tredici, 1999). Figure 7.3 shows the k_la values needed to avoid O_2 accumulation at a given photosynthetic efficiency and different equilibrium DO concentrations (150, 200 and 300%) for media with a saturation concentration of 7 mg L^{-1}. These calculations were made for two flat panel reactors with different optical paths (2.6 and 1.0 cm) and consequent different surface/volume (S/V) ratios. The incident light intensity was assumed to be 2000 μmol m^{-2} s^{-1} and the reactor dimensions (height x length x optical path) were 60 x 20 x 2.6 cm (Figure 7.3a) and 60 x 20 x 1 cm (Figure 7.3b) with corresponding S/V ratios of 38 and 100 m^{-1}, respectively. Hu et al. (1996) have measured the k_la in a flat panel reactor under different aeration rates and reported a maximal k_la value of 140 h^{-1} at a gas flow rate of 5 L L^{-1} h^{-1} (vvm). The maximum dissolved oxygen (DO) concentration reported by the same authors was 10 mg L^{-1} (ca. 150% saturation for a medium with a saturation value of 7 mg L^{-1}). Assuming 150% as the equilibrium DO concentration and a k_la of 140 h^{-1} (dotted line in Figure 7.3) it can be deduced from Figure 7.3a that a maximal photosynthetic efficiency of 15% can be reached without leading to oxygen accumulation. However, in the same flat panel with a smaller optical path (Figure 7.3b), a k_la of 140 h^{-1} would only support a maximal photosynthetic efficiency of ca. 6% at an equilibrium DO concentration of 150%, without leading to oxygen accumulation. At a higher equilibrium DO concentration of 300% saturation, a maximal photosynthetic efficiency of ca. 24% could be attained. A 300% saturation may inhibit photosynthesis in some microalgae species.

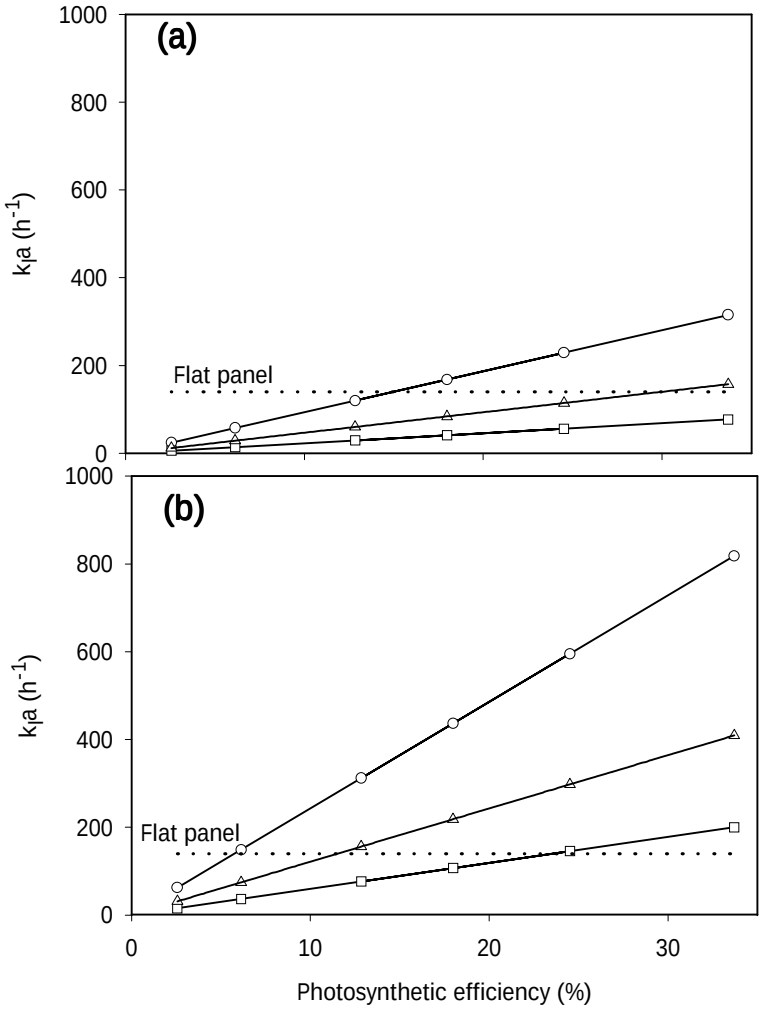

Figure 7.3. Theoretical k_la required at different photosynthetic efficiencies for steady-state oxygen concentrations. Degree of liquid-phase oxygen saturation, 150% (O), 200% (Δ) and 300% (□), for media with a saturation concentration of 7 mg L^{-1} (100%). Incident light intensity is assumed to be 2000 μmol m^{-2} s^{-1}. Calculations were made for a flat panel 0.60 m high and 0.20 m long with a optical path and surface/volume ratio of (a) 0.026 m and 38 m^{-1}, respectively and (b) 0.010 m and 100 m^{-1}, respectively. Dotted lines represent the k_la measured in a flat-panel reactor by Hu et al. (1996).

These calculations are meant to point out that decreasing the optical path and working at ultra-high cell densities may lead to mass-transfer limitations, even in flat-panel reactors. Moreover changes in the liquid properties such as viscosity and surface tension also affect the mass-transfer coefficient as discussed further in this manuscript.

For the above reasons is important to determine mass-transfer characteristics in high-cell density cultures in order to avoid oxygen accumulation and carbon dioxide limitation.

Future issues

High biomass concentrations can be reached in short-optical path flat panels. An optimal biomass concentration of 20 g L^{-1} has been reported by Hu et al. (1998) in a flat panel with an optical path of 1.4 cm and an incident light intensity of 2000 μmol m^{-2} s^{-1}. At this point one can envision new aspects that should be considered in order to have a successful process.

Reactor optical path

As explained before, the decrease in optical path can lead to a substantial improvement of the productivity due to a higher light efficiency. Certain limitations should be considered however, and the fluid dynamics should be more carefully looked at.

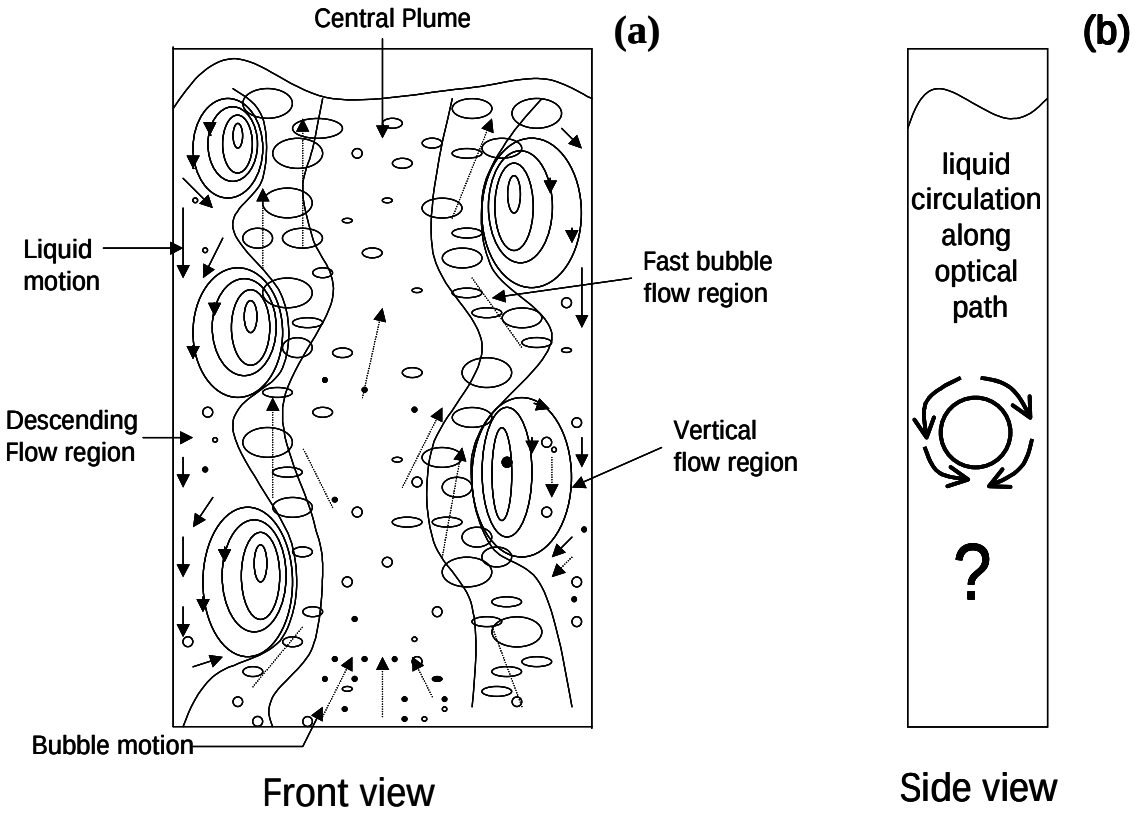

Figure 7.4. Scheme of a flat panel: (a) Flow pattern observed by Tzeng et al. (1993) in a flat panel (0.483 m x 1.6 m x 0.0127 m) with a gas distributor composed of multiple injectors, which were individually regulated, transition regime, front view (adapted from Tzeng et al. 1993); (b) side view, showing the important of liquid circulation time along the reactor optical path.

At the moment, in our lab we are undertaking some growth experiments with *Spirulina platensis* M2 grown in a flat panel with an optical path of 0.5 cm. Despite reaching very high biomass

concentrations, new problems arise. Due to the very small optical path, large bubbles occupying the entire optical path allow light to pass unabsorbed through the reactor. This effect is enhanced by bubble coalescence, which results in the formation of larger bubbles, allowing more light to pass through the reactor thereby becoming wasted. Moreover, with increasing biomass concentration (until 25 g L^{-1}) and a consequent increase in viscosity, a slug-flow regime could be seen, resulting in a large part of the light not being utilised by the algae (Figure 7.5) and in a poor mixing along the optical path (Figure 7.4b).

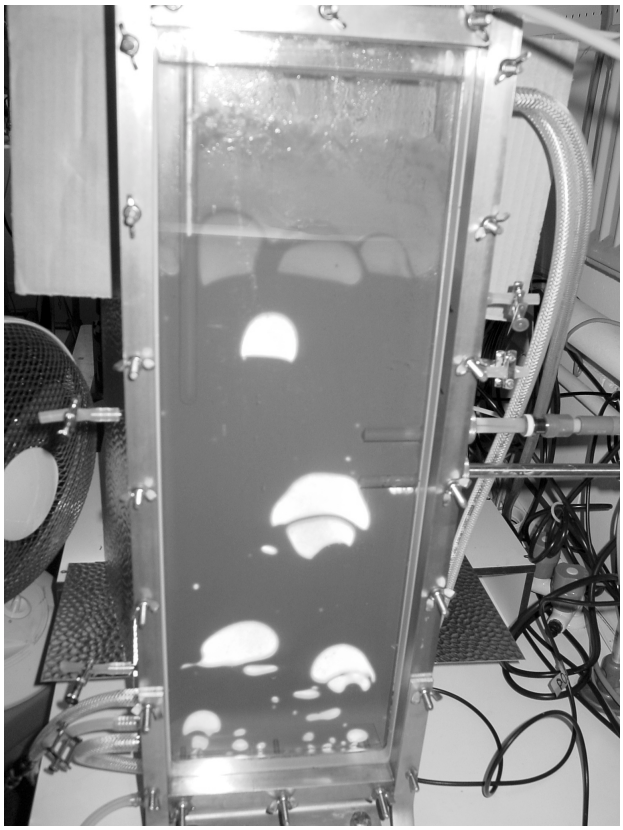

Figure 7.5. Slug flow regime in a flat panel (0.5 x 0.2 x 0.005 m) with an optical path of 0.5 cm and a biomass concentration of 25 g L^{-1} of *Spirulina platensis*. Gas-flow rate was 3.5 L min^{-1}

Therefore, in order to work with flat panels with short optical paths it is necessary to further investigate a current unknown area: the flow regimes that can be found in these systems and how to avoid slug flow regimes, keeping bubble sizes small all along the reactor width and height.

Sparger design

Depending on the liquid (culture and medium) properties, sparger design will determine the bubble size (Wu and Goosen, 1995; Contreras et al., 1999; Buwa and Ranade, 2002) and bubble size distribution (Buwa and Ranade, 2002; Polli et al., 2002).

Several parameters related to sparger design will influence bubble size: sparger type (sintered glass, perforated plate, -ring, -pipe and nozzle sparger), number and diameter of the orifice / nozzles and the distance between them (pitch) (Buwa and Ranade, 2002; Polli et al., 2002). The most practical and simple spargers to be used in flat panels are the perforated pipe and nozzle sparger.

For non-coalescing systems the sparger determines bubble size in the whole reactor (Schafer et al., 2002) while for coalescing gas-liquid systems the influence of the sparger configuration on bubble size distributions in large bubble columns is restricted mainly to a distance from the sparger to a distance of the order of magnitude of the vessel diameter (Polli et al., 2002). This is due to the suppression of the effect of primary gas dispersion by fast bubble coalescence at the point of entry into the reactor.

The main effects of sparger design on bubble-size distribution (BSD) are the following: (1) Gas-flow rate and orifice diameter have the same effect on BSD: the increase in the value of both parameters leads to a shift of the BSD towards larger bubble sizes; (2) Increasing the number of orifices, which is the same as decreasing the gas flow rate through each orifice, the BSD shifts to smaller sizes; (3) Breakage rate is faster on increasing gas velocity due to enhancement of bubble-bubble interactions. Increasing the superficial gas velocity, larger bubbles are produced but, after a certain distance from the sparger, smaller bubbles can be observed due to bubble breakage (Polli et al., 2002); (4) Decreasing the pitch, i.e. distance between nozzles, can lead to an increase in bubble diameter due to coalescence, when the ratio of the pitch to the orifice / pour diameter is less than approximately 8 (Miyahara et al., 1983).

There is no information on how sparger design will influence fluid dynamics. In microalgae cultivations, increasing the liquid-circulation time along the reactor optical path (Figure 7.4a, b) would be of great importance due to the decrease in the light/dark cycle frequency. Richmond and Hu (1997) and Hu et al. (1998) studied the effect of the optical path on productivity in a flat panel. The experiments were done in different reactors with different optical paths but with the same sparger, a perforated pipe extending along the bottom of the reactors. The amount of litres of air per litre culture suspension per minute (vvm) was kept constant as well as the incident light intensity. The optimal cell density decreased from 26.6 to 0.6 g L^{-1} and volumetric productivity decreased from 0.621 to 0.012 g L^{-1} h^{-1} with increasing optical path from 0.75 to 20 cm. The estimated average duration of the light/dark cycle increased linearly with increasing the length of the optical path at a constant superficial gas velocity (Richmond and Hu, 1997). This brought up the question if it would be possible, using a proper sparger design to enhance mixing along the reactor optical path as the optical path is increased. There are several design possibilities for designing a sparger. The nozzle diameter and number of nozzles should be chosen by taking into consideration the strain-dependent critical gas-entrance velocity, being therefore important

parameters in avoiding cell damage (Barbosa et al., 2003b, 2003 accepted). In addition, the spatial distribution of the nozzles should be designed considering the optimal pitch, in order to avoid immediate bubble coalescence. Even with these design criteria there are still different possible ways to design a sparger. It would be important therefore to study a possible effect of sparger design on the mixing along the reactor optical path. Computational fluid dynamics (CFD) would serve as a useful tool to bring insight in this field of research.

Liquid properties

The liquid properties that will play an important role in the future, as high-cell density cultures become common, are the coalescing capacity of the medium as well as the viscosity and surface tension. These properties will influence liquid circulation and bubble-size distribution (BSD), which are in turn a result of bubble formation as well as bubble coalescence and break-up.

Coalescence

Coalescence in aqueous systems decreases with increasing concentration of ions and hydrocarbons due to formation of a boundary layer at the gas-liquid interface. Bubble coalescence has been reported to increase when decreasing the sodium chloride concentration (Sanchez Mirón et al., 1999).

Since bubble size-distribution (BSD) is strongly influenced by the coalescence properties of the liquid, the light distribution and volumetric mass-transfer coefficient of the system are also influenced by the coalescing properties of the liquid.

Seawater, which is a common medium in microalgae biotechnology, has non-coalescing properties but due to the increase in biomass concentration, culture properties may change in time. Indeed, Calderbank et al. (1964) found that liquid viscosity largely determines the extent of bubble coalescence.

Viscosity

Fermentation broths may become viscous in high-cell density cultures. The effect of viscosity on fluid dynamics in photobioreactors is therefore of importance for cultivation of different microalgae and cyanobacteria strains. Glycerol producing strains such as *Dunaliella salina* can lead to a high-viscosity medium since glycerol is a thickening agent (Croughan et al., 1989).

A large number of cyanobacteria are characterized by the presence of polysaccharidic investments (i.e. sheaths, capsules and slimes) (De Philippis et al., 2001). Moreover, many polysaccharide-producing strains release into the culture medium alicots of their capsule or slime rich in a water-soluble polymer (De Philippis et al., 2001). Some red algae such as *Porphyridium sp*. and *Rhodella reticulata* are encapsulated within cell-wall polysaccharides, the external part of

which dissolves in the culture medium (Singh et al., 2000). In flat-panel reactors with *Porhyridium sp*., the rise in viscosity followed the same pattern as that of the increase in soluble polysaccharide, implying that viscosity was directly related to the extracellular release of soluble sulphated polysaccharides into the medium. In addition to product accumulation, which increases the viscosity of the cell free medium, the viscosity of cell suspension is also positively related to cell density for filamentous species (Tramper and van't Riet, 1991), as the majority of cyanobacteria.

Increasing the liquid viscosity leads to a reduction of the turbulence in the liquid flow (Schafer et al., 2002), reducing the liquid flow probably due to a greater frictional resistance to flow. The energy of eddies is reduced and bubble breakage damped, leading to increased bubble sizes (Schafer et al., 2002). For this reason, some viscosity-enhancing polymers are used as cell protective agents (Croughan et al., 1988).

In turbulent regimes (0.2-0.4 m s^{-1}), increasing viscosity from 0.001 to 0.075 Pa s did not change the radial distribution of liquid velocity and the centre-line liquid velocity in bubble columns of 0.38 m diameter and 2 m high (Baten and Krishna, 2001). The same was observed by Grima et al. (1999b), within a viscosity range of 0.00154 – 0.0195 Pa s in a split-cylinder airlift bioreactor operated in homogeneous and heterogeneous regimes. This was attributed to the compensation of any viscosity-associated increase in frictional resistance to flow by a corresponding increase in the driving force for liquid circulation (Grima et al., 1999b). The driving force is the difference between the gas hold-ups of the riser and downcomer, which increases with increasing viscosity (Grima et al., 1999b); as viscosity increases, the mean bubble size in the riser increases. Only the smaller bubbles are dragged into the downcomer zone; larger bubbles leave the reactor because their rise velocity far exceeds the downflow velocity of the liquid. Hence, with increasing viscosity and a consequent bigger bubble size, fewer and fewer bubbles move into the downcomer (Grima et al., 1999), leading to a decrease in the hold up. Other authors however have observed a decline in the liquid-circulation rate in air-lift reactors with increasing viscosity (Popovic and Robinson 1984; Weiland, 1984). This is a very important subject for microalgae cultures due to the requirement of short circulation times. If the liquid-circulation time increases due to an increase in viscosity, some measures should be taken in order to avoid a decline in productivity, such as increasing the gas flow rate.

Presently high microalgae cell densities and hence high viscous media can only be obtained in short-optical path flat panel-reactors. In these systems, the circulation rate along the optical path is a major parameter determining photosynthetic efficiency. In our lab, we have visually observed a decrease in the liquid mixing rate with increasing viscosity in flat panels with optical paths of 1.0 and 0.5 cm. Therefore, more knowledge on the effect of viscosity on the radial liquid-circulation time along the flat panel optical path is needed for a proper understanding of the effect of

increases in viscosity. It should be noted that viscosity could be reduced by addition of a commercial polysaccharide-hydrolysing enzyme preparation such as Glucanex® (Novo Nordisk, Neumatt, Switzerland) (de Swaaf et al., 2003)

The viscosity of the liquid, which is a property affecting the liquid-phase momentum, will affect both k_l and a, the latter most pronounced. Increasing viscosity has been reported to strongly decrease the mass transfer coefficient (k_la) in a 1L fermenter (de Swaaf et al., 2001) and in a bubble column (Elgozali et al., 2002). This might be due to the decrease in turbulence, a corresponding increase in the mean bubble size and a consequent decrease of the specific interfacial area (a). As previously discussed a good mass transfer is also important in microalgae cultivations in order to reduce O_2 pressure and supply carbon dioxide effectively.

Surface tension

Surface tension affects bubble coalescence and break-up, and therefore affects the interfacial area, although the mechanism by which this occurs is not clear (Merchuk et al., 1994). Decreasing surface tension may lead to an increase in the interfacial area (a) due to a decrease in coalescence. In addition, a decrease in the mass-transfer coefficient (k_l) may also occur due to the adsorption of surfactants to the gas-liquid interface. For this reason, a net reduction of the volumetric mass-transfer coefficient (k_la) can take place after adding surfactants such as pluronic (protective non-ionic surfactant used in animal cell culture) to the medium (Murhammer and Pfalzgraf, 1992). The specific effect on k_la depends on the type of surfactant used (Chisti, 1999).

For liquids with comparable physical properties lower surface tension results in smaller bubble size. This is seen by comparing nitrogen bubble sizes in water and in cyclohexane at ambient conditions (Schafer et al., 2002). For both systems, viscosity was nearly the same and liquid densities were comparable, but the surface tension of cyclohexane is almost one third of water. Despite the bubble size at the sparger being only slightly bigger for the system with water, bubble size increased with increasing height of the column (until a height of 0.7 m). In the cyclohexane system in contrast, with a much lower surface tension, bubble size did not change along the column.

In conclusion, Table 7.2 shows the main effects of liquid properties on the stable bubble size, k_la, coalescing properties, liquid circulation time and turbulence. It should be noted that this is a qualitative analysis. Due to its complexity, the interactions between fluid properties are not fully understood. Nevertheless, the present knowledge should be useful for running successful high-cell density cultures.

Table 7.2. Influence of liquid properties on different parameters.

	Cycle time	k_la	Coalescence	Bubble size	Turbulence
Ions and hydrocarbons ↑	-	↓	↓	↓	-
Viscosity ↑	contradictory	↓	↑	↑	↓
Surface tension ↓	-	[a]	↓	↓	-

[a] Depends on the type of surfactant

(-) Not known

Growth Inhibition

Several authors have reported growth inhibition in high-cell densities cultures. The exact inhibition factor is still unclear and remains controversial. Some authors suggest the production of autoinhibitory metabolites by some species (Pratt and Fong, 1940; Harris, 1971; Javanmardian and Palsson, 1991; Imada et al., 1992) as the inhibiting factor while others attribute the inhibition to an imbalance of nutrients in the culture medium (Mandalam and Palsson, 1995; 1998). In addition, the presence of particulate material in the culture medium, mainly cell-wall remains released during cell division, has been pointed out as a possible cause of growth inhibition (Rodolfi et al., in press). In order to achieve high cell-density microalgae cultures, a carefully balanced nutrient medium should be maintained and/or "growth inhibition" has to be removed, e.g. by ultrafiltration of the growth medium (Javanmardian and Palsson, 1991) or by complete replacement of culture medium with fresh medium (Richmond et al., in press; Richmond and Zou, 1999; Zou et al., 2000). Richmond et al. (2003) have shown a considerable improvement in the areal productivity by daily replacing the entire growth medium by fresh medium, in comparison to only adding nutrients to the culture medium, but not replacing it.

Recycling the growth medium, which demands improvement of medium quality before reutilisation, may be a way of reducing the need for big facilities to store and treat the waste medium as well as a means by which to reduce water usage, "growth inhibition" being removed during this step. Separation processes such as ultrafiltration and high-speed centrifugation could be used for the treatment of waste growth medium. This would require high costs, and therefore might only be advantageous for the production of high-value compounds such as pharmaceuticals. However, for a precise conclusion, an economical analysis should be done. On the other hand, if growth inhibition is mainly due to nutrient imbalance, a different measure, e.g. proper medium design, should be taken in order to be able to sustain high cell densities. More research is therefore needed in this field in order to maintain cost-effectively high cell densities in photobioreactors.

Concluding remarks

From previous works it can be concluded that high volumetric productivities and high light efficiencies can be obtained in flat-panel reactors. This brings along new aspects to be considered for future research and a new challenge for microalgae biotechnologists, i.e. manage cultures of high-biomass densities. The success of flat panels relies on the possibility of working with short optical paths, which allow fast circulation rates of cells from the light to the dark zones of the reactor at a high frequency.

The length of the optical path must yet be optimised in combination with the fluid dynamics in the system. Very small optical paths can lead to slug flow regimes (Figure 7.5) and a consequent decline in efficiency of light intensity used, due to light passing through the large bubbles. On the other hand, long optical paths lead to a decrease in productivity due to larger circulation times associated with wasteful dark period in the light/dark cycle. Avoiding slug flows in very short optical path reactors and/or improving the liquid circulation time along the reactor optical path are still new areas to be researched. They entail a proper sparger design and more knowledge on the liquid properties during microalgae cultivations, e.g. coalescence, viscosity surface tension and their effect on the fluid dynamics. The sparger design should aim at decreasing the liquid-circulation time, taking into consideration the specific stress-resistance capacity of each strain as cell death takes place at the sparger site. The liquid properties, especially viscosity, will be of relevance for high-cell density cultures. Several different strains of microalgae possess polysaccharides in their cellular membrane or polysaccharidic investments, which can lead to an increase in culture viscosity as cell density rises. This can lead to changes in bubble size and possibly in liquid-circulation time. The exact effects have yet to be studied, being an important factor in the process of optimisation of microalgal high-cell density cultures. Finally, and because an efficient photobioreactor must also be able to sustain cells at high concentrations, growth inhibition should be further studied. Despite existing clear evidences of this phenomenon at high cell densities, little is known on its exact nature. Presently, growth inhibition is thought to be due to the production of autoinhibitory molecules and/or to nutrients imbalance in the culture medium. However these phenomena are still far from being clearly understood.

References

Abalde J, Fabregas J. 1991. β-carotene, vitamin C and vitamin E content of the marine microalga *Dunaliella tertiolecta* cultured with different nitrogen sources. Bioresource Technol 38:121-125.

Abe K, Nishimura N, Hirano M. 1999. Simultaneous production of β-carotene, vitamin E and vitamin C by the aerial microalga *Trentepohlia aurea*. J Appl Phycol 11:331-336.

Aiba S. 1982. Growth kinetics of photosynthetic microorganisms. Adv Biochem Eng 23:85-156.

Albergaria H, Duarte LC, Amaral-Collaco MT, Girio FM. 2000. Study of *Saccharomyces uvarum* CCMI 885 physiology under fed-batch, chemostat and accelerostat cultivation. Food Technol Biotechnol 38:33-38.

Annadurai G. 2000. Design of optimum response surface experiments for adsorption of direct dye on chitosan. Bioprocess Eng 23:451-455.

Apt KE, Behrens PW. 1999. Commercial developments in microalgal biotechnology. J Phycol 35:215-226.

Babcock Jr RW, Malda J, Radway JC. 2002. Hydrodynamics and mass transfer in a tubular airlift photobioreactor. J Appl Phycol 14:169-184.

Barbosa M J, Janssen M, Ham N, Tramper J, Wijffels RH. 2003a. Microalgae cultivation in air-lift reactors: modeling biomass yield and growth rate as a function of mixing frequency. Biotechnol Bioeng 82:170-179.

Barbosa MJ, Albrecht M, Wijffels R. 2003b. Hydrodynamic stress and lethal events in sparged microalgae cultures. Biotechnol Bioeng 83:112-120.

Barbosa MJ, Hoogakker J, Wijffels EH. 2003c. Optimisation of cultivation parameters in photobioreactors for microalgae cultivation using the A-stat technique. Biomol Eng, in press.

Barbosa, MJ, Hadyianto, Wijffels R. 2003. Overcoming shear stress in sparged photobioreactors. Biotechnol Bioeng. Accepted for publication in Biotechnol Bioeng.

Baten JM, Krishna R. 2001. Eulerian simulations for determination of the axial dispersion of liquid and gas phases in bubble column operating in the churn-turbulent regime. Chem Eng Sci 56:503-512.

Benemann JR, Tillett DM, Weissman JC. 1987. Microalgae biotechnology. Trends Biotechnol 5:47-53.

Bosca C, Dauta A, Marvalin O. 1991. Intensive outdoor algal cultures: How mixing enhances the photosynthetic production rate. Bioresource Technol 38:185-188.

Brown MR, Hohmann S. 2002. Effects of irradiance and growth phase on the ascorbic acid content of *Isochrysis sp*. T.ISO (Prymnesiophyta). J Appl Phycol 14:211-214.

Broekmans WM, Berendschot TT, Klopping-Ketelaars IA, de Vries AJ, Goldbohm RA, Tijburg LB, Kardinaal AF, van Poppel G. 2002. Molecular pigment density in relation to serum and adipose tissue concentrations of lutein and serum concentrations of zeaxanthin. Am J Clin Nutr 76:595-603.

Bronnemeier R, Markl H. 1982. Hydrodynamic stress capacity of microorganisms. Biotechnol Bioeng 24:553-578.

Buwa VV, Ranade VV. 2002. Dynamics of gas-liquid flow in a rectangular bubble column: experiments and single/multi-group CFD simulations. Chem Eng Sci 27:4715-4736.

Camacho FG, Gomez AC, Fernandez FGA, Sevilla JMF, Grima EM. 1999. Use of concentric-tube airlift photobioreactors for microalgal outdoor mass cultures. Enzyme Microb Tech 24:164-172.

Camacho FG, Gomez AC, Sobczuk TM, Grima EM. 2000. Effects of mechanical and hydrodynamic stress in agitated, sparged cultures of *Porphyridium cruentum*. Process Biochem 35:1045-1050.

Camacho FG, Grima EM, Miron AS, Pascual VG, Chisti MY. 2001. Carboxymethyl cellulose protecs algal cells against hydrodynamic stress. Enzyme Microb Tech 29:602-610.

Calderbank PH, Moo-Young MB, Bibby R. 1964. Proc Third European Symp Chem Reaction Eng, North Holland, Amsterdam p 91.

Casper-Lindley C, Björkman O. 1998. Fluorescence quenching in four unicellular algae with different light-harvesting and xantophyll-cycle pigments. Photosynth Res 56:277-289.

Chalmers JJ. 1996. Shear sensitivity of insect cells. Cytotechnol 20:163-171.

Chisti MY. 1989. Air-lift bioreactors. London: Elsevier Applied Science. 339 p.

Chisti MY. 1999. Mass transfer. In: Flickinger MC, Drew SW (Eds). Encyclopedia of bioprocess technology: Fermentation, biocatalysis, and bioseparation. John Wiley & Sons, Inc. p 1607-1640.

Contreras A, Garcia F, Molina EM, Merchuk JC. 1999. Influence of sparger on energy dissipation, shear rate, and mass transfer to seawater in a concentric-tube airlift bioreactor. Enzyme Microb Tech 25:820-830.

Cohen Z. 1999. Products from microalgae. In Handbook of Microalgal Mass Culture. p 421-454.

Croughan MS, Sayre ES, Wang DIC. 1989. Viscous reductions of turbulent damage in animal cell culture. Biotechnol Bioeng 33:862-872.

Cornet JF, Dussap CG, Cluzel P, Dubertret G. 1992. A structured model for simulation of cultures of the cyanobacterium *Spirulina platensis* in photobioreactors: II. Identification of kinetic parameters under light and mineral limitations. Biotechnol Bioeng 40:826-834.

Deckwer W-D, Louisi Y, Zaidi A, Ralek M. 1980. Hydrodynamic properties of the Fischer-Tropsch slurry process. Ind Eng Chem Process Design Dev 19:699-708.

de Philippis R, Sili C, Paperi R, Vincenzini M. 2001. Exopolysaccharide-producing cyanobacteria and their possible exploitation: A review. J Appl Phycol 13:293-299.

de Swaaf ME, Grobben GJ, Eggink G, de Rijk TC, van der Meer P, Sijtsma L. 2001. Characterisation of extracellular polysaccharides produced by *Crypthecodinium cohnii*. Appl Microbiol Biotechnol 57:395-400.

de Swaaf ME, Sijtsma L, Pronk JT. 2003. High-cell-density fed-batch cultivation of the docosahenaenoic acid producing marine alga *Crypthecodinium cohnii*. Biotechnol Bioeng 81:666-672

Doba T, Burton GW, Ingold KU. 1985. Antioxidant and co-antioxidant activity of vitamin C. The effect of vitamin C, either alone or in the presence of vitamin E or water-soluble vitamin E analogue, upon the peroxidation of aqueous multilamellar phopholipid liposomes. Biochim Biophys Acta 835:298-303.

Dubinsky Z, Falkowski PG, Wyman K. 1986. Light harvesting and utilization by phytoplankton. Plant Cell Physiol 27:1335-1349.

Elgozali A, Linek V, Fiavola M, Wein O, Zahradnik J. 2002. Influence of viscosity and surfaace tension on performance of gas-liquid contactor with ejector type gas distributor. Chem Eng Sci 57:2987-2994.

Evers EG. 1991. A model for light-limited continuous cultures: growth, shading, and maintenance. Biotechnol Bioeng 38:254-259.

El-Helow E.R, Abdel-Fattah YR, Ghanem KM, Mohamad EA. 2000. Application of the response surface methodology for optimizing the activity of an aprE-driven gene expression system in *Bacillus subtilis*. Appl Microbiol Biotechnol 54:515-520.

Falkowski PG, Owens TG. 1980. Light-shade adaptation; two strategies in marine phytoplankton. Plant Physiol 66:592-595.

Falkowski PG, Owens TG, Ley AC, Mauzerall D. 1981. Effects of growth irradiance levels on the ratio of reaction centers in two species of marine phytoplankton. Plant Physiol 68:969-973.

Falkowski PG, LaRoche J. 1991. Acclimation to spectral irradiance in algae. J Phycol 27:8-14.

Fernandez FGA, Camacho FG, Perez JAS, Sevilla JMF, Grima EM. 1998. Modeling of biomass productivity in tubular photobioreactors for microalgal cultures: Effects of dilution rate, tube diameter, and solar irradiance. Biotechnol Bioeng 58:605-616.

Fabregas J, Herrero C. 1990. Vitamin content of four marine microalgae. Potential use as source of vitamins in nutrition. J Ind Microbiol 5:259-264.

Green B, Kühlbrandt W. 1995. Sequence conservation of light-harvesting and stress-response proteins in relation to the three-dimensional molecular structure of LHC II. Photosynth Res 44:139-148.

Grima EM, Camacho FG, Perez JAS, Sevilla JMF, Fernandez FGA, Gomez AC. 1994. A mathematical method of microalgal growth in light-limited chemostat culture. J Chem Technol Biotechnol 61:167-173.

Grima EM, Sevilla JMF, Perez JAS, Camacho FG. 1996. A study on simultaneous photolimitation and photoinhibition in dense microalgal cultures taking into account incident and averaged irradiances. J Biotechnol 45:59-69.

Grima EM, Acién Fernandez FG, Camacho FG, Chisti Y. 1999a. Photobioreactors: light regime, mass transfer and scale-up. J Biotechnol 70:231-247.

Grima EM, Contreras GA, Chisti MY. 1999b. Gas holdup, liquid circulation and mixing behavior of viscous newtonian media in a split-cylinder airlift bioreactor. Trans IChemE 77:27-32.

Grobbelaar JU. 1989. Do light/dark cycles of medium frequency enhance phytoplankton productivity? J Appl Phycol 1:333-340.

Grobbelaar JU. 1991. The influence of light/dark cycles in mixed algal cultures on their productivity. Bioresource Technol 38:189-194.

Gudin C, Chaumont D. 1991. Cell fragility - The key problem of microalgae mass production in closed photobioreactors. Bioresource Technol 38:145-151.

Hu Q, Richmond A. 1996. Productivity and photosynthetic efficiency of *Spirulina platensis* as affected by light intensity, algal density and rate of mixing in a flat plate photobioreactor. J Appl Phycol 8:139-145.

Handa A, Emery AN, Spier RE. 1985. On the evaluation of gas-liquid interfacial effects on hybridoma viability in bubble column bioreactors. Dev Biol Stand 66:241-253.

Harris DO. 1971. Growth inhibitors produced by the green algae (Volvocaceae). Arch Mikrobiol 76:47-50.

Harris EH. 1989. The *Chlamydomonas* sourcebook: a comprehensive guide to biology and laboratory use. San Diego: Academic press.

Haaland P. 1989. Experimental design in biotechnology. New York and Basel: Marcel Dekker, INC. 259 p.

Hu Q, Guterman H, Richmond A. 1996. A flat inclined modular photobioreactor for outdoor mass cultivation of photoautotrophs. Biotechnol Bioeng 51:51-60.

Hu Q, Zarmi Y, Richmond A. 1998. Combined effects of light intensity, light-path and culture density on output rate of *Spirulina platensis* (Cyanobacteria). Eur J Phycol 33:165-171.

Hwang S, Hansen CL. 1997. Modeling and optimisation in anaerobic bioconversion of complex substrates to acetic and butyric acids. Biotechnol Bioeng 54:451-460.

Imada N, Kobayashi K, Kasuaki I, Saito H, Kimura S, Tahara K, Oshima Y. 1992. Isolation and identification of an autoinhibitor produced by *Skeletonema costatum*. Nippon Suisan Gakkaishi 58:1687-1692.

Janssen M, Kuijpers TC, Veldhoen B, Ternbach MB, Tramper J, Mur LR, Wijffels R.H. 1999. Specific growth rate of *Chlamydomonas reinhardtii* and *Chlorella sorokiniana* under medium duration light/dark cycles: 13-87 s. J Biotechnol 70:323-333.

Janssen M, de Bresser L, Baijens T, Tramper J, Mur LR, Snel JFH, Wijffels RH. 2000a. Scale-up aspects of photobioreactors: effects of mixing-induced light/dark cycles. J Appl Phycol 12: 225-237.

Janssen M, de Winter M, Tramper J, Mur LR, Snel JFH, Wijffels RH. 2000b. Efficiency of light utilization of *Chlamydomonas reinhardtii* under medium-duration light/dark cycles. J Biotechnol 78:123-137.

Janssen M, Slenders P, Tramper J, Mur LR, Wijffels RH. 2001. Photosynthetic efficiency of *Dunaliella tertiolecta* under short light/dark cycles. Enzyme Microb Tech 29:298-305.

Janssen M, Tramper J, Mur LR, Wijffels RH. 2003. Enclosed outdoor photobioreactors: light regime, photosynthetic efficiency, scale-up and future prospects. Biotechnol Bioeng 81:193-210.

Jansson S. 1994. The light-harvesting chlorophyll *a/b*-binding proteins. Biochim Biophys Acta 1184:1-19.

Javanmardian M., Palsson BO. 1991. High-density photoautotrophic algal cultures: Design, construction and operation of a novel photobioreactor system. Biotechnol Bioeng 38:1182-1189.

Joshi JB, Vitankar VS, Kulkarni AA, Dhotre MT, Ekambra K. 2002. Coherent flow structures in bubble column reactors. Chem Eng Sci 57:3157-3183.

Jobses I, Martens D, Ramper JA. 1991. Lethal events during gas sparging in animal cell culture. Biotechnol Bioeng 37:484-490.

Joshi B, Sharma MM. 1979. A circulation cell model for bubble column. Trans IChemE 57:244-252.

Kask S, Laht TM, Pall T, Paalme T. 1999. A study on growth characteristics and nutrient consumption of *Lactobacillus plantarum* in A-stat culture. Antonie Van Leeuwenhoek Int J Gen Molec Microbiol 75:309-320.

Kok B. 1953. Experiments on photosynthesis by *Chlorella* in flashing light. In: Burlew JS, Editor. Algal Culture. Washington: Carnegie Institution of Washington. p 63-75.

Krinsky NI. 1964. Carotenoid de-epoxidation in algae. I. Photochemical transformation of antheraxanthin to zeaxanthin. Biochim Biophys Acta 1184:1-19.

Kusmic C, Barsacchi R, Barsanti L, Gualtieri P, Passarelli V. 1999. *Euglena gracilis* as source of the antioxidant vitamin E. Effect of culture conditions in the wild strain and in the natural mutant WZSL. J Appl Phycol 10:555-559.

Lee YK, Pirt SJ. 1981. Energetics of photosynthetic algal growth: influence of intermittent illumination in short (40 s) cycles. J. Gen. Microbiol. 124: 43-52.

Matthijs HCP, Balke H, Hes van HM, Kroon BMA, Mur LR, Binot RH. 1996. Application of light-emitting diodes in bioreactors: Flashing light effects and energy economy in algal culture (*Chlorella pyrenoidosa*). Biotechnol Bioeng. 50:98-107.

Märkl H, Bronnexnmeier R, Wittek, B. 1991. The resistance of microorganisms to hydrodynamic stress. Int Chem Eng 31:185 197.

Meijer EA, Wijffels RH. 1998. Development of a fast, reproducible and effective method for the extraction and quantification of proteins of micro-algae. Biotechnol Techniques 12:353-358.

Melis A. 1999. Photosystem-II damage and repair cycle in chloroplasts: what modulates the rate of photodamage *in vivo*? Trends Plant Sci 4:130-135.

Melis A, Neidhart J, Benemann JR. 1999. *Dunaliella salina* (Chlorophyta) with small chlorophyll antenna sizes exhibit higher photosynthetic productivities and photon use efficiencies than normally pigmented cells. J Appl Phycol 10:515-525.

Merchuk JC, Ben ZS, Niranjan K. 1994, Why use bubble column bioreactors? Trends Biotechnol 12:501-511.

Merchuk, JC, Ronen M, Giris S, Arad S M. 1998. Light/dark cycles in the growth of the red microalga *Porphyridium* sp. Biotechnol Bioeng 59:705-713.

Merchuk JC, Gluz M, Mukmenev I. 2000. Comparison of photobioreactors for cultivation of the red microalga *Porphyridium sp*. J Chem Tech Biotechno 75:1119-1126.

Mandalam RK, Palsson BO. 1995. *Chlorella vulgaris* (Chlorellaceae) does not secret autoinhibitors at high cell densities. Am J Bot 82:955-963.

Mandalam RK, Palsson BO. 1998. Elemental balancing of biomass and medium composition enhances growth capacity in high-density *Chlorella vulgaris* cultures Biotechnol Bioeng 59:605-611.

Michele V, Hempel DC. 2002. Liquid flow and phase holdup-measurement and CFD modeling for two-and three-phase bubble columns. Chem Eng Sci 57:1899-1908.

Miyahara T, Matsuha Y, Takahashi T. 1983. The size of bubbles generated from perforated plates. Int Chem Eng 23:517-523.

Murhammer DW, Pfalzgraf EC. 1992. Effects of Pluronic F-68 on oxygen transport in agitated, sparged bioreactor. Biotechnol Techn 6:199-202.

Murhammer DW, Goochee CF. 1990. Sparged animal cell bioreactors: mechanism of cell damage and Pluronic F68 protection. Biotechnol Prog 6:391-397.

Nedbal L, Tichy V, Xiong F, Grobbelaar JU. 1996. Microscopic green algae and cyanobacteria in high-frequency intermittent light. J Appl Phycol 8:325-333.

Niki E. 1987. Interaction of ascorbate and α-tocopherol. Ann NY Acad Sci 498:186-199.

Nusch EA. 1980. Comparison of different methods for chlorophyll and phaeopigment determination. Archiv fuer Hydrobiologie Beiheft, Ergebnisse der Limnologie 14:14-36.

Ogbonna JC, Tomiyama S, Tanaka H. 1999. Production of α–tocopherol by sequential heterotrophic-photoautotrophic cultivation of *Euglena gracilis.* J Biotechnol 70:213-221.

Paalme T, Kahru A, Elken R, Vanatalu K, Tiisma K, Vilu R. 1995. The computer-controlled continuous culture of *Escherichia coli* with smooth change of dilution rate (A-stat). J Microbiol Meth 24:145-153.

Paalme T, Elken R, Kahru A, Vanatalu K, Vilu R. 1997a. The growth rate control in *Escherichia coli* at near to maximum growth rates: The A-stat approach: Antonie Van Leeuwenhoek Int J Gen Molec Microbiol 71:217-230.

Paalme T, Elken R, Vilu R, Korhola M. 1997b. Growth efficiency of *Saccharomyces cerevisiae* on glucose/ethanol media with a smooth change in the dilution rate (A-stat): Enzyme Microb Technol 20:174-181.

Palozza P, Krinsky NI. 1992. β-carotene and α-tocopherol are synergistic antioxidants. Arch Biochem Biophys 297:184-187.

Phillips JN, Myers JN. 1954. Growth rate of *Chlorella* in flashing light. Plant Physiol 29:152-161.

Phillips LG, Cowan AK, Rose PD, Logie MRR. 1995. Operation of the xanthophyll cycle in non-stressed and stressed cells of *Dunaliella salina* Teod. in response to diurnal changes in incident irradiation: A correlation with intracellular β-carotene content. J Plant Physiol 146:547-553.

Polli M, Di Stanislao M, Bagatin R, Bakr EA, Masi M. 2002. Bubble size distribution in the sparger region of bubble columns. Chem Eng Sci 57:197-205.

Popovic M, Robison CW. 1984. Proceedings of the 34th Canadian Chemical Engineering Conference, Quebec City. Estimation of some important design parameters for non-Newtonian liquids in pneumatically-agitated fermenters. p 258-263.

Pratt R, Fong J. 1940. Studies on *Chlorella vulgaris* II. Further evidence that Chlorella cells form a growth inhibiting substance. Am J Bot 27:431-436

Pulz O, Scheibenbogen K. 1998. Photobioreactors: Design and performance with respect to light energy input. In: Scheper T, editor. Advances in Biochemical Engineering/Biotechnology. Berlin Heidelberg, Springer-Verlag 59:123-152.

Pulz O, Scheibenbogen K, Grob W. 2001.Biotechnology with cyanobacteria and microalgae. In: Rehm HJ, Reed G, Puhler A, Stadler P (Eds). Biotechnology. Weinheim: Wiley-VCH. Vol 10 p 107-136.

Richmond A. 1996. Efficient utilization of high irradiance for production of photoautotrophic cell mass: a survey. J Appl Phycol 8:381-387.

Richmond A. 2000. Microalgal biotechnology at the turn of the millennium: A personal view. J Appl Phycol 12:441-451.

Richmond A, Hu Q. 1997. Principles for efficient utilization of light for mass production of photoautotrophic microorganisms. Appl Biochem Biotechnol 63-65:649-658.

Richmond A, Zou N. 1999. Efficient utilisation of high photon irradiance for mass production of photoautotrophic micro-organisms. J Appl Phycol 11:123-127.

Richmond AZ, Cheng-Wu. 2001. Optimization of a flat plate glass reactor for mass production of *Nannochloropsis* sp. outdoors. J Biotechnol 85:259-269.

Richmond A, Cheng-Wu Z, Zarmi Y. 2003. Efficient use of strong light for high photosynthetic productivity: interrelationships between the optical path, the population density and cell-growth inhibition. Biomol Eng, in press.

Rodolfi L, Zittelli GC, Barsanti L, Rosati G, Tredici M. 2003. Growth medium recycling in *Nannochloropsis sp.* mass cultivation. Biomol Eng, in press.

Sanchez MA, Contreras GA, Garcia CF, Grima EM, Chisti MY. 1999. Comparitive evaluation of compact photobioreactors for large-scale monoculture of microalgae. J Biotechnol 70:249-270.

Sanchez MA, Camacho FG, Gomez AC, Grima EM, Chisti MY. 2000. Bubble-column and air-lift photobioreactors for algal culture. AIChE 46:1872-1887.

Schafer R, Merten C, Eigenberger G. 2002. Bubble size distributions in a bubble column reactor under industrial conditions. Exp Thermal Fluid Sci 26:595-604.

Shigeoka S, Onishi T, Nakano Y, Kitaoka S. 1986. The contents and subcellular distribution of tocopherols in *Euglena gracilis.* Agric Biol Chem. 50:1063-1065

Silva HJ, Cortinas T, Ertola HJ. 1987. Effect of hydrodynamic stress on *Dunaliella* Growth. J Chem Tech Biotechnol 40:41-49.

Singh S, Arad SM., Richmond A. 2000. Extracellular polysaccharide production in outdoor mass cultures of *Porphyridium sp.* in flat plate glass reactors. J Appl Phycol 12:269-275.

Skulberg OM. 2000. Microalgae as a source of bioactive molecules - experience from cyanophyte research. J Appl Phycol 12:341-348.

Sluis C, Westerink B, Dijkstal M, Castelein S, Boxtel A, Giuseppin M, Tramper J, Wijffels R H. 2001. Estimation of steady-state culture characteristics during acceleration - stats with yeasts. Biotechnol Bioeng 75:267-275.

Smith PK, Krohn RI, Hermanson GT, Mallia AK, Gartner FH, Provenzano MD, Fujimoto EK, Goeke NM, Olson BJ, Klenk DC. 1985. Measurement of protein using bicinchoninic acid. Analyt Biochem 150:76-85.

Speek AJ, Schrijvers J, Schreurs WHP. 1984. Fluorimetric determination of total vitamin C and total vitamin iso-C in foodstuffs and beverages by high performance liquid chromatography with pre-column derivatization. J Agr Food Chem 32:352-355.

Speek AJ, Schrijvers J, Schreurs WHP. 1985. The vitamin E composition of some seed oils as determined by high performance liquid chromatography with fluorimetric detection. J Chromatogr 224:389-397.

Suzuki T, Matsuo T, Ohtaguchi K, Koide K. 1995. Gas-sparged bioreactors for CO_2 fixation by *Dunaliella tertiolecta*. J Chem Tech Biotechnol 62:351-358.

Tani Y, Tsumura H. 1989. Screening for tocopherol-producing microorganisms and α-tocopherol production by *Euglena gracilis* Z. Agric Biol Chem. 53:305-312.

Takeyama H, Kanamaru A, Yoshino Y, Kakuta H, Kawamura Y, Matsunaga T. 1997. Production of antioxidant vitamins, β-carotene, vitamin C, and vitamin E, by two-step culture of *Euglena gracilis* Z. Biotechnol Bioeng 53:185-190.

Terry KL. 1986. Photosynthesis in modulated light: Quantitative dependence of photosynthetic enhancement on flashing rate. Biotechnol Bioeng 28:988-995.

Threlfall DR, Goodwin TW. 1967. Nature, intracellular distribution and formation of terpenoid quinones in *Euglena gracilis*. Biochem J 103:573-588

Torzillo G, Accolla P, Pinzani E, Masojidek J. 1996. *In situ m*onitoring of chlorophyll fluorescence to assess the synergistic effect of low temperature and high irradiance stresses in *Spirulina* cultures grown outdoors in photobioreactors. J Appl Phycol 8:283-291.

Tramper J, Williamn JB, Joustra D, Vlak JM. 1986. Shear sensitivity of insect cells in suspension. Enzyme Microbiol Technol 8:33-36.

Tramper J, Joustra D, Vlak JM. 1987. Bioreactor design for growth of shear-sensitive insect cells. In: Webb C, Mavintuna F (Eds). Plant and Animal Cell Cultures: Process Possibilities. Ellis Horwood, Chichester, UK p 125-136.

Tramper J, Vlak JM. 1988. Bioreactor design for growth of shear sensitive mammalian and insect cells. In: Mizrahi A, editor. Adv Biotechnol Process. New York: Alan R Liss, Inc.

Tramper J, Smit D, Straatman J, Vlak JM. 1988. Bubble column design for growth of fragile insect cells. Bioprocess Eng 2:37-41.

Tredici MR. 1999. Bioreactor, Photo. In Flixkinger MC, Drew SW (Eds). Encyclopedia of bioprocess technology : Fermentation, biocatalysis, and bioseparation. John Wiley & Sons, Inc. p 395-419.

Tzeng JW, Chen RC, Fan LS. 1993. Visualisation of flow characteristics in a 2D-bubble column and three phase fluidized bed. Am Inst Chem Eng J 39:733-744.

Van't Riet K, Tramper. 1991. Basic bioreactor design. Marcel Dekker, Inc. New York.

Vonshak A, Torzillo G, Tomaseli L 1994. Use of chlorophyll fluorescence to estimate the effect of photoinhibition in outdoor cultures of *Spirulina platensis.* J Appl Phycol 6:31-34.

Weiland P. 1984. Influence of draft tube diameter on operation behaviour of air-lift loop reactors. Ger Chem Eng 7:374-385

Wu J. 1995. Mechanisms of animal cell damage associated with gas bubbles and cell protection by medium additives. J Biotechnol 43:81-94.

Wu J, Goosen MFA. 1995. Evaluation of the killing volume of gas bubbles in sparged animal cell culture bioreactors. Enzyme Microb Tech 17:1036-1042.

Wu X, Merchuk J C. 2001. A model integrating fluid dynamics in photosynthesis and photoinhibition processes. Chem Eng Sci 56:3527-3538.

Wu X, Merchuk JC. 2002. Simulation of algae growth in a bench-scale bubble column bioreactor. Biotechnol Bioeng 80:156-168.

Young AJ, Orset S, Tsavalos AJ. 1997. Methods for carotenoid analysis. In: Pessarakli M, editor. Handbook of Photosynthesis. New York: Marcel Dekker. p 575-596.

Zhu CJ, Lee YK. 1997. Determination of biomass dry weight of marine microalgae. J Appl Phycol 9:189-194.

Zou N, Zhang C, Cohen Z, Richmond R. 2000. Production of cell mass and eicosapentaenoic acid (EPA) in ultrahigh cell density cultures of *Nannochloropsis sp* (Eustigmatophyceae). Eur J Phycol 35:127-133.

Zou N, Richmond A. 2000. Light-path length and population density in photoacclimation of *Nannochloropsis* sp. (Eustigmatophyceae). J Appl Phycol 12:349-354.

Summary

Microalgae and cyanobacteria are a very interesting source of a wide range of compounds. For many of the applications, monoalgal or even axenic cultures are required. This can be obtained in closed photobioreactors. In these systems, besides the main scale-up parameters, which are associated to all microbial fermentations: mass transfer, mixing rate and hydrodynamic stress, the light regime has also to be considered because light energy is the limiting substrate. However, these parameters cannot be controlled independently, as they are closely interrelated. Therefore the whole process has to be examined. In this thesis, tools for a proper scale-up and optimisation of vertical gas-sparged photobioreactors are given. More attention is put on light regime, hydrodynamic stress and optimisation tools.

Inside photobioreactors there will be a photic zone, close to the illuminated surface and a dark zone, further away from this surface. This is due to light absorption by the cells and mutual shading. The light regime is determined by the light gradient and the liquid circulation time. As a result of mixing, cells will circulate between the light and the dark zone of the reactor at a certain frequency, which is dependent on reactor design and gas input. These light/dark cycles will determine the efficiency at which the microorganisms can utilize the light energy given, i.e. photosynthetic efficiency.

From literature is known that short light/dark cycles in the range 40 ms to 1 s, can enhance photosynthetic efficiency. Because it is difficult to establish these cycles in large-scale photobioreactors, it was studied if medium-duration cycles would also lead to higher photosynthetic efficiency. Medium-duration light/dark cycles in the ranges 10-100 and 1-4 s can be found in the well-studied airlift and bubble column reactors, respectively. For this reason, in Chapter 2, the effect of medium-duration light gradient/dark cycles on microalgal productivity is clarified and modelled.

Light/dark cycles are associated with two basic parameters: first, the light fraction, i.e. the ratio between the light period and the cycle time (ε) and second, the length of the light/dark cycle (t_c). The biomass yield and growth rate is mainly affected by the light fraction, whereas cycle duration only has a small influence. The yield of biomass on light energy is lower under light-gradient/dark cycles in comparison to a light gradient only ($\varepsilon = 1$). Only in the situation where the duration of the dark period is relatively short the biomass yield approaches the yield under a light gradient without an additional dark period. A statistical model, describing the effect of light fraction and cycle time on the biomass yield and growth rate is developed and is used to simulate the implications of theses cycles on the design and operation of air-lift reactors. This can be done only under the assumption that the downcomer comprises the photic zone with a constant light

gradient (1200 to 50 µmol m^{-2} s^{-1}), the riser equals the dark zone, the incident light intensity is approximately 1200 µmol m^{-2} s^{-1}, $10 < t_c < 100$ and $0.1 < \varepsilon < 1$. The effect of reactor height, superficial gas velocity in the riser and the downcomer to riser cross-sectional area on cycle time, light fraction and consequently on biomass yield on light energy are simulated.

Air-lift reactors seem to be inefficient for microalgae cultivation due to the presence of light/dark cycles of 10 to 100 s. Only at high light fractions ($\varepsilon \geq 0.67$) biomass yield will be comparable to the yield obtained under a continuous light gradient without a dark period. This yield, on its turn, is much lower than the yield described in literature in a flat panel reactor with an optical path of 2.6 cm and a light intensity of 1800 µmol m^{-2} s^{-1}, 0.27 as opposed to 1.48 g mol^{-1}.

These findings clearly show that light/dark cycles of several seconds to tens of seconds do not result in enhanced photosynthetic activities. In the following chapters of this work, only bubble columns and flat panels are considered due to the possibility of attaining shorter light/dark cycles at high gas power inputs.

High gas inputs can lead to cell death due to hydrodynamic stress. The growth rates of some microalgae have been reported to increase initially with increasing turbulence, probably due to the improved supply of light or CO_2, but upon an optimum level, the growth decreases sharply with further increase of the superficial gas velocity. In Chapter 3, the effect of superficial gas velocities up to 0.085 m s^{-1} is studied in cultures of the strains *Dunaliella tertiolecta*, *Chlamydomonas reinhardtii* wild type and cell wall lacking mutant cultivated in bench-scale and pilot-plant bubble columns. *D. tertiolecta* and *C. reinhardtii* are selected because they are reported as being the most sensitive microalgae strains due to the lack of a rigid cell wall. Both *C. reinhardtii* wild type and cell wall deficient mutant are chosen to verify the protective effect of the cell wall against hydrodynamic shear.

No cell damage is found for *D. tertiolecta* and *C. reinhardtii* (wild type) up to superficial gas velocities of 0.076 and 0.085 m s^{-1}, respectively. These findings suggest that high superficial gas velocities cannot be responsible for cell death and therefore the bursting of the bubble is not the cause for cell injury. A death rate of 0.46 ± 0.08 h^{-1} was found for *C. reinhardtii* (cell wall lacking mutant) at a superficial gas velocity of 0.076 m s^{-1} and increased to 1.01 ± 0.29 h^{-1} with increasing superficial gas velocity to 0.085 m s^{-1}. This shows that shear sensitivity is strain dependent and the cell wall plays to some extent a role in the protection against hydrodynamic shear.

The increase in cell death rate constant with increasing superficial gas velocity might be due to the increased frequency of bubble burst at the culture, but it can also be due to an increase in the gas-entrance velocity at the sparger as a consequence of increasing the gas flow rate without changing the number and diameter of the nozzles. In order to confirm that cell death takes place at the sparger and to further investigate other possible causes for cell damage, the effect of gas

entrance velocity, culture height and nozzle diameter on the cell death constant is studied in Chapter 4 for *Dunaliella tertiolecta* and *Dunaliella salina*. The cause for cell death of these two different microalgae strains, cultivated in bench-scale bubble columns is identified and cell death rates are quantified. After reaching a certain critical gas-entrance velocity, which is strain dependent, a further increase of the gas-entrance velocity leads to an increase in the cell-death rate. Bubble rising and bubble bursting are not responsible for cell death and that small nozzles, which produce small bubbles, are more detrimental to cells. Bubble formation is proven to be the main cause for cell death in gas-sparged photobioreactors.
These findings contribute to optimal design, operation and scale-up of photobioreactors in terms of minimising shear-related cell death. The strategy to follow when a reactor needs to be scaled-up and/or high superficial-gas velocities need to be used is to determine the critical gas velocity at the sparger for the strain of interest and to keep the gas velocity at the sparger lower than the critical value by increasing the number of nozzles or/and increasing the nozzle diameter.

The maximization of productivity and light efficiency implies the optimisation of cultivation parameters. The knowledge on the response of microorganisms to changes in the physical environment is an essential step to obtain a cost-effective process. Steady-state culture characteristics are usually determined in chemostat cultivations, which are very time consuming. Acceleration-stat (A-stat) cultivations can supply more information and reduce experimental time. In the A-stat the dilution rate is continuously changed at a constant acceleration rate, which leads to different average light intensities inside the photobioreactor. The acceleration rate should be small enough to keep the system in steady state and as high as possible in order to reduce experimental time. In Chapter 5 simulations of the A-stat are done with different acceleration rates to have an indication of the best rate to use. An A-stat is performed in a pilot plant bubble column with *D. tertiolecta* as a model organism. The results show that the A-stat is a fast and accurate tool to determine kinetic parameters and to optimise cultivation conditions in continuous cultivations of a specific photobioreactor. Its applicability to another photobioreactor (flat panel reactor), to other light regimes and to optimise the production of compounds of interest (vit C, vit E, lutein and β-carotene) is proven in Chapter 6. In order to validate the simulations of the effect of the acceleration rate on the pseudo-steady state conditions, four different accelerations are studied. Pseudo-steady state is maintained at acceleration rates of 0.00016 and 0.00029 h^{-2} and results are similar to those of the chemostat. An increase in the acceleration rate leads to an increase in the deviation between the results obtained in the A-stat and those in the chemostats obtained at the same dilution rate. From this work it is concluded that it is advantageous to use the A-stat instead of chemostats to determine culture characteristics and optimise a given photobioreactor.

For the above reasons, the biomass and product yield of continuous cultures of *Dunaliella tertiolecta* is optimised in a flat panel reactor using the A-stat. The effect of the average light intensity inside the photobioreactor on the production of vitamin C and E, lutein and β-carotene is studied. Different product concentrations are obtained at different average light intensities, showing the importance of optimising each product on average light intensity.

Finally in Chapter 7 the possibility of attaining high-cell density cultures in flat-panel reactors with a small optical path, in which short liquid-circulation times can be induced, is discussed. An overview of the important operational and design parameters to be considered for an optimal process is given. New issues and challenges that will be decisive for the success of high-cell density cultivations in photobioreactors are pointed out, namely flow regime, liquid properties and growth inhibition.

Samenvatting

Microalgen en cyanobacteriën (blauw-groene algen) zijn een erg interessante bron voor een breed scala van verbindingen. Voor veel van deze toepassingen is het noodzakelijk monoculturen te gebruiken, in sommige gevallen zelfs zonder bacteriën. Dergelijke monoculturen kunnen gekweekt worden in gesloten fotobioreactoren. Naast de belangrijkste parameters die van belang zijn tijdens de opschaling van alle microbiële fermentaties: massaoverdracht, mengsnelheid en hydrodynamische stress, moet ook het lichtregime in ogenschouw genomen worden omdat licht energie het limiterende substraat is. Deze parameters kunnen echter niet onafhankelijk gecontroleerd worden omdat ze nauw met elkaar verbonden zijn. Daarom moet het gehele proces in zijn geheel worden onderzocht. In dit proefschrift worden hulpmiddelen aangeleverd voor de opschaling en optimalisatie van verticale beluchte fotobioreactoren zoals bellenzuilen. De nadruk is gelegd op het lichtregime en de hydrodynamische stress in zulke fotobioreactoren en ook op optimalisatie strategieën voor bestaande reactoren.

In een fotobioreactor kan onderscheid gemaakt worden tussen een zone (volume) aan het belicht oppervlak waarin de cellen blootgesteld zijn aan licht en een donkere zone in het inwendige van de reactor. Dit wordt veroorzaakt door de absorptie van licht door de cellen zelf waardoor ze andere cellen in de schaduw plaatsen. Het lichtregime wordt daarom gekarakteriseerd door een lichtgradiënt in het belicht volume en door de snelheid waarmee de vloeistof, en dus de cellen, circuleert tussen belicht en donker volume. Ten gevolge van de menging van de vloeistof circuleren de cellen met een bepaalde frequentie welke afhankelijk is van het reactorontwerp en de beluchtingssnelheid. Deze zogenaamde licht/donker cycli hebben een grote invloed op de efficiëntie waarmee de microorganismen licht gebruiken, de fotochemische efficiëntie.

Uit de literatuur is het bekend dat korte licht/donker cycli van 40 ms tot 1 s de fotochemische efficiëntie kunnen verbeteren. Omdat het moeilijk is zulke cycli te induceren in fotobioreactoren op productieschaal, is onderzocht of ook middellange cycli kunnen leiden tot een hogere efficiëntie. Licht/donker cycli van 1 tot 4 s of 10 tot 100 s kunnen namelijk bereikt worden in respectievelijk bellenzuilen en ‘air-lift’ reactoren. In hoofdstuk 2 wordt daarom het effect van middellange licht/donker cycli op de productiviteit van algenculturen onderzocht en gemodelleerd.

Licht/donker cycli worden gekarakteriseerd door 2 parameters: ten eerste, de lichtfractie, dit is de verhouding tussen de verblijftijd in het belicht volume en de duur van de gehele licht/donker cyclus (ε), en ten tweede de circulatietijd, de duur van de licht/donker cyclus (t_c). De biomassaopbrengst en de groeisnelheid werden met name beïnvloed door de lichtfractie, terwijl

de circulatietijd slechts een kleine invloed had. De biomassaopbrengst is lager onder blootstelling aan licht/donker cycli dan onder continue belichting ($\varepsilon = 1$), waarbij tijdens belichting altijd éénzelfde lichtgradiënt is gehandhaafd in de cultuur. Alleen in de situatie waarbij de periode in het donker van relatief korte duur was, benadert de biomassaopbrengst de opbrengst zonder blootstelling aan een donkere periode. Een statistisch model is opgezet om het effect van lichtfractie en circulatietijd op de biomassaopbrengst en de specifieke groeisnelheid te beschrijven en dit model is gebruikt om de invloed van licht/donker cycli op het design en de werking van air-lift reactoren te simuleren. Deze simulaties zijn gedaan onder de aanname dat de 'riser' van de air-lift reactor samenvalt met het donkervolume en dat de 'downcomer' samenvalt met het belicht volume met éénzelfde lichtgradiënt als gebruikt tijdens de experimenten: 1200 μmol m^{-2} s^{-1} aan het oppervlak naar 50 μmol m^{-2} s^{-1} aan het donkervolume. Verder is het model alleen valide voor: 10 s < t_c < 100 s en 0.1 < ε < 1. De effecten van reactor hoogte, superficiële gassnelheid in de riser en de verhouding tussen de dwarsdoorsneden van downcomer en riser op de circulatietijd, lichtfractie en, als gevolg daarvan, de biomassaopbrengst zijn gesimuleerd.

Air-lift reactoren lijken niet efficiënt te zijn voor algenkweek vanwege de aanwezigheid van middellange licht/donker cycli van 10 tot 100 s. Alleen onder hoge lichtfracties ($\varepsilon \geq 0.67$) is de biomassaopbrengst vergelijkbaar aan de situatie zonder een donkere periode. Sterker nog, deze biomassaopbrengst is veel lager dan de opbrengst van een vlakke plaatreactor (rechthoekige bellenzuil) met een lichtweg van 2.6 cm en een lichtintensiteit van 1800 μmol m^{-2} s^{-1}: 0.27 g mol^{-1} in vergelijking tot 1.48 g mol^{-1}.

Deze resultaten laten duidelijk zien dat licht/donker cycli van enkele tot tientallen seconden niet leiden tot een verbetering van de fotosynthetische activiteit. In de volgende hoofdstukken worden daarom alleen bellenzuilen en vlakke plaatreactoren (rechthoekige bellenzuilen) in beschouwing genomen vanwege de mogelijkheid om in deze reactoren kortere licht/donker cycli op te leggen bij hoge beluchtingsnelheden.

Hoge beluchtingsnelheden kunnen tot celdood leiden vanwege een te grote hydrodynamische stress (afschuifspanningen). Voor sommige microalgen is een toename van de groeisnelheid beschreven als gevolg van een toename van de turbulentie en dit wordt waarschijnlijk veroorzaakt door een verbetering van de licht- en/of koolstofdioxide toevoer. Als de beluchtingsnelheid (superficiële gassnelheid) echter verder verhoogd wordt tot boven het optimale niveau neemt de groeisnelheid snel af. In hoofdstuk 3 is het effect van verschillende superficiële gassnelheden (tot 0.085 m s^{-1}) op de microalgen *Dunaliella tertiolecta* en *Chlamydomonas reinhardtii* (wildtype en celwandloze mutant) beschreven. Deze experimenten zijn uitgevoerd in labschaal en 'pilot' schaal bellenzuil reactoren. *D. tertiolecta* en *C. reinhardtii* werden gekozen omdat deze gevoelig zouden

kunnen zijn voor hydrodynamische stress vanwege het feit dat ze niet beschikken over een rigide celwand. Van *C. reinhardtii* is het wildtype en een celwandloze mutant gekozen om de beschermende werking van de celwand te kunnen verifiëren.

Celbeschadiging is niet opgetreden tot superficiële gassnelheden van 0.076 en 0.085 m s^{-1} voor respectievelijk *D. tertiolecta* en *C. reinhardtii* (wildtype). Deze resultaten doen vermoeden dat hoge superficiële gassnelheden niet leiden tot celdood en dat daarom het knappen van de luchtbellen aan het vloeistofoppervlak niet de oorzaak van celbeschadiging kan zijn. Voor de celwandloze mutant van *C. reinhardtii* is een afstervingsnelheid van 0.46 ± 0.08 h^{-1} gevonden bij een superficiële gassnelheid van 0.076 m s^{-1} en deze nam toe tot 1.01 ± 0.29 h^{-1} bepaald bij een superficiële gassnelheid van 0.085 m s^{-1}. Dit laat zien dat gevoeligheid voor afschuifspanningen soortafhankelijk is en dat de celwand een zekere mate van bescherming biedt tegen hydrodynamische stress.

De evenredige toename van de afstervingsnelheid met een toename van de superficiële gassnelheid zou kunnen worden veroorzaakt door een toename van de frequentie waarmee bellen knappen aan het vloeistofoppervlak. Maar de toename van de gassnelheid bij de gasverdelers zou ook een verklaring kunnen zijn voor de toename van de afsterving. Deze gassnelheid nam toe omdat de beluchtingsnelheid toenam bij een gelijkblijvend aantal gasverdelers. Om deze hypothese te testen en om andere mogelijke oorzaken voor celbeschadiging te onderzoeken is in hoofdstuk 4 de invloed van de gassnelheid bij de gasverdelers, de hoogte van de vloeistofkolom en de diameter van de verdelers op de afstervingsconstante van *Dunaliella tertiolecta* en *Dunaliella salina* onderzocht. Voor deze microalgen is de oorzaak van celdood onderzocht in labschaal bellenzuil reactoren en de afstervingsnelheid is gekwantificeerd. Na het bereiken van een zekere soortafhankelijke kritische gassnelheid bij de verdeler treedt celdood op en leidt een verdere verhoging tot een toename in de afstervingsnelheid. Het opstijgen van de luchtbellen en het knappen van luchtbellen aan het vloeistofoppervlak zijn niet verantwoordelijk voor celdood. Gasverdelers van kleine diameters die kleine gasbellen produceren richten meer celschade aan. Het is aangetoond dat het proces van bellenvorming bij de gasverdelers de belangrijkste oorzaak is voor celdood in gas gemengde fotobioreactoren.

Deze bevindingen dragen bij aan het optimale ontwerp, operatie- en opschalingstrategie met betrekking tot het minimaliseren van celdood veroorzaakt door hydrodynamische stress. In de situatie dat een reactor opgeschaald moet worden of dat hoge superficiële gassnelheden toegepast moeten worden, moet eerst de kritische gassnelheid bij de gasverdeler voor de desbetreffende algensoort bepaald worden. De daadwerkelijke gassnelheid moet lager gehouden worden dan de kritische snelheid door het aantal gasverdelers of de diameter van de verdelers aan te passen.

De kweekomstandigheden moeten geoptimaliseerd worden om de productiviteit en dus de fotochemische efficiëntie te maximaliseren. Het verkrijgen van inzicht in de aanpassing van microorganismen aan veranderingen in de kweekomstandigheden is een essentiële stap op weg naar een rendabel proces. De karakteristiek van culturen in evenwicht met de omstandigheden worden gewoonlijk bepaald in een chemostaat. Dit is erg tijdrovend en een Accelaratie-staat (A-stat) kan meer informatie geven in een kortere tijd. In een A-stat wordt de verdunningssnelheid continu verhoogd met een constante versnelling (acceleratiesnelheid) en dit resulteert in een toename van de gemiddelde lichtintensiteit in de fotobioreactor. De versnelling moet voldoende laag gehouden worden om het systeem in (pseudo-)evenwicht te houden maar tegelijkertijd moet deze zo hoog mogelijk gehouden worden om de experimentele tijd te reduceren. In hoofdstuk 5 is de A-stat gesimuleerd voor *Dunaliella tertiolecta* met verschillende versnellingen om een inschatting te maken van de beste versnelling voor een experiment. Daarna is de A-stat uitgevoerd in een 'pilot' schaal bellenzuil reactor met *D. tertiolecta* als modelorganisme. De resultaten tonen aan dat de A-stat een snel en accuraat middel is om de kinetische parameters te bepalen en de kweekomstandigheden in een fotobioreactor te optimaliseren. In hoofdstuk 6 wordt de toepasbaarheid voor andere fotobioreactoren (vlakke plaatreactor) met andere lichtregimes aangetoond. Ook wordt aangetoond dat deze techniek gebruikt kan worden voor de optimalisatie van specifieke producten (vitamine C en E, luteïne en β-caroteen). Verder zijn vier verschillende acceleratiesnelheden getest om de simulaties van het effect van de versnelling op het pseudo-evenwicht te valideren. Pseudo-evenwicht wordt gehandhaafd onder versnellingen van 0.00016 en 0.00029 h^{-2} en de resultaten zijn vergelijkbaar met die verkregen in een serie chemostaten. Een toename van de acceleratiesnelheid leidt tot een toename in de afwijking tussen de resultaten verkregen in een A-stat en een serie chemostaten. Uit dit onderzoek is geconcludeerd dat het voordelen heeft om een A-stat te gebruiken in plaats van een serie chemostaten om de karakteristieken van een algencultuur te bepalen en een willekeurige fotobioreactor te optimaliseren.

Om bovengenoemde redenen is een A-stat gebruikt om de biomassa- en productopbrengst van *Dunaliella tertiolecta* in een vlakke plaatreactor te optimaliseren. De invloed van de gemiddelde lichtintensiteit in de fotobioreactor op de productie van vitamine C en E, luteïne en β-caroteen is onderzocht. Verschillende productconcentraties zijn gevonden onder verschillende lichtintensiteiten, wat duidelijk het belang aantoont, om voor ieder product de gemiddelde lichtintensiteit te optimaliseren.

Tenslotte wordt in hoofdstuk 7 de mogelijkheid besproken om hoge celdichtheden te bereiken in vlakke plaatreactoren met een korte lichtweg. In zulke reactoren kunnen zeer korte vloeistofcirculatietijden bereikt worden. Er wordt een overzicht gegeven van belangrijke operatie-

en ontwerpparameters die meegenomen moeten worden om een optimaal proces te verkrijgen. Nieuwe aspecten en uitdagingen die beslissend zijn voor het succes van hoge celdichtheidskweken in fotobioreactoren worden toegelicht namelijk, vloeistofstromingsprofiel, vloeistof- of medium eigenschappen en groei inhibitie.

Acknowledgements

And here we are **Wijffels**, at the most exciting lines of this thesis, which everyone will read!
René, it was an incredible experience to have you as my supervisor. You have been very important for my scientific, professional and personal development during these four and a half years. You knew how to motivate me during my PhD deeps, you believed in me and gave me the responsibility and the necessary space to "grow"! Your creativeness, optimism, support, trust and good laughs were essential to me to get here. Your non-conventional comments on my manuscripts or abstracts for conferences, such as "Maria, this is boring", made me think, laugh and improve my scientific writing. I hope you're still not bored at this point, because this kind of writing we did not cover and I still have a lot to say! Thanks to you, working has been a lot of fun. You've been a great boss and a wonderful friend. Reading my manuscripts in one day if necessary, looking for "caracoles" in restaurants in Granada during a whole evening (without finding them!), sitting for hours in a pub (despite the headache on the day after), learning how to "correctly" pronounce "Puuuurrrrtugal" are a few of the good moments we have spent together. You will always be a very special friend "con mucho corazion!". Thank you and **Ida** for always making me feel welcome and at home in your house. Next time in Portugal…you still have a lot to learn about our gastronomy!
Hans, I would like to thank you for being my promoter, for your always friendly smile and for never complaining even if sometimes I was a "bit loud" in lab 632, meaning a bit loud also in your office next door. My stay at Bioprocess Engineering will always be an important step in my career.
To my students **Bram** (Bramy!), **Nienke**, **Marco** (Marquito!), **Jeroen**, **Jan-Willem** (sweety!), **Hady** and **Adri**, thank you for the good work you've done and your enthusiasm! I would certainly not have succeeded to promote within four years without your help.
And to all the students of Marine Biotechnology thanks for making the lab 632 and the pubs in Wageningen so "gezellig". Coincidently most of you were always in the mood for more than one drink after work.
Marcel, you were my first deep contact to the dutch way of working and living… I could not wish for a better friend! You have given advices and ideas, complained, helped, stressed out, overworked, corrected manuscripts, criticised, stressed me, encouraged me, worried with me, and almost starved in Portugal while waiting for lunch time…you have always been present… also as co-author of Chapter 2 and 7! Daaaaaankejewel Marcelito!!!! **Dorien**, thanks for making Marcel a bit more relaxed (little by little we will get there!).
Catrinus (now Ninus!), you're my tallest and sweetest Frisian friend! (I hope not to be spoiling your reputation!). I am so happy that you were there when I started! You made me feel so at home. Thank you for always caring as only you can do!

Ronald (Roneeeee!)**,** your unique sense of humor and willing to shock me (without succeeding!) led to the most silly and funny conversations. I always had a good time (and a good laugh) with you around!

Jorge, you gave me the feeling I had driven 2500 km from Portugal to get to Portugal. Thank you "pelas boas vindas a Wageningen", your friendship and your delicious Portuguese feijoada.

Carlos (Carlitos!), you came for a few months and ended up as a friend for life! Conversámos horas e horas, rimos que nem doidos, gozámos um pouquinho com os macaquinhos holandeses e partilhámos os momentos mais importantes da nossa vida. A friendship like yours comes once in a lifetime…Besitos!!!!

Rouke, people say we make a lot of noise together, but in reality they mean a lot of loud enthusiastic and happy sounds!!! I cannot imagine these four and a half years without you…or maybe I can think of a "few" less after-party headaches! Your friendship has been very important to me, and your creative ideas and the capacity of solving practical problems in the lab (in a few seconds!) only for " een zakje dropjes" are also in this thesis. Bedankt Roukita!!!!!

Mohammad (Mr President!), we did it!!!!!!!!!! We have started and finished our PhD thesis at the same time! We have shared similar experiences, discussed our different cultures, we laughed and stressed together and suddenly, in a blink, here we are! You, **Zahra Selva** and **Maryam** will always be "my Iranian family".

Detmer, with you I spent the most time during these years. We have discussed reality and the imaginary. I have tasted your extremely weird food combinations and you have learned to enjoy my garlic obsession. Life is made of small details … we have shared a life together! Beijinhos Dety!!!

Yovita, you have been always "marine" to me! There are no words to describe our friendship… it just came with a lot of hours talking about everything and nothing. You are one of the reasons I call Wageningen my sweet home! Kusjes!

Isabel, thank you for you friendship, support and GOOD advices. My house will always be yours! Beijocas!

Wim, "netjes" as you I had never seen! The lab was never so shiny as when you were working with us! **Sebastiaan** and **Eira**, good luck with your PhD!

Fred, you saved my live 1000 times, i.e. you solved 1000 problems during my cultivations. You came, said "Que pasa, huuuuun?????" and problem solved! **Gerrit** no one screams Mariiiiiiiiiiia like you, and **Jos** I promise not to order beer again! Harstikke bedank voor jullie adviezen en hulp!

Dirk, thank you for reading my manuscript on shear, for your advices and sympathy. **Arjen**, it has always been great talking to you and trying to understand your point of view…but there is no way for you of escaping the last dance! **Pieter**, luckily you found the pâté of sardines or else I would have never been able to explain you how incredible Portugal is! **Maurice** thank you for the nice

game evenings! **Marian**, it was a lot of fun, some headaches and a wonderful adventure to organise the PhD trip to South Africa with you and Yovita… I would not choose anyone else! **Martin**, thank you for taking care of all financial matters regarding my holidays….ooooopsss!!!!, I mean my travels to conferences!, for your good mood and for the beautiful Wit's Coffee Corner. **Joyce** and **Hedy** thank you for your sympathy, good mood, and help whenever necessary. **Rolf**, the last one to leave the "borrels" and the MacGyver of the department, thank you for having a weird time-schedule just like me! **Marieke**, I had never met anyone so relaxed in life and so Nordic as you! It was good laughing with you! **René**, thank you for the nice dinners and the private piano concerts! To my first roommates, **Mariska** and **Marjolein** thank you for the nice chatting and pleasant atmosphere in our room.

Verder, wil ik de mensen van de werkplaatsen bedanken, **Jan**, **Eric**, **André**, **Evert**, **Reinoud**, **Peter**, **Hans en Jurrie**, zonder jullie had ik nooit gelukt!!!!

To all my colleagues in **Proceskunde** thank you for the "gezelligheid", the inumerous "borrels", Christmas dinners, "labuitjes", movie nights, and especially the good daily work environment. It feels so good to wake up in the morning and go to work with a smile on the face!

Evelien, I was so happy to find so many things in common with you. You and Roukita were both very important to me. I would not change our dinners for nothing in this world and I hope to once be able to make you feel the same way in Portugal: at home! **Vagner**, thank you for opening my eyes for things in live that I had never thought before. Your kindness has no limits and your friendship will always be precious to me. Um beijão! **Clara**, un gran beso para ti!, **Timo**, you have taught me my first dutch word: the most important thing in the kitchen–koelkast and you and **Thijs** made my short stay in Rijnsteeg worth while! Bedankt! **Herma**, para ti só vou escrever português! Nós as duas fizemos as lições de Português e Holandês mais divertidas do mundo. Pessoas como tu sabem ser felizes em qualquer parte do mundo. Fico contente por teres escolhido Portugal! **Hans**, I had never thought that being a ceremony master would be so much fun until we had to do it together. We had a great time and you have amazed me with your simple and clear perspective of live. Thank you Yovita and Catrinus for giving me a very special and unique friend! I am starting to be a fan of Frisians!

I will now fly to Portugal…

Filipe, pipinho do coração, it always felt good to have you so close by in Rotterdam. Para mim Roterdão é como aquele cantinho do mundo à beira mar plantado, ora o caldo verde, ora o bacalhau, batatinhas a murro, um ombro amigo, cantoria e muita conversa! My world would not be the same without you!

Ana, being with you after one year always felt as if I had seen you everyday…with the exception that we had to talk even longer to update our lives. I believe that this is what is meant with friendship! **Paulinha**, **Andreia**, **Sofia e Pi**, there's no "Porto" without you!

Sandra, amiga como tu só tu! Morri de saudades tuas, I talked and talked about you and I often wished you would be next to me: in the most silly and funny moments where only you would understand my big laugh and laugh even louder, in the bar drinking some "bejecas" and also in the hard moments when I felt like throwing everything to space. It is now, on this precise moment that I realise that in fact you have always been by my side and helped me to get here! Não há amizade maior que a nossa!

Henriqueta e **Agostinho,** your joy of living will always be an example for me. Thank you for always caring!

Patricia e **Paulo**, your stays in Amsterdam were a total refreshment of my energy. I cannot really explain how good it felt each time you were here, but it was something like family mixed with love, warmth and tenderness with some spices on top calling me back home! Obrigada primos!

Tia **Nini**, tia **Lourdes**, Sarocas, **Helinha** e Patricia, vocês tornaram a ceia de Natal no dia mais esperado do ano! **Sarocas**, in you I saw the most incredible changes during these years. If you could only imagine how proudly I talk about you!

Avó Isilda, para si vai toda a minha admiração! Para toda a minha familia um muito obrigada!

António, mano, you're my favourite brother but also my special friend. You've always tried to look after me and protect me since we were kids. If something was wrong I just had to scream Antoooonioooo!!!!!!!!. You have given me support in all important moments of my live and if it involved party you were definitely present! Thank you for your love, friendship, trust and all the fun we had together!

Jorge, you have shown me the beauty of simplicity, with you there are no limits in life…

Papá e mamã, vocês viveram comigo o dia a dia, todas as alegrias, tristezas, preocupações, inseguranças e euforias. Ouviram-me, aconselharam-me, apoiaram-me e disseram-me quando estava errada… ensinaram-me a viver feliz.

O vosso amor foi a minha força e determinação

A minha maior felicidade são vocês

Esta é a nossa tese!

Mania

Curriculum Vitae

PERSONAL DATA

Maria João Barbosa
Born 2nd April 1974, Luanda, Angola
Nationality: Portuguese

ACADEMIC CARRER

1999-03 PhD in Nutrition, Food technology and Biotechnology, speciality Bioprocess Engineering, by Wageningen University, The Netherlands

1993-97 MSc in Food Engineering, Superior School of Biotechnology, Catholic University, Portugal.

PROFESSIONAL ACTIVITIES

1999-03 Food and Bioprocess Engineering Group, Wageningen University, the Netherlands
PhD thesis entitled Closed microalgal photobioreactors: Scale-up and optimisation.

1999 Food and Bioprocess Engineering Group, Wageningen University, The Netherlands.
Junior researcher in the Dutch national project: Biological Hydrogen Production

1998 Multinational company Sara Lee, "Carnes Nobre", Production Management Department, Portugal.
Professional trainee.

1997 INRA – Institut National de la Recherche Agronomique, Saint-Pée-sur-Nivelle, France and Superior School of Biotechnology, Catholic University, Portugal.
Research assistant: Microalgae as a natural source of astaxanthin for aquaculture.

1997 CNR–Centro Nazionale della Ricerca, Florence, Italy.
Scientific traineeship: Cultivation of microalgae as a source of PUFAs for aquaculture.

1996 Necton – Portuguese Company of Marine Cultures, Portugal.
Industrial traineeship: Cultivation of microalgae for aquaculture and cosmetic industry.

SCIENTIFIC PUBLICATIONS

PEER-REVIEWED JOURNALS

Barbosa MJ, Zijffers JW, Nisworo A, Vaes W, Schoonhoven J, Wijffels RH. 200?. Optimisation of biomass, vitamins and carotenoid yield on light energy in a flat panel reactor using the A-stat technique. Submitted.

Barbosa MJ, Janssen M, Richmond A, Wijffels RH. 200?. High-cell density cultures: design and operational charachteristics of photobioreactors. Submitted

Barbosa MJ, Hadyianto, Wijffels R.H. 2003. Overcoming shear stress in sparged photobioreactors. Biotechnol Bioeng (in press).

Barbosa MJ, Hoogakker J, Wijffels RH. 2003. Optimisation of cultivation parameters in photobioreactors for microalgae cultivation using the A-stat technique. Biomol Eng (in press).

Luiten EEM, Akkerman I, Koulman A, Kamersmans P, **Barbosa MJ**, Sipkema D, Wijffels RH. 2003. Realising the promises of Marine Biotechnology. Biomolecular Engineering (in press).

Barbosa MJ, Albrecht M, Wijffels RH. 2003. Hydrodynamic stress and lethal events in sparged microalgae cultures. Biotechnol Bioeng 83:112-120.

Barbosa MJ, Janssen M, Ham N, Tramper J, Wijffels RH. 2003. Microalgae cultivation in air-lift reactor: modeling biomass yield and growth rate as a function of mixing frequency. Biotechnol Bioeng 82: 170-179.

Barbosa MJ, Rocha MS, Tramper J, Wijffels RH. 2001. Acetate as a carbon source for hydrogen production by photosynthetic bacteria. J Biotechnol 85: 25-33.

Rocha JS, **Barbosa MJ**, Wijffels RH. 2000. Hydrogen production by photosynthetic bacteria: culture media, yield and efficiency. In: Miyake J, Matsunaga T. and San Pietro A. (Eds.), Biohydrogen II, pp. 1-31.

Barbosa MJ, Morais R, Choubert G. 1999. Effect of carotenoid source and dietary lipid content on blood astaxanthin concentration in rainbow trout (*Oncorhynchus mykiss*). Aquaculture 176: 331-341.

COMMUNICATIONS IN CONGRESSES

Barbosa MJ, Albrecht M, Hadiyanto, Wijffels RH. 2003. Overcoming hydrodynamic stress in sparged photobioreactors.International Marine Biotechnology Conference, Tokyo, Japan.

Janssen M., **Barbosa MJ**, Hoekema S. 2003. Towards the application of high-density phototrophic cultures. 5th European Workshop. Biotechnology of Microalgae, Berlin, Germany.

Barbosa MJ, Wijffels RH. 2003. A dynamic approach to optimize product and biomass yield in photobioreactors: Basics and Applications, Matalascanas, Spain (poster).

Barbosa MJ, Wijffels RH. 2003. Hydrodynamic stress and lethal events in sparged microalgae cultures. Symposium Marine Biotechnology: Basics and Applications, Matalascanas, Spain (poster).

Bosma R, **Barbosa MJ**, Wijffels RH. 2003. Marine Biotechnology in education. Symposium Marine Biotechnology: Basics and Applications, Matalascanas, Spain (poster).

Barbosa MJ, Tramper J, Wijffels RH. 2002. A-stat: A new tool for photobioreactor optimization. 9th International Conference on Applied Algology and 1st Congress of International Society for Applied Phycology, Aguadulce, Spain (poster).

Barbosa MJ, Zijffers JW, Vaes W, Wijffels RH. 2002. Optimisation of biomass, vitamins and carotenoid yield on light energy. Natural products from marine microorganisms. Greifswald, Germany.

Barbosa MJ, Tramper J, Wijffels RH. 2001. Scale-up parameters for microalgae cultivation. The Fourth Asia-Pacific Marine Biotechnology Conference, Hawaii, USA.

Barbosa MJ, Bosma R, Tramper J, Wijffels RH. 2000. Light Regime in gas-sparged bioreactors for microalgae cultivation. 8th Netherlands Biotechnology Congress, Ede, The Netherlands (poster).

Barbosa MJ, Bosma R, Tramper J, Wijffels RH. 1999. Microalgae cultivation in bubble columns and air-lift reactors. 8th International Conference on Applied Algology, Montecatini Terme, Italy (poster).

Rocha JS, **Barbosa MJ**, Tramper J, Wijffels RH. 1999. Potential of microalgal biomass and photosynthetic bacteria for hydrogen production. 8th International Conference on Applied Algology, Montecatini Terme, Italy (poster).

Barbosa MJ, Morais R, Choubert G. 1999. Astaxanthin absorption in rainbow trout *Oncorhynchus mykiss*: Effect of carotenoid sources and dietary lipid content. 12th International Carotenoid Symposium, Cairns, Australia (poster).

Barbosa MJ, Choubert G, Morais R, Serna Rico A, Gómez R, Gobantes I, Salvador AM, Milicua JCG. 1999. Astaxanthin transport in rainbow trout *Oncorhynchus mykiss*: Effect of dietary lipid level. 1st International Congress on Pigments in Food Technology, Seville, Spain (poster).

Barbosa MJ, Morais R, Choubert G. 1998. Effect of dietary lipid content on astaxanthin serum absorption and on flesh pigmentation of rainbow trout fed diets supplemented with *Haematococcus* and with synthethic astaxanthin. BIOTEC 98, IV Iberian Congress on Biotechnology, I Ibero – American Meeting on Biotechnology, Guimarães, Portugal.

Barbosa MJ, Gonçalves A, Raposo F, Morais R. 1996. Effect of vegetable hormones on the growth of the microalga Dunaliella salina, X National Congress of Biochemistry, Braga, Portugal (poster).

This work was carried out at Wageningen University, Department of Agrotechnology and Food Sciences, Food and Bioprocess Engineering Group, P.O. Box 8129, 6700 EV Wageningen, The Netherlands.

The research described in this thesis was sponsored by the Portuguese Ministry of Science and Technology, "Fundação para a Ciência e Tecnologia" with a Portuguese doctoral fellowship PRAXIS XXI/BD/19539/99.

The printing and representation costs of this thesis were financially supported by Food and Bioprocess Engineering Group, Wageningen University, The Netherlands; J.E. Jurriaanse Stichting, Rotterdam, The Netherlands and "Fundação para a Ciência e Tecnologia", Lisbon, Portugal.

Printed by Ponsen & Looijen BV, Wageningen, The Netherlands